

International Atomic Energy Agency

INDC(SEC)-62/L

INDC

INTERNATIONAL NUCLEAR DATA COMMITTEE

CONSOLIDATED PROGRESS REPORT FOR 1976

ON NUCLEAR DATA ACTIVITIES

OUTSIDE THE NDS SERVICE AREA

Austria

Belgium

Canada

Netherlands

Norway

Switzerland

Turkey

October 1977

IAEA NUCLEAR DATA SECTION, KÄRNTNER RING 11, A-1010 VIENNA

Reproduced by the IAEA in Austria
October 1977
77-8772

CONSOLIDATED PROGRESS REPORT FOR 1976

ON NUCLEAR DATA ACTIVITIES

OUTSIDE THE NDS SERVICE AREA

Austria

Belgium

Canada

Netherlands

Norway

Switzerland

Turkey

October 1977

FOREWORD

This consolidated progress report for 1976 has been prepared for countries outside the NDS service area. A second report, INDC(SEC)-61/L, covers countries within the NDS service area.

The report is arranged alphabetically by country, and reproduces the content of each individual report as it was received by the INDC Secretariat. Progress reports of other countries which have received already wide distribution, are not reproduced in this report.

As in all progress reports the information included here is partly preliminary and is to be considered as private communication. Consequently, the individual reports are not to be quoted without the permission of the authors.

TABLE OF CONTENTS

	pages
<u>Austria</u>	1-14
Atominstitut der Oesterreichischen Universitaeten Wien	
Institut fuer Radiumforschung und Kernphysik der Oesterreichischen Akademie der Wissenschaften, Wien	
Institut fuer Theoretische Physik und Reaktorphysik der Technischen Universitaet Graz	
<u>Belgium</u>	15-118
S.C.K./C.E.N., Mol	
Ghent State University	
<u>Canada</u>	119-133
Atomic Energy of Canada Limited Chalk River Nuclear Laboratories	
<u>Netherlands</u>	135-150
Netherlands Energy Research Foundation (ECN), Petten	
R.J. Van de Graaff Laboratory, State University, Utrecht	
<u>Norway</u>	151
<u>Switzerland</u>	153-180
Institut de Physique, Université de Neuchâtel	
Laboratorium f. Kernphysik, Eidg. Technische Hochschule Zuerich	
Institut f. Physik der Universitaet Basel	
Physik-Institut der Universitaet Zuerich	
Eidg. Institut f. Reaktorforschung, Wuerenlingen	
<u>Turkey</u>	181-204
Cekmece Nuclear Research and Training Center, Istanbul	
Middle East Technical University, Ankara	
Hacettepe University, Ankara	

PROGRESS REPORT TO INDC AND NEANDC
FROM AUSTRIA

April 1977

O.J.Eder, Editor

This report contains abstracts about work performed at

Atominstitut der Österreichischen Universitäten, Wien

Institut für Radiumforschung und Kernphysik der
Österreichischen Akademie der Wissenschaften, Wien

Institut für Theoretische Physik und Reaktorphysik der
Technischen Universität Graz

Österreichische
Studiengesellschaft
für Atomenergie
A-2444 Seibersdorf
Austria

This report contains
partly preliminary data.
The information given
is to be considered as
private communication
and is not to be quoted.

ATOMINSTITUT DER ÖSTERREICHISCHEN UNIVERSITÄTEN, WIEN

1. NEUTRON SOURCES AND NEUTRON DETECTION

1.1 Measurement of the emission spectra of Sb-Be, Ga-D₂O, In-Be, Mn-Be and Ga-Be photoneutron sources

E.Zankl, F.Bensch

The energy distribution of the photoneutrons produced in said sources was measured by a proton-recoil proportional counter. The sources were surrounded by spherical lead-shields to reduce the very intense gamma field. Various methods of (n,γ)-discrimination were investigated and the best results were obtained by an electronic division method which used the quotient of the rise-time to the pulse height of each pulse. The experimental results showed for the Sb-Be source that there exists also a continuous neutron contribution, produced by the ${}^9\text{Be}(\gamma, n)\alpha$ -reaction, besides the sharp neutron peak at 24keV. Good agreement with earlier theoretical calculations was obtained for the Ga-D₂O source. For the first time there exist accurate measurements of the energy distribution of In-Be, Mn-Be and Ga-Be photoneutrons; these sources have several neutron groups with discrete energies.

2. NEUTRON SCATTERING

2.1 Electric and Nuclear Scattering of Slow Neutrons by Atoms

G.Eder

The electric scattering of neutrons by the Coulomb field of the nucleus and the electrons of a free, neutral and non-magnetic atom is due to the internal charge distribution, the magnetic moment, and the electric polarizability of the neutron. The interference between electric and nuclear interaction of slow neutrons ($l = 0$) is discussed. Expressions for differential cross sections and final state polarization are derived. The electric polarizability modifies essentially the left-right asymmetry of the scattering cross section for polarized neutrons.

2.2 Parameter Systematic for a Neutron-Nucleus Optical Potential*)

G.Eder, H.Leeb and H.Oberhummer

The functional relations between the potential depth and the half density radius of the phenomenological optical neutron-nucleus potential are studied. Parameter systematics for the energy range from 4MeV to 30MeV are constructed which include this ambiguity. It is demonstrated that besides the usually assumed isospin dependence of the real potential depth there must also exist a dependence on the mass number of the target nucleus. The work confirms once more shell effects in the surface absorption term and suggests a method to separate volume and surface absorption by their energy dependence.

*)The work is partly supported by Kulturstiftung der Stadt Wien.

3. NEUTRON INTERFEROMETRY

3.1 Measurements of Scattering Lengths by Neutron Interferometry

H.Rauch, U.Bonse*, W.Bauspiess**, H.Kaiser, G.Badurek

The perfect crystal neutron interferometer which was developed during the last years (Phys.Lett. A47 (1974) 369) is used for high precision measurements of coherent scattering lengths of various gases. The measurements are carried out at the high flux reactor in Grenoble. The results serve for a deeper understanding of nuclear-, electromagnetic- and few-body-interaction (Proc.Gatlinburg CONF-760601-P2, p. 1094 (1976) and Proc.Lowell CONF-760715-P2, p. 1027). We got the following values for the bound coherent scattering length (in 10^{-13} cm):

Al	3.449 ± 0.005	H	-3.42 ± 0.03
Bi	8.502 ± 0.012	He	3.007 ± 0.03
Mg	5.375 ± 0.003	N	8.975 ± 0.07
Nb	7.054 ± 0.003	O	5.735 ± 0.05
Sn	6.228 ± 0.004	Ar	2.017 ± 0.02
V	-0.382 ± 0.001		
Zn	5.686 ± 0.003		

3.2 Magnetic Effects in Neutron Interferometry

H.Rauch, U.Bonse*, A.Zeilinger, G.Badurek, W.Bauspiess**, H.Kaiser, W.Schindler

* Institut für Physik, Universität Dortmund

** Institut für Physik, Universität Dortmund and Institut Laue-Langevin, Grenoble

The neutron interferometer is sensitive to nuclear and magnetic phase shifts as well. After we have verified the 4π -periodicity for spinor rotation (Phys.Lett. 54A (1975) 425) new modulation and polarization effects are observed for simultaneous nuclear and magnetic phase shifts (Phys.Rev. D14 (1976) 1177; Nuovo Cim. 34B (1976) 76). New neutron interferometric measurements with an advanced magnetic field positioning yield an accuracy of about 2% for the 4π -factor and about 1% for the determination of magnetic forward scattering lengths. Experiments with polarized incident neutrons are in preparation.

4. NEUTRON DEPolarIZATION

4.1 Search for Magnetic Order in Selected Pseudobinary Systems down to Milli Kelvin Temperatures

R.Goblirsch, H.W.Weber, G.Hilscher*, R.Grössinger*,
W.Steiner**

Magnetization and neutron depolarization experiments performed on the pseudobinary systems $Y_6(Fe_xMn_{1-x})_{23}$, $Zr(Fe_xCo_{1-x})_2$ and $Y(Fe_xAl_{1-x})_2$ are reported. At some intermediate concentrations bulk magnetization measurements did not show a Curie temperature down to 2K. Neutron depolarization measurements down to 30mK confirm the absence of any spontaneous order in these systems. However, the magnetization curves obtained indicate the existence of magnetic clusters. This assumption is supported by the appearance of a field induced magnetic short range order observed by neutron depolarization experiments. The results are discussed in terms of a simple cluster model.

4.2 Instrumental Developments in Polarized Neutron Research

G.Badurek, H.Rauch, J.Hammer

A fully transistorized electronic spin-flip chopper system for polarized neutron beams based on a modified Mezei spin-flip device could be developed, which represents an improved version of the originally described DC flipper-chopper (Nucl.Instr.Meth. 128 (1975) 315) and provides a quasi elastic time resolution in the $1\mu s$ range and a minimum pulse width of about 3 - $5\mu s$. Feasibility studies on the application of the pseudo-statistical correlation method for that type of chopper clearly showed the disturbing influence of systematical errors introduced by deviations of the modulation function from their mathematically ideal value. The conclusion could be drawn that the correlation technique is useful only for moderate resolution, i.e. elementary pulse widths of more

* Institut für Experimentalphysik, TU Wien

** Institut für Angewandte Physik, TU Wien

than 20 μ s, and low modulation depth as it is frequently the case, if spin-dependent scattering is investigated only without the use of an analysing crystal.

A further development is concerned with the extension of the well established neutron depolarization method to dynamic process and relaxation phenomena. At present the electronic setup for the pulsed analyzation has been completed and a search for magnetic after-effects in Dy single and polycrystals is in progress.

5. NEUTRON DIFFRACTION

5.1 Fourier Neutron TOF-Diffractometry

G.Badurek, G.P.Westphal, P.Ziegler

A computer controlled time-of-flight diffractometer for thermal neutrons has been developed (Atomkernenergie 29 (1977) 27), allowing efficient use of the available intensity. An especially designed so-called Fourier-chopper modulates the incident polychromatic beam periodically in time with different frequencies. From the frequency dependent count rate the Fourier transform of the TOF distribution of the scattered neutrons is derived by means of a four-quarter-period phase sensitive detector system. This distribution containing the structural information of the scattering sample can be obtained by performing the corresponding inverse transformation by means of a computer program. The safe maximum rotational speed of the chopper rotor is about 11000 rpm, corresponding to a maximum modulation frequency of the beam of 100kHz. The time resolution of the instrument for a flight path length of 1 - 2m is of the order of 1%. It could be shown (Nucl.Instr.Meth. 137 (1976) 595) that the presence of the higher harmonics in the nearly triangular chopper modulation function causes only negligible systematic errors in the determination of the Fourier components of the neutron TOF-distribution, thus making complicated stator shaping procedures for sinusoidal modulation not necessary. Preliminary test measurements on poly- and single crystal specimens could demonstrate the correct function of the instrument.

5.2 Development of a new Small-Angle X-Ray and Neutron Diffractometer

D.Bader, H.Rauch, A.Zeilinger

A perfect crystal diffractometer for the study of small-angle diffraction was developed. The device is both applicable to X-ray and neutron diffraction. Therefore measurements with these radiations on the same sample with the same geometry are possible. The angular

resolution is in the order of seconds of arc. An optical control system was constructed which is only sensitive to the relative position of the two monochromators and therefore measures the parallelity and deviations from parallelity of these two crystals.

6. NEUTRON RADIOGRAPHY

6.1 Neutron Radiographic Measurements of the Diffusion of H in Metals

W.A.Pochman, A.Zeilinger

Neutron radiography was used to measure hydrogen diffusion in metals (J.Appl.Phys. 47 (1976) 5478; J.Phys.F: Metal.Phys., in print). It is possible to work in a range of exposures where the optical density distribution on the radiographic film directly represents the hydrogen distribution in the sample. The method is essentially non-destructive and the hydrogen need not penetrate surfaces during the measurement. The diffusion coefficients of H in β -Ti, V, Nb and Ta in qualities as usually delivered were measured for temperatures between 50 to 110°C. The results indicate that the diffusion coefficient of H in β -Ti, Nb and Ta is not very sensitive to chemical composition and impurity content. It is concluded that for most technical applications regarding the H transport properties it is not necessary to use extremely pure metals.

6.2 Neutron Radiography of TRIGA Fuel Rods

C.Koberger, W.A.Pochman, H.Rauch, A.Zeilinger, H.Böck

Neutron radiographic investigations of fresh TRIGA fuel rods showed cracks in two elements running right through the fuel briquette. As the new elements were not radioactive, the radiographs could be taken with Gd-foils using the direct method (Atomkern-energie 29 (1977) 231). After the exposition time of several minutes the fuel elements became slightly radioactive showing a radiation level of 100mrem/h measured on contact immediately after radiographing. This activity decayed within a few hours. Further measurements of irradiated fuel elements using the track etch technique are under progress.

INSTITUT FÜR RADIUMFORSCHUNG UND KERNPHYSIK DER
ÖSTERREICHISCHEN AKADEMIE DER WISSENSCHAFTEN, WIEN

1. Precise measurement of the $^{63}\text{Cu}(n,\alpha)^{60}\text{Co}$ cross section with 14MeV neutrons

G.Winkler

The $^{63}\text{Cu}(n,\alpha)^{60}\text{Co}$ reaction is a crucial fluence monitor in reactor dosimetry and it is of great importance in unfolding the high-energy part of neutron spectra by foil activation techniques. As significant discrepancies exist in the literature data the $^{63}\text{Cu}(n,\alpha)$ cross section has been remeasured with 14 MeV neutrons with an accuracy of a few per cent.

2. Activation Analysis Applications in Archaeology

W.Czerny, G.Winkler

The use of 14MeV neutrons for the analysis of ancient pottery has been investigated. A comparison technique using Al-foils as a standard was introduced. The main components Si, Al, Mg and Fe could be evaluated within a short time with an error of a few per cent thus differentiating between samples of different origin. It has been shown that also the analysis of minor components in pottery such as Na, Ca, Sc, Ti, Mn, Ni, As, Rb, Y, Zr, Cs, Ce can be performed by activation with fast neutrons with moderate precision using a Ge(Li) γ -spectrometer system. The work will be published in the Journal of Radioanalytical Chemistry.

3. Measurement of differential elastic and inelastic scattering cross sections with 14MeV neutrons on elements of practical importance

K.Hansjakob, G.Staffel, G.Winkler, F.Wenninger,
A.Chalupka, H.Vonach

Using time-of-flight techniques for neutron spectroscopy a program has been started to measure the elastic scattering cross sections $(\frac{d\sigma}{d\Omega})_{el}(\theta)$ in the region $\theta = 20^\circ - 135^\circ$ with an accuracy of about 10%, the high energy part of the inelastic neutron spectra $(\frac{\delta^2\sigma}{\delta E_n \delta \Omega})(\theta)$ as a function for θ and $E_n = 3 - 14\text{MeV}$ with an energy resolution of about 0.5MeV. In the beginning emphasis is

laid on measurements on Ba in its natural isotopic composition and on measurements of the cross sections for forming the first 2^+ level of ^{138}Ba . Furthermore measurements of the low-energy part of the neutron spectra from (n,n') - and $(n,2n)$ -reactions in the region $E_n = 0.5 - 3\text{MeV}$ averaged over θ are planned.

4. Multiparameter-coincidence study of the reaction
 $\text{Zn}(n,n'\gamma)$ at 14MeV

H.Kratschmar, S.Tagesen

A sample of natural Zn has been irradiated with 14MeV neutrons from a nanosecond pulsed beam facility. Coincidence-events have been recorded as 3-word items containing neutron time-of-flight, recoil energy (in NE 213) and γ -ray energy (Ge(Li)-detector). Neutron energy spectra for transitions to the first excited levels of $^{64,66,68}\text{Zn}$ will be extracted and compared to results of statistical model calculations.

5. On the low-energy performance of the Munich PSD system

A.Chalupka and G.Stengl
M.R.Maier* and P.Sperr*

The performance of the Munich pulse-shape discrimination (PSD) circuit was tested at very low particle energies. n - γ separation turned out to be possible down to $E_{el} \approx 30\text{keV}$ also for relatively large ($5'' \times 1''$) NE 213 scintillators. Even at the lowest energies rejection of 99% of the γ -pulses could be achieved if a loss of about 30% of the neutron pulses was permitted.
(Will be published in Nucl.Instr. and Meth.)

6. Temperature dependence of the pulse shape
discrimination properties of NE 213

A.Chalupka, G.Stengl and H.Vonach

The temperature dependence of the pulse shape discrimination (PSD) properties of the liquid scintillator NE 213 was investigated in the temperature range $-15^\circ - +30^\circ\text{C}$. The large temperature dependence of the PSD properties reported in the literature could not be confirmed. Even in very sensitive measurements no change in the PSD properties was observable. This indicates that both intensity ratio of the fast and slow components of the scintillation and the scintillation decay times have very small temperature coefficients.
(Will be published in Nucl.Instr. and Meth.)

* Physikdepartment, TU München

7. Statistical and optical model calculations of neutron induced reaction cross sections for $^{134-138}\text{Ba}^*$

B. Strohmaier and M. Uhl

Average neutron induced reaction cross sections for $^{134-138}\text{Ba}$ for incident energies between 20keV and 20MeV have been calculated by means of the optical and the statistical model with consideration of preequilibrium emission. The calculations comprise the total, the nonelastic, the differential elastic, the (n,γ) , $(n,xn\gamma)$, $(n,p\gamma)$, $(n,pn\gamma)$ and $(n,np\gamma)$ cross sections, as well as the production spectra of neutrons, protons and gamma-rays. For the model calculations a consistent set of parameters based on experimental data as far as possible was employed. The accuracy of the calculated cross sections was estimated.

8. Statistical model calculations of neutron induced cross sections for $^{31}\text{P}^*$

B. Strohmaier and M. Uhl

Average $(n,xn\gamma)$, $(n,\gamma\gamma)$, $(n,pn\gamma)$, $(n,np\gamma)$, $(n,\alpha\gamma)$, $(n,\alpha n\gamma)$ and $(n,n\alpha\gamma)$ cross sections as well as particle and gamma-ray production spectra for ^{31}P have been calculated for incident energies between threshold and 20MeV. Preequilibrium emission was accounted for. Good agreement between computed and experimental cross sections could be achieved by use of a single set of model parameters.

9. Measurement of energy spectra and angular distributions of charged particles emitted in nuclear reactions induced by 14MeV neutrons

P. Hille, M. Uhl, K. Richter, C. Derndorfer, R. Nowotny, G. Stengl

Measurement of the reaction $^{56}\text{Fe}(n,\alpha)$ has been completed and compared to statistical model calculations. The new improved version of the cylindrical multiwire chamber is now tested.

10. Age-determination of bones by activation with 14MeV neutrons

P. Hille, H. Vonach, P. Eisenbarth

In cooperation with the Palaeontological Institute of the University of Vienna the N/P- and F/P-ratios of fossil bones are determined by activation analysis and compared to age determination by other methods. Work is now concentrated on bone material found in Austrian caves.

* Work supported by the European Communities (EURATOM)

11. Measurement of γ -multiplicities after (n,n')-reactions with 14MeV neutrons

P.Grabmayr, P.Hille

The project described in the last report has been started by calibrating the γ -detector using inelastic 2 - 3MeV neutron scattering on Li-, Si- and Fe-targets.

12. Neutron sputtering

G.Stengl, P.Hille

Using the pulsed high intensity neutron generator at the Institut für Radiumforschung it is planned to study 14MeV neutron sputtering of several materials. TOF-technique will be used for mass identification of sputtered atoms and compounds. Neutron sputtering is an important problem for the development of fusion reactors.

INSTITUT FÜR THEORETISCHE PHYSIK UND REAKTORPHYSIK DER
TECHNISCHEN UNIVERSITÄT GRAZ

1. On the Determination of the Resonance Selfshielding in Materials of Medium Atomic Weight*

M.Heindler

In the present study the theoretical basis for a computer code (SEFAC) has been worked out that allows for resolved resonances the correct calculation of the energy- and temperature dependence on cross-sections, on non-shielded and effective group cross-sections and on resonance selfshielding factors of medium-heavy elements.

With the help of this programme and a set of resonance parameters for iron, evaluated by Le Coq and Ribon, the cross-sections and the selfshielding factors for the radiative capture in iron have been calculated, dependent on the energy of the neutrons, on the temperature of iron, the form of the neutron spectre in the regarded reactor type, and on the dilution cross-section of the iron in the considered reactor zone.

The data gained by this programme SEFAC for the effective group

* Habil. T.U. Graz, 1976

cross-sections and the selfshielding factors of medium heavy elements will enter into the version IV of the CADARACHE-cross-section data files, which will be made use of when projecting the fast 1200MWe reactor "Super Phénix".

2. Diffusiontheoretical Treatment of Coupled Cores*

H.Rabitsch

The associated flux distributions of weakly coupled slab- and cylindergeometrical cores are calculated by applying the one-group diffusion theory. From the integral representation of the neutron flux by its boundary values the explicit terms of the associated flux distributions for approximately calculated boundary fluxes are derived. A first order perturbation theory makes it possible to determine the buckling change and the resulting flux distributions of coupled systems from the associated flux distributions. The buckling changes are evaluated for coupled cores in slab geometry and for cores of a cross-section in circular ring sector shape; their results are compared with each other.

3. Transporttheoretical Treatment of Spherically Symmetric Cores*

H.Hubmer

From the view of reactor safety the fine structure of the flux in a light water-cooled statistical pebble bed reactor is of considerable interest. Calculation models are applied to make the use of analytical methods possible - e.g. one considers the neighbouring sphere of a reference sphere as distributed on a concentric shell. The applicability of integrodifferential as well as of integral transport theoretical methods on the model of spherically symmetric assembled cores is to be investigated.

4. The Second Order Correlation Functions of the Neutron Field Dealt with in the n-Group Diffusion Theory

E.Ledinegg

Beside the direct method of incore spectroscopy there are also integral methods of interest that can be used for testing multigroup parameters. For reactors of low power also stochastic methods can be applied which refer to the inner pile noise, respectively to the correlation behaviour of neutron chains of the same or different energy groups.

In the present study the cross- and autocorrelation function of two optionally chosen energy groups are calculated; only statistical

* Diss. T.U. Graz, 1976

moments of second order are dealt with. Green's function in the correlation terms is determined by using a n-group diffusion equation, which is decoupled by means of a principle axis transformation after having applied a Laplace transformation. In the transformed system the demanded Green's functions can be easily stated in form of bilinear developments.

5. Electromagnetic Wave Propagation in Plane Plasma Layers Subjected to Uniform Static Magnetic Field of Arbitrary Direction*

E.Ledinegg, B.Schnizer

To find the field representation of the electromagnetic field in an anisotropic plasma, it is necessary to calculate the mode continuum in infinite space, which requires the solution of the dispersion equation. This is a fourth order equation. The twodimensional case, in which the electromagnetic field depends only on two coordinates and the quartic becomes biquadratic, is an approximation sufficient in many practical cases. At first the corresponding system of modes and the integral representation of the electromagnetic field are given for only one plasma layer. Then the transition to a multiple-layer plasma requires the matching of tangential field components along the boundary, which task can easily be accomplished by solving a system of linear equations.

6. Wave Propagation in Plane Waveguides in an Anisotropic Plasma with Given Primary Current Distribution**

E.Ledinegg, W.Papousek

A multi-layered plasma is considered, where each layer becomes anisotropic by an arbitrary oriented static magnetic field. Wanted is an integral representation of the electromagnetic field excited by an arbitrary source distribution in the stratified plasma. Our method is similar to that of ARBEL and FELSEN, but extends the latter by assuming arbitrarily oriented static magnetic fields. The electromagnetic field is given as an integral representation, constructed from the modes of the transversal parts of the field equations. In case of a nonlinear interaction between plasma and electromagnetic field the obtained solution can be taken as a first order approximation to develop an iteration technique for the equations of magnetohydrodynamics.

7. A Diffusiontheoretical Method for the Flux Calculation in Multisphere Configurations

F.Schürerer

* Int.Congr. "Waves and Instabilities in Plasmas" Book of Abstracts, University of Innsbruck, 1975

** Kleinheubacher Berichte, Vol. 19, 1975

Starting from the exactly solvable problem of the flux determination of a point source of neutrons in an infinite medium, which contains a spherical impurity zone eccentric to the point source, an approximation method for the calculation of the flux distribution of two neighbouring spherical fuel elements in infinite diffusion media is developed. An iterative method allows by alternately satisfying the conditions of continuity of the two spherical fuel elements to proceed to continually improving approximations.

8. On the Calculation of the Doppler-effect of Reactor Materials

M.Heindler

A weak point in the safety analysis of fast breeders is the defective knowledge of the temperature effects on materials of medium atomic weight (60 volume % in fast breeders) that have a direct and indirect influence on the results of the calculations of the Doppler coefficient. The results derived from a quantum mechanical reactorphysical investigation of the relations between resonance structures of reaction rates and temperature effects show up the weak points of the usual calculation methods.

9. Neutron Physical Study on a Light Water Pebble Bed Reactor*

M.Heindler

The advantages of the pebble bed reactor, which have already been demonstrated in practice for the gas-cooled high temperature reactor, suggested the investigation of this principle for the application in reactors with liquid cooling as well. The results of various studies make pebble bed cores also for liquid cooled reactors appear as an interesting alternative to conventional core principles. On the basis of a parameter study of the neutron physical qualities of a pebble bed reactor with liquid cooling especially the neutron physical and thermodynamic characteristics of the fuel elements are discussed after describing the calculation methods. Unsolved problems are referred to.

10. Pulsed Neutron Source Measurements at the SAR Graz

W.Ninaus

Von Dardel suggested to determine the prompt kinetic behaviour of sub-critical assemblies with the help of the pulsed neutron tech-

* ATW, 11, p.574 - 580, Nov. 1975

nique. For applying this method, a pulsed neutron source for the installation in the central channel of the SIEMENS-ARGONAUT-Reactor in Graz has been designed and constructed. The principle of this pulsed neutron source is based on the periodical short utilization of the (γ, n) reaction in beryllium. The prompt neutron life time 1_0 was determined with the method of Simmons and King. For the two core configurations, two-slab and ring-core, the measured values were compared with the results from the Rossi- α -measurements (Stribel and Thury).

11. A Contribution to the Measurement of the Neutron Flux with Wire Probes

Hj. Müller

For the determination of the neutron flux in reactors generally the induced beta and gamma activity will be measured in disk probes. At large flux profiles, the use of wire probes is advantageous, because by only one activation a very large field of the profile is determined. Sometimes it is possible to point out the fine structures of the flux, depending on the evaluation method. The results of the measurements will be discussed according to the evaluation of the beta and gamma activity as well as to the limits of the accuracy.

S.C.K./C.E.N., Mol

Contribution to the Annual Scientific Report for

1976

from the

NEUTRON PHYSICS DEPARTMENT

- <u>Experimental Nuclear Physics</u>	pg.
Neutron Spectrometry	16
Fission Physics and Chemistry	19
Nuclear Spectroscopy	22
- <u>Theoretical Nuclear Physics</u>	24
- <u>Laser Isotope Separation</u>	27
- <u>Neutron Inelastic Scattering by Condensed Matter</u>	28
- <u>Instrumentation</u>	29
Appendix I (Publications)	31
Appendix II (Colloquia, Seminars, Symposia)	35
Appendix III (Theses)	38
Appendix IV (Seminars)	39
Appendix V (External Relations)	41
List of the members and guests of the Department for 1976.	42

1. Experimental Nuclear Physics

1.1. Neutron Spectrometry

(Joint SCK/CEN-CBNM-RUCA neutron cross-section programme)

Resonance Parameters of ^{238}U

E. CORNELIS^{***}, L. MEWISSEN, F. POORTMANS, G. ROHR^{*}, R. SHELLEY^{*},
T. VAN DER VEEN^{*}, G. VANPRAET^{***}, H. WEIGMANN^{*}
(Contract SCK/CEN-IAEA ; N° 1636/RB).

The transmission, scattering, capture and self-indication experiments on ^{238}U performed in the course of 1975 (cfr. previous annual report, BLG 515) were analysed.

The analysis of the transmission data is completed for all samples thicknesses in the energy range between 9 eV and 4262 eV. The analysis of the capture measurements is finished for the three thinnest samples in the same energy range. The scattering measurements were performed up to 1.2 keV. The analysis of these data is nearly completed.

Up to now, the neutron width has been determined for 286 levels below 4262 eV and the capture width for 62 levels up to 3.9 keV. Taking into account the l-assignments of ^{238}U resonances by Corvi et al. (F. Corvi, G. Rohr and H. Weigmann, Proceedings of the Conference on Neutron Cross Sections and Technology, NBS Spec. Publ. 425 (1975), p. 733) we have deduced the following results for the average properties of s-wave neutron resonance parameters (energy range 0 - 4260 eV) :

s-wave strength function : $S_0 = (1.06 \pm 0.11) 10^{-4}$ (number of resonances : 174)

mean-s-wave level spacing : $D_0 = 21.82 \pm 0.85$ eV

mean s-wave capture width : $\Gamma_\gamma = 23.43 \begin{cases} + 0.11 \text{ meV (1}\sigma\text{-statistical error)} \\ - 0.70 \text{ meV (systematic error)} \end{cases}$

The distribution of the Γ_γ values around the mean value is very narrow, the dispersion being only 0.85 meV. No correlation between Γ_γ and Γ_n^0 has been found.

The results mentioned above are of preliminary nature. Minor changes could be necessary after completion of the analysis of all the data. The analysis of the capture experiments with the two thickest samples is in progress. An analysis of the scattering data was started initially taking into account only the effect of self-screening and of

* CBNM, Geel

*** RUCA, University of Antwerp

absorption of the scattered neutrons. Meanwhile an area analysis code has been written which contains Monte-Carlo methods to correct for multiple scattering effects.

Resonance Parameters of ^{237}Np

A. ANGELETTI^{*}, E. CORNELIS^{**}, L. MEWISSEN, F. POORTMANS, G. ROHR^{*},
T. VAN DER VEEN^{*}, G. VANPRAET^{**}, H. WEIGMANN^{*}

The analysis of our ^{237}Np data in the energy range from 8 eV to 204 eV has been completed. A shape and area analysis of the transmission measurements was performed using the Atta-Harvey code. The capture and scattering cross section data were analysed with the area method.

The neutron widths were determined for 213 resonances up to 204 eV. The following value was obtained for the s-wave strength function

$$S_0 = (0.95 \pm 0.09) 10^{-4}$$

By fitting the reduced neutron width distribution to a Porter-Thomas distribution above a bias of $\Gamma_n^0 = 0.02$ meV, we obtained the following result for the s-wave mean level spacing :

$$D_0 = 0.74 \pm 0.03 \text{ eV}$$

The total capture width was deduced from a shape analysis of the transmission data with various sample thicknesses, of capture and of scattering data up to 50 eV. As a result of this analysis the capture width was obtained for 27 resonances. The mean value is :

$$\overline{\Gamma}_\gamma = 41.2 \pm 0.5 \text{ meV} \quad (1\sigma \text{ -statistical error})$$

The fluctuation of Γ_γ around this mean value are small (standard deviation = 3 meV) except for three resonances at 38.3 eV, 39.0 eV and 40.0 eV, respectively, for which Γ_γ is about 50 % larger.

Resonance Parameters of ^{93}Nb

L. MEWISSEN, F. POORTMANS, G. ROHR^{*}, T. VAN DER VEEN^{*}, J. WINTER^{*}

The low energy γ -ray spectrum from the $^{93}\text{Nb}(n,\gamma)^{94}\text{Nb}$ reaction has been measured in individual resonances up to a neutron energy of 2.6 keV with a Ge(Li)-detector.

The 100 keV, 114 keV and 293 keV γ -rays depopulate the low lying level with $J = 2^-, 5^+$ and 2^+ , respectively. As expected, the

* CBNM, Geel

** RUCA, University of Antwerp.

intensity ratios fall into groups which allow a resonance spin classification.

From these data spin values for 24 further resonances could be determined. Most of the parity assignments are, known from the transmission data.

The analysis of the total and capture cross section measurements on ^{93}Nb performed in 1975, has been finished. The analysis of scattering cross section data is in progress. A paper describing this work was presented at the International Conference on the Interactions of Neutrons with Nuclei, Lowell, USA, July, 1976.

Bidimensional data handling system for capture measurements

L. MEWISSEN

A HP 2112 A processor with 56 K memory has been prepared for two-parameter capture measurements, recording simultaneously neutron time-of-flight and energy of the prompt γ -rays. A prototype of the 2 ns CBNM timecoder is coupled, via a Camac crate controller, to the processor.

A HP-Assembler program has been developed to build up the frequency distribution with 8 different pulseheight-groups, each consisting of 6144 time channels. The final histogram is written, in an IBM compatible format, on a coupled magnetic tape unit.

1.2. Fission Physics and Chemistry

Heavy ion interaction barrier.

P. del MARMOL, M. BERLANGER^{4*}, F. HANAPPE^{4*}, J. PETER^{5*}, C. NGO^{5*},
B. TAMAIN^{5*}.

To measure the nuclear part of the interaction barrier and owing to the low beam intensities given previously by the cyclotron at Louvain-la-Neuve (see BLG 515/76) the experiment has been repeated by bombarding ¹¹²Sn and ¹²⁴Sn targets with Ar ions of various energies and measuring their Rutherford scattering.

From a simple parametrization of the barrier value :

$$B = \frac{1.44 Z_1 Z_2}{Z_e (A_1^{1/3} + A_2^{1/3})} \quad \text{and if no dynamical deformation occurs during}$$

the reaction one should expect for a given incident ion (Ne or Ar) that the difference $\Delta B = B_{124} - B_{112}$ should be negative. This was observed in the present work, in contradiction with the results from experiments of other groups working on ¹¹⁶Sn and ¹²⁴Sn in targets.

JOINT SCK/CEN-CBNM-R.U.Gent STUDIES IN FISSION PHYSICS AND STANDARDS.
(Contract EUR/C/4146/67f)

Scattering of fission fragments.

G. CODDENS^x and C. WAGEMANS^{xx}

With an improved experimental set-up, allowing the simultaneous recording of 8 pulse-height spectra taken under different scattering angles, the scattering of fission fragments on gold has been studied. The results are under analysis.

Neutron induced fission cross-section of ²³⁵U in the energy region from 0.008 eV to 30 keV

C. WAGEMANS^{xx} and A.J. DERUYTTER^{xxx}

The results of these measurements were published in Ann. of Nucl. En. with the following abstract : "The neutron induced fission

* IWONL/IRISIA bursar, R.U. Gent and SCK/CEN
** NFWO/FNRS, R.U. Gent and SCK/CEN
*** Nuclear Physics Laboratory, R.U. Gent
4* I.I.K.W./I.I.S.N., U.L.B.
5* Institut de Chimie Nucléaire, Orsay.

cross-section of ^{235}U was measured up to 30 keV at a 30 m flight-path of the CBNM Linac. The fission reaction rate and the neutron flux were determined simultaneously with surface barrier detectors placed on each side of back-to-back ^{235}U and ^{10}B layers. The fission cross-section was calculated assuming a $1/v$ -behaviour of the $^{10}\text{B}(n,\alpha)^7\text{Li}$ cross-section and normalized to $\int_{7.8 \text{ eV}}^{11 \text{ eV}} \sigma_f(E) dE = 240 \text{ barn}\cdot\text{eV}$. The average fission cross-section was calculated in several energy regions and compared with other results. Also the fission integral $\int_{1 \text{ eV}}^{1000 \text{ eV}} \sigma_f(E) dE$ was calculated yielding 16.16 barn. keV; for the episcadmium resonance integral we obtained $I_f = 280 \pm 7 \text{ barn}''$.

Fission fragment kinetic energy and mass-distributions for the neutron induced fission of ^{235}U

C. WAGEMANS^{*}, G. WEGENER-PENNING^{**}, H. WEIGMANN^{***}

All data taken before the stop of the Linac have been analysed. The results indicate that new measurements covering other neutron energies are required in order to allow a clear conclusion.

To improve the experimental conditions for these further measurements, a detector cooling system was installed, resulting in a better energy resolution.

Determination of some characteristics of the thermal neutron induced sub-barrier fission of ^{231}Pa , ^{232}Th and ^{237}Np .

C. WAGEMANS^{*}, M. ASGHAR^{4*}, P. D'HONDT^{5*}, A. DERUYTTER^{5*}, A. EMSALLEM^{4*}
(Collaboration with R.U. Gent and I.L.L.Grenoble on thermal neutron induced reactions).

The results of these measurements are in print with the following abstract: "Some characteristics of the thermal neutron induced fission of ^{231}Pa , ^{232}Th and ^{237}Np were studied using a highly pure thermal neutron beam of the Grenoble High Flux Reactor. For the thermal neutron induced fission cross-section we obtained $(20 \pm 4) \text{ mb}$ for ^{237}Np , $(19 \pm 4) \text{ mb}$ for ^{231}Pa and smaller than $2.5 \mu\text{b}$ for ^{232}Th , in agreement with calculations based on a double humped fission barrier. We also determined a mean total fission fragment kinetic energy of $(172.8 \pm 2.5 \text{ MeV})$ for ^{237}Np ,

* NFWO/FNRS, R.U. Gent and SCK/CEN

** SCK/CEN trainee

*** CBNM, Geel

^{4*} I.L.L. Grenoble

^{5*} R.U. Gent

which fits into the semi-empirical systematic of \bar{E}_K versus $Z^2/A^{1/3}$.
Finally, we determined LRA/B ratios of $(1.94 \pm 0.17) \cdot 10^{-3}$ for ^{237}Np and
 $(1.67 \pm 0.14) \cdot 10^{-3}$ for ^{231}Pa , in disagreement with the theoretical
predictions of Feather, but consistent with the semi-empirical systematic
of Halpern."

Thermal neutron induced (n, α)-reactions in heavy nuclei

C. WAGEMANS*, P. D'HONDT**, A. DERUYTTER**, M. ASGHAR***, A. EMSALLEM***

Preliminary measurements on the reactions $^{209}\text{Bi}(n,\alpha)$, $^{232}\text{Th}(n,\alpha)$
and $^{237}\text{Np}(n,\alpha)$ were performed, yielding an upper-limit of typically a few
 μ barn for the (n, α)-cross-sections. A ΔE -E telescope detector system
is being tested for obtaining an unambiguous detection of the α -particles.

* NFWO/FNRS, R.U. Gent and SCK/CEN

** R.U. Gent

*** I.L.L. Grenoble

1.3. Nuclear Spectroscopy

Neutron capture gamma-ray studies with Ge(Li) detectors (Joint ULB-CEN/SCK programme)

J.C. DEHAES* and P. FETTWEIS

An apparatus for the study of thermal and average resonance neutron capture is under construction at the R1 beam hole of BR2 reactor. Besides direct spectra, the measurement of γ - γ coincidences and angular correlations both for the determination of transition multipolarities and the study of hyperfine interaction between excited nuclear levels and their host lattice are foreseen.

The following items have been installed :

- 1) A Bi-monocrystalline filter for the obtention of a thermal neutron beam. Its actual length of 50 cm has still to be adjusted in order to optimize neutron flux and gamma background. Flux values of up to 10^7 n/cm² s are expected.
- 2) A polycrystalline filter consisting of 25 cm Fe, 30 cm Al and 5 cm S giving rise to a beam of 24 keV neutrons due to the Fe resonance interference minimum at this energy. The neutron energy distribution has been measured with the help of a proton recoil spectrometer. As expected, weak neutron groups at 357, 279, 133 and 72 keV besides the 24 keV neutron flux is about 10^4 n/cm² s.
- 3) The angular correlation table is being assembled, together with the sample holder and a final shielding against the room background, which is almost exclusively due to the capture of scattered neutrons in Fe, Cu and Ba, elements which are found in the vicinity of the Ge(Li)-detector.

Search for ^{82}Y

P. del MARMOL, P. FETTWEIS, F. HANAPPE***, J. VAN HORENBEECK***

Contradictory results have been published concerning the half-life of ^{82}Y . A preliminary experiment at the cyclotron of Louvain-la-Neuve was attempted. By bombarding Zn with ^{20}Ne ions, it was hoped to follow the decay of known transitions from excited states in ^{82}Sr .

Some of these γ -rays were masked by other rays of similar energy belonging to neighbouring isotopes. One of these could belong to the decay of ^{82}Y but owing to low statistics the results are still inconclusive and further experiments are in progress.

* U.L.B. Brussels

** I.I.K.W./I.I.S.N., U.L.B. Brussels

*** F.N.R.S.

Joint KUL-SCK/CEN programme

Nuclear structure of the transitional ^{151}Sm nucleus

P. VAN ASSCHE, G. VANDENPUT^{*}, L. JACOBS^{*}, J.-M. VANDEN CRUYCE^{**}

A series of nuclear structure calculations aiming at a detailed reproduction of the low energy spectroscopic characteristics of ^{151}Sm have been concluded. Initially these calculations only included a diagonalization of the rotation-particle coupling in a limited basis of quasi-particle configurations. Although most of the levels below 500 keV was fairly well accounted for serious discrepancies remained at somewhat higher energies and some transition rates were off by a few orders of magnitude. It was believed that at least some of these differences could be due to the neglect of the influence of collective vibrations. Thereupon, the model space was extended by the inclusion of quadrupole vibrations of β - and γ -type around an axially symmetric equilibrium shape. The interaction Hamiltonian in addition to Coriolis coupling also contained quasi-particle-phonon and rotation-vibration coupling. The interaction matrix was diagonalized for the negative parity case in a space spanned by 2^4 basis states. The mixed wave functions were used to calculate absolute transition probabilities. Despite this more elaborate effort, however, most of the discrepancies resulting from the first series of calculations could not be resolved in a satisfactory way.

Bent crystal spectrometer at BR2 (L. JACOBS^{*}, P. VAN ASSCHE)

After assembling a new source holder mechanism in soft-iron, the bent crystal diffractometer at BR2 was further improved. Based on measurements on an iridium (n, γ) source of 0.05 mm thickness, the linewidth was determined as 2.9 sec of arc, corresponding to an energy resolution of $\Delta E = 4.3 \cdot 10^{-6} E^2$ ($E, \Delta E$ in keV). The total reflectivity of the Si-crystal^v was measured and displayed the two expected characteristics: a higher absolute value and a smaller decrease at higher gamma energies.

The behaviour of a GeLi detector to detect the diffracted γ -rays, instead of a NaI scintillator, has been investigated.

* I.I.K.W./I.I.S.N., K.U. Leuven

** K.U. Leuven

Decay of Nb^{90m}

P. FETTWEIS, A. MEYKENS*, M. NEVE de MEVERGNIES

Some additionnal measurements were performed so as to check and complete the previous results (cfr. Annual Scientific Report Blg-515, p. 5.18). The final analysis is under way.

2. Theoretical nuclear physics

Triaxial shapes in A = 10 nuclei

M. BOUTEN**, M.-C. BOUTEN and E. FLERACKERS**

Projected Hartree-Fock (PHF) calculations for nuclei in the p shell have been found to be very successfull, as was described in previous reports. A serious discrepancy, however, was observed in the A = 10 nuclides. A PHF calculation for ¹⁰Be yields a good energy spectrum for the low-lying states but calculating the B(E2)'s from the lower two 2+ states to the ground state shows an inversion of the 2+ levels as compared to experiment. Whereas experiment finds a strong B(E2) from the lowest 2+ level to the ground-state, the PHF functions show a strong B(E2) from the second 2+ level and a weak B(E2) from the first 2+ level to the ground state.

Several attempts have been made during the last years to solve these difficulties and we were led to consider triaxial deformations. A more general computer program has been written to carry out PHF calculations for non axially symmetric nuclei.

In the case of ¹⁰Be, an increase in binding energy of the order of 1,0 to 1,5 MeV is obtained as compared to previous (axially symmetric) calculations. This indicates that ¹⁰Be must be considered as a triaxially deformed nucleus in its low-lying states. The largest energy gain is obtained for the K = 0 L = 2 state, the smallest gain for the K = 2 L = 2 state so that the separation between these two states has become much smaller and a reasonable spin-orbit strength ξ will cause the crossing of the two levels.

* K.U. Leuven

** L.U.C. Hasselt

The $B(E2)$'s from the lower two $2+$ levels to the ground state are given in table 1 for three values of ξ . We show also for comparison, the corresponding values for the axial calculation. Satisfactory quantitative agreement with experiment is obtained in the triaxial case for $\xi = 5$ MeV.

Table 1 : $B(E2)$ values in units $e^2 \text{ fm}^4$

	Axial			Triaxial			Exp
	$\xi = 3$	$\xi = 4$	$\xi = 5$	$\xi = 3$	$\xi = 4$	$\xi = 5$	
$B(E2; 2 \rightarrow 0)$	4.25	5.76	7.00	5.76	7.42	8.42	10.4 ± 1
$B(E2; 2^* \rightarrow 0)$	7.68	6.06	4.71	5.77	3.98	2.87	

2^* means the second state with $J = 2$.

Short range correlations in light nuclei

M. BOUTEN*, M-C. BOUTEN and P. VAN LEUVEN**

In the description of light nuclei by the projected Hartree-Fock method, some discrepancies also remained in the form factors for electron scattering at large momentum transfers. In order to remedy for this, we tried to introduce correlation functions of the Jastrow type in the wave functions of the p-shell nuclei. Such correlation functions prevent the particles of coming too close to each other when repulsive nucleon-nucleon interactions are used. On the other hand, they soon become equal to unity when the distance between the particles is greater than the range of the repulsive core.

We use correlation functions of the form

$$F = \prod_{i < j=2}^N \left(1 + \lambda e^{-\left(\frac{r_{ij}}{\mu}\right)^2} \right)$$

with $r_{ij} = \left| \vec{r}_i - \vec{r}_j \right|$.

N is the number of particles; λ and μ are parameters that should be chosen in such a way that the binding energy becomes minimum.

* L.U.C. HASSELT

** R.U.C.A. Antwerp

As calculations with correlation functions are very complicated even in the case of few-nucleon systems, approximation methods have to be developed. In order to test these methods by comparison with exact calculations, we first study ${}^4\text{He}$.

In a first approach we have neglected all terms containing powers of λ greater than 4. We consider wellknown soft-core interactions such as Volkov and Brink-Boeker's forces and we calculated the binding energy for various values of the parameters

$$(0,1 \leq \mu \leq 0,9) \text{ and } (-0,05 \leq \lambda \leq -0,8).$$

We find that in the Brink-Boeker case where the repulsive core is more pronounced, the energies are very sensitive to the introduction of the short range correlations and can be lowered by several MeV. As the method seems to be promising, in a next step, we go over to an exact calculation in which all powers of λ are taken into account.

The Sp(2,R)-Model (F. ARICKX^{*}, M. BOUTEN^{**}, P. VAN LEUVEN^{*})

The results on the group theoretical structure of the ${}^8\text{Be}$ spectrum have been published. An analyse of the particle density revealed a strong α -cluster structure of the Sp(2,R)-wave functions. Hence a comparison with the α -particle model was required. This comparison showed that the Sp(2,R)-model describes better the global structure of the spectrum but is less good for the ground state band.

Generate Coordinates (L. LATHOUWERS^{*}, M. BOUTEN^{**}, P. VAN LEUVEN^{*})

Various mathematical methods for solution of the Hill-Wheeler equation have been worked-out and published. A double perturbation theory where the Hamiltonian- as well as the Overlap-kernels are perturbed, has been established and tested on the Lipkin Model. This method can be useful for the study of anharmonic effects.

* R.U.C.Antwerpen
** L.U.C.Hasselt

3. Laser Isotope Separation

P. del MARMOL, P. FETTWEIS, M. NEVE de MEVERGNIES

Various gaseous compounds absorbing the 10 micron radiation from our TEA-CO₂ laser were studied, so as to check their potentialities for the separation of the isotopes of some light elements.

SF₆

The study of the relationship between the ³⁴S isotope enrichment factor and the focal distance of the lens used to concentrate the laser beam was finalised. From these data one derives a threshold power of 26 MW/cm² for photodissociation, a mean absorption of 100 photons of 10.59 μm wavelength per ³²SF₆ dissociation, and a dependence of the enrichment factor on the 3/2 power of the laser pulse energy.

A report has been prepared for publication.

N₂F₄

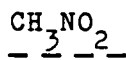
Tetrafluorohydrazine of good purity was prepared in the laboratory. Some evidence was obtained as well for photodissociation as for chemical reaction of N₂F₄ with NO under CO₂ laser pulses. However, it was not possible to obtain quantitative results due to parasitic reaction of N₂F₄ with the glass walls of the irradiation cell. A new cell is being prepared for further experimentation.

BCl₃

Some irradiation tests on boron trichloride were run. It was found that parasitic reactions occur between BCl₃ and the halocarbon grease of the stopcocks of the irradiation cell. A new cell is being prepared for further experimentation.

H₂Se

Hydrogen selenide was prepared with adequate purity in the laboratory. Photodissociation under CO₂ laser pulses is found to occur, but no isotopic selectivity was detected, even at fairly low pressures (0.5 Torr). This is probably due to the fact that the isotopic shift of H₂Se in the 10 micron absorption band is too small (less than 0.5cm⁻¹).



A study of the reaction between nitromethane and H_2 was started. It was found that under proper pressure conditions interaction occurs under focused CO_2 laser pulses. Mass-spectrometric analysis of the irradiated gas show that the main products are HCN , H_2O , H_2CO and N_2O , thus two different reaction channels seem to be open, one preserving the C-N bond, and another one breaking this bond. Spectrographic recordings of the light emitted by the reaction products were obtained and analyzed.

Further work will be done to increase the reaction probability for HCN -formation, and to check if this reaction channel has some isotopic selectivity.

4. Neutron inelastic scattering by condensed matter

Cerium hydrides

P. VORDERWISCH^{*}, S. HAUTECLER, J.B. SUCK^{**}, W.D. TEUCHERT^{**}, H. DACHS^{*},
G.G. LIBOWITZ^{***}

The crystal field splitting of the ground state $^2F_{5/2}$ of Ce^{3+} in fcc cerium hydride has been investigated using deuterated samples CeD_x with concentrations between $x = 1.94$ and $x = 2.75$. For all samples investigated three crystal field transitions are observed which cannot be explained without taking into account a non-cubic surrounding of part of the Ce ions.

The phonon dispersion curves in cerium dihydride have been obtained using a single crystalline sample of composition $\text{CeD}_{2.12}$. The experimental acoustical branches agree reasonably well with predicted

* Hahn-Meitner-Institut, Berlin

** Institut Laue-Langevin, Grenoble

*** Allied Chemical Corporation, Morristown, USA

curves obtained from a simple central force model using parameters derived from our previous analysis of neutron incoherent scattering experiments on polycrystalline samples. However, with regards to the optical branches the deviations between experimental and calculated curves are more important which means that the D-D interactions are not adequately described by the simple model.

Molecular rotations studied by neutron inelastic scattering.

W. WEGENER, J. VANDERHAEGHEN^{*}, S. HAUTECLER, L. VAN GERVEN^{**}

Previously measured quasielastic neutron spectra of ethylene-oxide clathrate have been corrected for multiple-scattering effects. Model fits to the new data showed much more clearly the consistency of the model assumed for the guest molecule reorientations (instantaneous rotational jumps). The resulting values for residence times and activation energy were essentially the same as those from uncorrected data. The low temperature inelastic spectra were interpreted in terms of transitions belonging to librations around principal molecular axes. Wall heights for a model hindering potential were derived; they agree well with results from other experimental methods. At higher temperatures the inelastic spectra could be described using rotational correlation functions.

Analog experiments have been performed with Silane (SiH_4) in the solid (plastic and crystalline) phases. The results for the plastic phase are being analysed in the same manner as those of the clathrate measurements, i.e. the quasielastic region is described in terms of rotational jumps, the inelastic region in terms of librations or correlation functions.

5. Instrumentation (P. D'HOGHE, E. MIES, L. VANSTEELANDT)

Nuclear Physics

The new apparatus for $\gamma\gamma$ -angular correlation measurements on neutron capture gamma rays is almost assembled. Several improvements have been performed at the R1 beam equipment of BR2: the fore-collimator has been checked; the collimator drum has been equipped with an automatic

* IIKW/IISN Bursar, K.U. Leuven

** K.U. Leuven

remote control and loaded with a Bi and an Fe-Al-S neutron filter; an adequate shielding has been mounted in the beam-port for attenuation of the radiation background.

The Linac apparatus for cross-section measurements was improved with a new collimation equipment. The collimator near the Linac target room is installed; the construction of the other parts is started.

Interfaces were built to link the fast FACIT reader on punch to the microprocessor HP 2112A, a magnetic tape system model 7970 A was also coupled to this microprocessor.

A study was made to connect a 2n timecoder to a Camac Crate Controller model N504.

A multiple-input mixer counting system has been tested, it operates now together with a HP 2115 A Computer and a Northern 8K ADC.

Laser isotope separation

A quadrupole mass-spectrometer (from Vacuum Generators, U.K., Mod. Q7B) was received and tested. It can be connected "on-line" with the cell containing the gas irradiated by the laser beam, thus in principle its chemical and isotopic composition can be followed under or immediately after irradiation.

A high vacuum pumping system, needed for the operation of the mass spectrometer, has been assembled and mounted near the irradiation cell of the CO₂ laser. A vacuum of better than $5 \cdot 10^{-8}$ Torr is routinely obtained.

APPENDIX I

PUBLICATIONS

NUCLEAR PHYSICS

A New Quantum Number in the description of ^8Be

F. ARICKX

Nucl. Phys. A268, 347-357 (1976)

The ^{238}U (n, α) ^{235}Th reaction with thermal neutrons

M. ASGHAR, A. EMSALLEM, R. CHERY, C. WAGEMANS, P. D'HONDT, A. DERUYTTER

Nucl. Phys. A259, 429-434 (1976)

Configuration mixing in the positive parity states of ^{182}Ta

M.K. BALODIS, M.N. PLATE, J.J. TAMBERGS, J.M. VAN DEN CRUYCE,

G. VANDENPUT, L. JACOBS, P. VAN ASSCHE

International Conference on the Interactions of Neutrons with Nuclei,
Lowell, Vol. II, 1439 (1976)

The positive parity band mixing in ^{182}Ta

M.K. BALODIS, M.N. PLATE, J.J. TAMBERGS, J.M. VAN DEN CRUYCE,

G. VANDENPUT, L. JACOBS, P. VAN ASSCHE, H.A. BAADER, H.R. KOCH,

W. DELANG, P. GOTTEL, B. HRASTNIK, H. SEYFARTH

All-Union Conference, Baku, (USSR), p. 126 (1976)

Investigation of the low-lying levels of ^{179}Hf with the (n, γ) and
(n, e^-) reactions

M. BEITINS, N. KRAMER, P. PROKOFJEV, J. TAMBERGS, L. JACOBS, G. VANDENPUT,

J.M. VAN DEN CRUYCE, P. VAN ASSCHE, D. BREITIG, H.A. BAADER, H.R. KOCH

Nucl. Phys. A262, 273-300 (1976)

How rotational are the rotational bands in light nuclei ?

M. BOUTEN, M-C. BOUTEN

Proc. Int. Symposium on Nuclear Structure, 1-6 Sept. 1975, Balatonfured,
Hungary, Ed. I. Fodor-Lovas and G. Palla, Vol. I, p. 209, Budapest (1976)

Possible perturbation of the decay rate of ^{90m}Nb by implantation in
metals

P. FETTWEIS, M. NEVE de MEVERGNIES, A. MEYKENS

Hyperfine Interactions, 2, 419-420 (1976)

Weak low energy gamma transitions in ^{182}W

A.M. HASSAN, A.A. EL KADY, N.B. ROFAIL, P. FETTWEIS

Arab Journ. Nucl. Sc. &Appl., 9, 169-174 (1976)

(n, γ)-Measurements at the Grenoble HFR

H.R. KOCH, H. BORNER, W.F. DAVIDSON, D. HECK, J.A. PINSTON, R. ROUSILLE,

P. VAN ASSCHE

International Conference on the Interactions of Neutrons with Nuclei,
Lowell, Vol. II, 1229 (1976)

A new approach to canonical orthonormalisation

L. LATHOUWERS

Int. J. Quant. Chem., X, 413-418 (1976)

APPENDIX I (continued)

A supereigenvalue problem for the solution of the generator coordinate integral equation

L. LATHOUWERS

J. Math. Phys., 17, 1274-1275 (1976)

On the limit of approximate solutions of generator coordinate integral equations

L. LATHOUWERS

J. Phys. A: Gen. Math., 9, 1235-1240 (1976)

Bi-orthonormal bases in Hilbert space

L. LATHOUWERS, in "Methods and Structure of Quantum Science", Plenum Press, New York (1976)

The generator coordinate method in a natural state formalism

L. LATHOUWERS

Ann. of. Phys., 102, 347 (1976)

Hyperfine structure constants in the Li atom by the projected Hartree-Fock method

S. LUNELL, B. LASKOWSKI, P. VAN LEUVEN

Ann. Phys., 98, 555-565 (1976)

Resonance parameters for ^{237}Np

L. MEWISSEN, A. ANGELETTI, E. CORNELIS, F. POORTMANS, G. ROHR, G. VANPRAET
H. WEIGMANN

International Conference on the Interactions of Neutrons with Nuclei, Lowell, Vol. II, 1263 (1976)

Cross sections and neutrons resonance parameters for ^{238}U below 4 keV

F. POORTMANS, E. CORNELIS, L. MEWISSEN, G. ROHR, R. SHELLEY,
T. VAN DER VEEN, G. VANPRAET, H. WEIGMANN

International Conference on the Interactions of Neutrons with Nuclei, Lowell, Vol. II, 1264 (1976)

Gamma-ray spectra of ^{44}Ca from thermal neutron capture

W. RATYNSKI, P. VAN ASSCHE, H. BORNER, W.F. DAVIDSON, J.A. PINSTON

International Conference on the Interactions of Neutrons with Nuclei, Lowell, Vol. II, 1301 (1976)

Rotations and vibrations in transitional ^{151}Sm

G. VANDENPUT, P. VAN ASSCHE, L. JACOBS, J.M. VAN DEN CRUYCE

International Conference on the Interactions of Neutrons with Nuclei, Lowell, Vol. II, 1438 (1976)

Deformed Orbitals in the Li-atom

P. VAN LEUVEN

Phys. Lett., 56A, 23-24 (1976)

Deformed atoms and the projected Hartree-Fock method

P. VAN LEUVEN, in "Methods and Structure of Quantum Science", Plenum Press, New York (1976)

APPENDIX I (continued)

Measurement and normalization of the relative ^{241}Pu fission cross-section
in the thermal and low resonance energy region

C. WAGEMANS, A. DERUYTTER

Nucl. Sci. & Engn. 60, 44-52 (1976)

The thermal neutron induced fission cross-section of ^{232}Th

C. WAGEMANS, P. D'HONDT, A. DERUYTTER, A. EMSALLEM, M. ASGHAR

Nucl. Phys., A259, 423-428 (1976)

The neutron induced fission cross-section of ^{235}U in the energy region
from 0.008 eV to 30 keV

C. WAGEMANS, A. DERUYTTER

Ann. of Nucl. Engn., 3, 437-445 (1976)

Mesuré et calcul de la section efficace de fission induite par neutrons
thermiques en dessous du seuil pour quelques noyaux lourds

C. WAGEMANS, P. D'HONDT, A. DERUYTTER, M. ASGHAR, A. EMSALLEM

Rapport BLG 514 (1976)

Spin and parity assignments of ^{93}Nb neutron resonances

J. WINTER, L. MEWISSEN, F. POORTMANS, G. ROHR, R. SHELLEY

International Conference on the Interactions of Neutrons with Nuclei,
Lowell, Vol. II, 1248 (1976).

APPENDIX I (continued)

SOLID STATE PHYSICS

Magnetic interactions in Co_3O_4

D. SCHEERLINCK, S. HAUTECLER

Phys. Stat. Sol., (b) 73, 223-228 (1976)

Reorientations of cyclic ether molecules in clathrate deuterates

J. VANDERHAEGHEN, W. WEGENER, S. HAUTECLER, E. LEGRAND, L. VAN GERVEN

Proc. of the Conference on Neutron Scattering, Gatlinburg, Tennessee, USA, June 6-10, p. 281-287 (1976).

APPENDIX II

COLLOQUIA, SEMINARS and SYMPOSIA

All-Union Conference, Baku (U.S.S.R.), 3-6.2.1976

- Determination of Gamma Energy Standards
P. VAN ASSCHE, H.R. KOCH, J.A. PINSTON, W.F. DAVIDSON and H. BORNER
- Progress in the Study of the Transitional ^{151}Sm Nucleus
G. VANDENPUT, L. JACOBS, J.M. VAN DEN CRUYCE, P. VAN ASSCHE,
T. VON EGIDY, K. SCHRECKENBACH, H.A. BAADER, D. BREITIG, H.R. KOCH
- Gamma Diffractometry at the Institut Laue-Langevin
P. VAN ASSCHE, H.R. KOCH, J.A. PINSTON, W.F. DAVIDSON, H. BORNER

Institute of Physics, Latvian SSR Academy of Sciences, Riga, 10.2.1976

- Study of some Deformed Nuclei with a Gamma Diffractometer
P. VAN ASSCHE, H.R. KOCH, J.A. PINSTON, W.F. DAVIDSON, H. BORNER

Nuclear Physics Institute, USSR Academy of Sciences, Gatchina, Leningrad
11.2.1976

- Nuclear Structure Research at the Institut Laue Langevin
P. VAN ASSCHE, H.R. KOCH, J.A. PINSTON, W.F. DAVIDSON, H. BORNER

Egyptian Society of Nuclear Sciences and Applications, Cairo, 24.2.1976

- Some Basic Remarks on Ge(Li) Detectors
P. FETTWEIS

Atomic Energy Establishment, Cairo, 2.4.1976

- Fabrication and Applications of Ge(Li) Detectors
P. FETTWEIS

Seminar on Inelastic Neutron Scattering, Delft, 5.5.1976

- Crystal Field Splitting in CeD_2
S. HAUTECLER, P. VORDERWISCH

Middle East Technical University, Ankara, Turkey, 10-13.5.1976

- Perturbation of Nuclear Decay Rates
M. NEVE de MEVERGNIES
- Separation of Isotopes by Means of Lasers
M. NEVE de MEVERGNIES
- The Decay of $^{235}\text{m}\text{U}$
M. NEVE de MEVERGNIES

Nuclear Research Center of Çekmece, Istanbul, Turkey, 14.5.1976

- Separation of Isotopes by means of Lasers
M. NEVE de MEVERGNIES

Journées d'Etude sur la Fission, Aussois, 24-26.5.1976

- Mesure et calcul de la section efficace de fission induite par neutrons thermiques en dessous du seuil pour quelques noyaux lourds
C. WAGEMANS

APPENDIX II (continued)

Algemene Wetenschappelijke Vergadering van de Belgische Natuurkundige Vereniging

Réunion Scientifique Générale de la Société Belge de Physique

Ottignies, 3-4.6.1976

- Crystal Field Effects Investigation in CeD_2 by Inelastic Neutron Scattering

S. HAUTECLER, P. VORDERWISCH

- Effets géométriques dans la photodissociation isotopiquement sélective de SF_6 par laser CO_2 pulsé

M. NEVE de MEVERGNIES, P. FETTWEIS

- Onderzoek van door-thermische neutronen in ^{237}Np geïnduceerde fissie
C. WAGEMANS, P. D'HONDT, A. DERUYTTER, M. ASGHAR, A. EMSALLEM

- Studie van de reakties ^{237}Np (n, α) en ^{238}U (n, α)

P. D'HONDT, C. WAGEMANS, A. DERUYTTER, A. EMSALLEM, R. CHERY

- Resonance Parameters for ^{238}U

F. POORTMANS, E. CORNELIS, L. MEWISSEN, G. ROHR, R. SHELLEY,
T. VAN DER VEEN, G. VANPRAET, H. WEIGMANN

Conference on Neutron Scattering, Gatlinburg (Tenn. USA), 6-10.6.1976

- Reorientations of Cyclic Ether Molecules in Clathrate Deuterates

J. VANDERHAEGHEN, W. WEGENER, S. HAUTECLER, E. LEGRAND, L. VAN GERVEN

National Research Council of Canada, Division of Chemistry,

Ottawa, 13.6.1976

- Molecular Motions in Clathrates Studied by Quasielastic Neutron Scattering

W. WEGENER

National Bureau of Standards, Washington, 2.7.1976

- Nuclear Gamma Ray Spectra Calibration Problems

P. VAN ASSCHE

Sagamore V Conference on Charge Spin and Momentum Density,

Helsinki (Finland), 25-30.8.1976

- Spin and Symmetry Projection in HFS Calculations

S. LUNELL, P. VAN LEUVEN

2nd International Conference on Crystal Field Effects in Metals and Alloys, Zürich, 1-4.9.1976

- Neutron Spectroscopy of the Crystal Field Splitting in Cerium Hydride

P. VORDERWISCH, S. HAUTECLER, J.B. SUCK, H. DACHS

Future of Quantum Chemistry, A Symposium in Honour of P.O. Löwdin,

Dalseter (Noorwegen), 1-6.9.1976

- Deformed Orbitals and PHF (Invited Talk)"

P. VAN LEUVEN

- Optimal Properties of Canonical Orthonormalisation

L. LATHOUWERS

APPENDIX II (continued)

Quantum Chemistry Group, University of Uppsala (Sweden), 17.11.1976

- Perturbation Theory for Generalised Eigenvalue Problems
L. LATHOUWERS

Information Meeting on Research with BR2 Neutron Beams, Mol, 24.11.1976

- Reactor Neutron Beams
M. NEVE de MEVERGNIES
- Neutron Spectrometers
F. POORTMANS
- Neutron Capture Gamma Ray Spectroscopy with Ge(Li) Detectors
P. FETTWEIS
- Neutron Capture Gamma Ray Spectroscopy with a Bent Crystal
Diffractometer
L. JACOBS
- Fission Experiments
C. WAGEMANS
- Inelastic Neutron Scattering Studies with a Time-of-flight
Spectrometer :
 1. Lattice Dynamics; Atomic Spectroscopy in the Solid State;
Molecular Motions in Adsorbed Gases and in Liquids
S. HAUTECLER
 2. Molecular Motions in Plastic Crystals and in Clathrates;
Spin Dynamics
W. WEGENER

Quantum Chemistry Group, University of Uppsala (Sweden), 2.12.1976

- To Cross or not to Cross... Some Recent Results on the Non-Crossing
Rule
L. LATHOUWERS

University of Aarhus (Denmark), 16.12.1976

- Survey of the Generator Coordinate Method
L. LATHOUWERS

University of Münster (West Germany), 17.12.1976

- Survey of the Generator Coordinate Method
L. LATHOUWERS

APPENDIX III

THESES

The Sp (2,R) Model and its Application to ^8Be
F. ARICKX (V.U.B.)
Doctor in de wetenschappen - V.U.B.

The Mathematical Foundations of the Generator Coordinate Method
for Bound States
L. LATHOUWERS (V.U.B.)
Doctor in de Wetenschappen - V.U.B.

De laag-energetisch structuur van de overgangskern ^{151}Sm : Kwasi-
deeltjesexcitaties, kollektieve rotaties, kwadrupoolvibraties en hun
interakties
G. VANDENPUT (K.U.L.)
Doctor in de Wetenschappen - K.U. Leuven

APPENDIX IV

SEMINARS HELD AT S.C.K./C.E.N.

A. By S.C.K./C.E.N. Personnel

10-11.3.1976

Introduction to Quantum Mechanics

M. BOUTEN, P. VAN LEUVEN

2.4.1976

Electron Scattering from Nuclei

M. BOUTEN

7.4.1976

Interlude on Experimental Methods

G. VANPRAET

21.4.1976

The Nuclear Shell Model

M. BOUTEN

28.4.1976

The Nuclear Collective Model

P. VAN LEUVEN

5.5.1976

Towards a Unified Theory

P. VAN LEUVEN

25.5.1976

Rotaties en vibraties in de overgangskern ^{151}Sm

G. VANDENPUT

13.7.1976

Recent Progress in laser isotope separation

M. NEVE de MEVERGNIES

7.10.1976

Investigation of some aspects of thermal neutron induced sub-barrier fission

C. WAGEMANS

B. By Guest Speakers

3.2.1976

Neutron beam research at the I.L.L.

R.L. MOSSBAUER (I.L.L. Grenoble)

25.3.76

Nonuniform states of liquid helium

C. GARROD (Univ. of California, Davis, USA)

B. By Guest Speakers (continued)

24.11.1976

- Technical and industrial applications of neutrons
C. WEITKAMP (G.K.S.S. mbH. Geesthacht)
- Standard fission cross section measurements
E. WATTECAMPS (C.B.N.M. Euratom Geel)
- Survey of the neutron beams and their applications around Cyclone
J.P. MEULDERS (U.C.L.)
- Theory of inelastic neutron scattering in solids
K. MICHEL (U.I.A. and Univ. Saarbrücken)
- Biological applications of thermal neutron scattering
D.L. WORCESTER (A.E.R.E. Harwell, U.K.)
- Chemical research with neutrons
J.W. WHITE (Associate Director I.L.L., Grenoble, France)

APPENDIX V

External Relations

P. FETTWEIS, Jan. 13 - April 12, 1976.

Field mission as an IAEA-expert in Nuclear Science and Engineering at the Reactor and Neutron Physics Department of the Nuclear Research Center, Atomic Energy Establishment, Cairo, Egypt.

P.H.M. VAN ASSCHE, March 1974 - July 1976

Part-time group leader at the German-British-French High-Flux Reactor Institute in Grenoble.

List of the members and guests of the
NEUTRON PHYSICS DEPARTMENT
for 1976

Staff members

CEULEMANS, Hugo *
BOUTEN-DENYS, Marie-Claire
Jel MARMOL, Patrick
D'HOOGE, Paul
FETTWEIS, Paul
HAUTECLER, Serge
MEWISSEN, Louis
MIES, Edward
NEVE de MEVERGNIES, Marcel
(Department Head)
POORTMANS, Freddy
VAN ASSCHE, Piet
VANSTEELANDT, Lionel
WEGENER, Wolter

Technical and Administrative Support

BROUWERS, Jan
COSTERS, Fernand
DE WINTER-DELEN, Julienne
GERARD, Arlette
GOOS, André
GOOSSENS, August
MACHIELS, Jos
PAGGERS, Jacques
VAN DER VEKEN, Robert
VAN DE WATERING- DE CORTE, Germaine
VAN VELTHOVEN, Frans
VERMEULEN, Louis

Guest Scientists

ARICKX, Frans (RUCA, Antwerp)
BOUTEN, Marc (L.U.C., Hasselt)
CODDENS, Gerrit (IWONL/IRSI bursar, R.U. Gent)
CORNELIS, Etienne (RUCA, Antwerp)
DEHAES, Jean-Claude (U.L.B. Brussels)
FLERACKERS, Eddy (L.U.C. Hasselt)
JACOBS, Ludo (IIKW/IISN, K.U.L., Leuven)
LATHOUWERS, Luc (RUCA, Antwerp)
VAN DEN CRUYCE, Jean-Marie (IIKW/IISN, K.U.L., Leuven)
VANDENPUT, Gilbert (IIKW/IISN, K.U.L., Leuven)
VANDERHAEGHEN, Jacques (IIKW/IISN bursar, K.U. Leuven)**
VAN LEUVEN, Piet (RUCA, Antwerpen)
VANPRAET, Georges (RUCA, Antwerp)
WAGEMANS, Cyriel (NFWO/FNRS, R.U. Gent)
WEGENER-PENNING, Gerda (SCK/CEN trainee).

* moved to the Division "Applied Research" on 1/11/1976.

** also guest of the Materials Study Department of CEN/SCK.



GHENT STATE UNIVERSITY

NUCLEAR PHYSICS LABORATORY
LABORATORIUM VOOR KERNFYSICA

ANNUAL REPORT 1976

INTRODUCTION

Beginning 1976 the new set-up of the linear electron accelerator has been thoroughly checked. Measurements have been performed between 10 MeV and 70 MeV electron-energy. The guaranteed values for the CGR MeV sections were obtained: 50% of an accelerated pulse current of 200 mA, passing through a slit system, defining the energy to $\pm 0.5\%$ at 60 MeV.

The machine was used for our programmes in photofission, photonuclear reactions, nuclear spectroscopy and dosimetry. Our programme in positron annihilation studies was continued. Several studies in connection with our programme have been performed in collaboration with other laboratories (ILL Grenoble; SCK-CEN Mol; NRC, Ottawa; Université de Lyon; Stony Brook, New York; Orsay). The status of the development of these programmes is described in the present report. A publication list is joint to the report and more detailed information on the research-status can be obtained by contacting our laboratory: Nuclear Physics Laboratory, Proeftuinstraat 86 B 9000 Gent (Belgium).

The reported research has been made possible by the substantial help of the IIKW (Interuniversity Institute for Nuclear Sciences, Brussels). We want to thank this institute and its "Committee for low energy nuclear physics" for this support.

Prof. Dr. A.J. Deruytter.

Director of the Nuclear Physics
Laboratory.

Table of contents

	Page
1. Linear Accelerator	47
1.1. Linac Operation	47
1.2. Linac Radioactivity Control - Radiation monitoring	49
2. Fission Studies and (n_{th}, α) Measurements	51
2.1. Introduction	51
2.2. Experimental arrangements and techniques	51
2.2.1. Extension of the PDP-11 data handling system	51
2.2.2. Other experimental arrangements	52
2.3. Study of the photofission of ^{235}U and ^{238}U	53
2.3.1. The photofission of ^{235}U and ^{238}U with 25 MeV bremsstrahlung	53
2.3.2. Photofission of ^{235}U and ^{238}U at different excitation energies of the compound nucleus	56
2.4. Measurement of short-lived fission products produced in photofission	56
2.5. Study of long-range α 's emitted in ternary fission	57
2.6. β -decay of ^{118g}In and ^{118}Sb to excited states of ^{118}Sn	57
2.7. Short-lived isomers (micro- and millisecon) in fission products	59
2.8. Study of some characteristics of the thermal neutron induced sub-barrier fission of ^{231}Pa , ^{232}Th and ^{237}Np	59
2.9. Scattering of fission fragments	60
3. Photonuclear Reactions	63
3.1. Introduction	63
3.2. The total $^{208}\text{Pb}(\gamma, n)$ cross section	63
3.3. Photoneutron energy spectra experiments	64
3.3.1. Bremsstrahlung spectra at 17 and 18 MeV endpoint energy	64
3.3.2. The $^{19}\text{F}(\gamma, n)$ reaction	65
3.3.3. Study of the 90° photoneutron spectrum from ^{89}Y	65
3.3.4. Photoneutron angular distributions for ^{208}Pb	68
3.4. Photoproton spectra and angular distributions	69
3.4.1. The $^{12}\text{C}(\gamma, p)$ reaction	69
3.4.2. Structure in the photoproton cross section of ^{16}O	70
3.4.3. Preliminary results on the $^{19}\text{F}(\gamma, p)$ reaction	73
3.4.4. Study of the $^{89}\text{Y}(\gamma, p)^{88}\text{Sr}$ reaction in the G.R. region	75

3.5.	The $^{12}\text{C}(\gamma, n\alpha)^7\text{Be}$ reaction	76
3.6.	Positron production and acceleration	78
4.	Nuclear Spectroscopy and Positron Annihilation	79
4.1.	First test on the anti-compton spectrometer	79
4.2.	Measurement of the angular shapefactor in deformed copper	79
4.3.	Measurement of the Doppler-broadened positron annihilation lineshape in Indium	80
4.4.	The effect of thermal expansion on the Doppler-broadened positron annihilation lineshape factor	82
4.5.	Electro-optical stabilisation of the positron annihilation life-time equipment	83
4.6.	Positron annihilation study of neutron-irradiation induced voids in Aluminium	85
5.	Dosimetry	87
5.1.	Cavity theory and related transport problems	87
5.2.	Calorimetry	88
5.3.	Film dosimetry	88
5.4.	Chemical dosimetry	88
5.5.	Atmospheric pollution of ^{85}Kr	90
5.6.	Nuclear energy	94
6.	Nuclear theory	95
6.1.	Coexistence of spherical and deformed states near closed shells	95
6.1.1.	Unified description of odd-mass In nuclei	95
6.1.2.	$J^\pi = 9/2^+$ deformed states in odd-mass Sb, I nuclei	99
6.1.3.	Anharmonicities in N=81, 83 isotones	101
6.2.	Magnetic moment of the isomeric $J^\pi = 6^+$ level in ^{134}Te	102
6.3.	Study of isobaric analog resonances (IAR) in fp-shell nuclei	103
6.4.	Microscopic nuclear structure calculations with effective three-body forces	104
6.4.1.	Removal of shortcomings of the Skyrme force by addition of a momentum dependent three-body interaction	104
6.4.2.	Self-consistent treatment of pairing correlations with effective three-body forces	105
6.5.	Dissipation in quantum mechanical systems with inclusion of collective motion	109
	Publications by members of the Laboratory-1976	111
	Publications in print	114
	Conference or symposia contributions	116

1. LINEAR ACCELERATOR

1.1. Linac Operation

(K.Kiesel , W.Mondeleers)

After the reconstruction of the linear electron accelerator of the Nuclear Physics Laboratory of the Ghent State University at the end of 1975, the first electrons were accelerated in the renewed machine the very last days of the same year.

January 1976 was mainly used for the "aging" of the tubes in the modulators and the outgassing of the new waveguides and sections under RF-power.

In February, the guaranteed values for the CGR-MeV-sections were obtained: 50% of an accelerated pulse current of 200 mA, passing through a slit-system, defining the energy to $\pm 0,5$ % at 60 MeV.

The first experiments with the new set-up of the machine started in March, although at a low repetition-rate of 50 Hz, due to the remaining outgassing.

In April and May, the repetition-rate was gradually increased from 50 Hz to 100 Hz, 150 Hz and finally to the maximum of 300 Hz.

From June on, the accelerator became fully operational. Experiments have been running at energy-levels as low as 10 MeV and up to 70 MeV, but the machine has been tested at even lower and higher levels.

During the year 1976, a total of 2376 h machine-time has been realised (see fig.1).

LINAC OPERATION DURING 1976

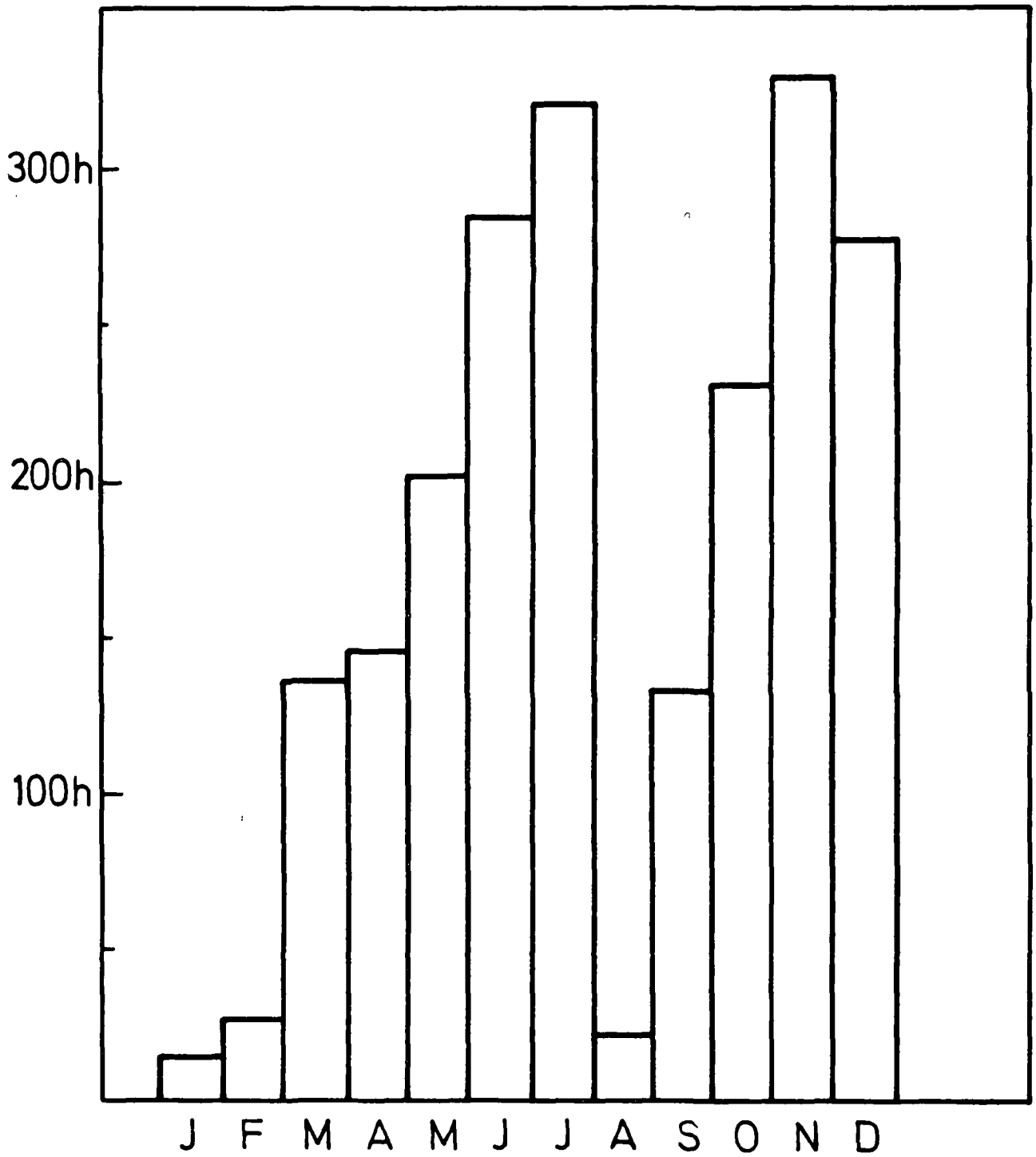


Fig.1. Distribution of linac operating time during 1976.

1.2. Linac Radioactivity control - Radiation monitoring

(M.Dorikens)

The radioactive level around the linear electron accelerator and the deflection system has been controlled weekly. The measurements were performed on Mondays, i.e. approximately 60 hours after the last acceleration, in order to determine the activities with lifetimes longer than 1/2 day, and to monitor the long-term build-up of activities.

In the accelerator bunker, the magnetic switchyard, the target hall, the modulators, the accelerator hall, a total of 96 control points were indicated by numerals (also to be found on the ground-plan of the hall). The activity at the 36 most important of these points was followed weekly (the other points presenting negligible radiation hazards). The measured activity exceeds 2.5 mR/hr at 8 measuring points only. These are illustrated in fig.2 ; their location is indicated in table 1.

All activities are given in mR/hr. The measuring instrument was a Nardeux Babyline 61 beta-gamma monitor. The peaks in the activities are due either to proceeding long irradiation periods (e.g. 3 days on a 24 hour schedule) or to high energy irradiations (above 30 MeV). An upper limit for continuous irradiations at 70 MeV is to be set as not exceeding 2 days. The activity of the slit on channel east (measuring point 35) has to be followed carefully since the increasing level may cause difficulties if replacement should become necessary.

Table 1.

Location of the most important measuring points	
12	entrance of acceleration section II
16	collimator after section II
25	entrance of magnetic switchyard
26	magnet West 1
27	magnet West 2
29	magnet East 1
32	window direct beam
35	slit channel East

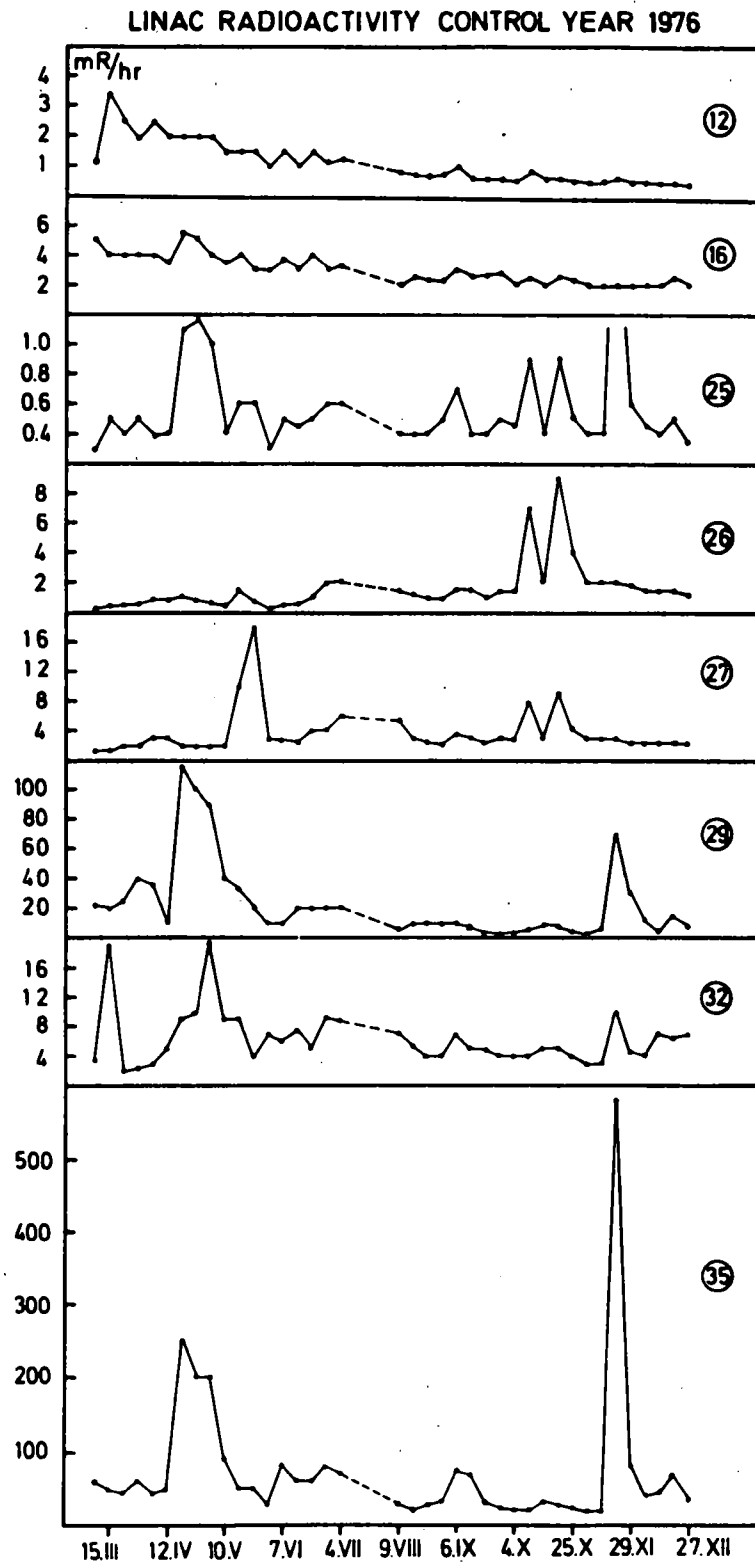


Fig.2. Radioactivity at 8 different locations around the linac as measured weekly.

2. FISSION STUDIES AND (n_{th}, α) MEASUREMENTS

(E.Jacobs, D.De Frenne, A.De Clercq, H.Thierens, P.D'hondt,
P.De Gelder, C.Wagemans* and G.Coddens**)

2.1. Introduction :

During 1976 the experimental arrangements and techniques, especially the data handling system based on a PDP 11, were extended. The data obtained in 1975 on the photofission of ^{235}U and ^{238}U with 25 MeV bremsstrahlung were published together with some additional information obtained in 1976. The decay of $^{118\text{g}}\text{In}$ was studied in collaboration with K.Heyde. Tests to use a particle identification system for the study of long range α ternary fission and tests to extend the study of the yields of fission products to short-lived isotopes were performed. The study of the photofission of ^{235}U and ^{238}U as a function of the bremsstrahlung endpoint energy was started. Catcher foil measurements were performed with 12, 15, 20, 30 and 70 MeV bremsstrahlung. In collaboration with J.Uyttenhove (Laboratorium voor Natuurkunde-Groep II, RUG) some preliminary tests to study milli-and(or) microsecond isomers in the fission products obtained in the photofission of ^{238}U were done. Results on the thermal neutron induced fission of ^{231}Pa , ^{232}Th and ^{237}Np were obtained and some preliminary measurements were performed on ^{40}K , ^{209}Bi , $^{235}\text{U}(n_{th}, \alpha)$ reactions by C. Wagemans and P.D'hondt at the ILL-Grenoble. Scattering of fission fragments was studied by C.Wagemans and G.Coddens at a neutron beam of the BR2 at the SCK/CEN-Mol.

2.2. Experimental arrangements and techniques

2.2.1. *Extension of the PDP 11 data handling system*

The existing system was extended with a Hewlett-Packard HP1317A

* NFWO, University of Ghent and SCK/CEN-Mol

** IWONL, University of Ghent and SCK/CEN-Mol

display . A system to multiplex two 4096 channels ADC data (12 bit) into one 13 bit data channel (the 13th bit identifying the ADC) was constructed. This allows the two ADC's to work in one single memory increment DMA channel. A Camac module used as a scaler (in photonuclear reaction experiments or in experiments on short-lived isomers) or to indicate the linac status (beam ON-OFF) in photofission experiments, was constructed. A plotter interface, allowing the control of the CALCOMP plotter of the PDP-15 system, with the PDP-11 system using the DL 11 asynchronous serial line interface, was built.

PHA4M, an extension of the existing linear PHA4K program, was written. It provides the possibility to measure simultaneously two spectra of 4096 channels, each containing 2^{24} ($\sim 16 \cdot 10^6$) counts. The linac status (beam ON-OFF) can be indicated, allowing registration of γ -ray spectra of irradiated samples at predefined time intervals relative to the irradiation time. For reasons of limited memory the program is written in different overlay disk resident segments.

PHAFR, a version of PHA4K includes the possibility to register the charge collected in an ionization chamber, produced by the brems - strahlungsbeam. It is used e.g. in photonuclear reaction work.

2.2.2. Other experimental arrangements

The γ -ray spectra of the fission products, caught in Al catcher foils, are analyzed on a PDP-15 system using the standard program GASPAN. A modification of this program is planned and studies for this purpose were started.

The technique of chemical separation of Cd from the fission products caught in an Al foil or in an $\text{UO}_2(\text{NO}_3)_2 \cdot 6\text{H}_2\text{O}$ target, based on the method of C.Gleit and C.Coryell [*Phys.Rev.*135, B9(1964)], was adapted to our experimental conditions by J.Buysse.

For dual parameter experiments performed outside our laboratory (i.e measurements in the SCK/CEN-Mol of ILL-Grenoble), a data recording system based on a Philips digital incremental cassette recorder was built. The necessary electronic equipment was constructed. The system is suited for low count rates (up to 75 data pairs per sec). A simple check of the data during the experiments is possible. After the measurements the data are handled by the PDP 11 - PDP 15 systems of the laboratory.

The required software for an INTEL 8080 microprocessor to compile

and write programs into PROMS by means of the PDP-15 was written in FORTRAN IV. Some expected applications are : read-out of a digital voltmeter, read-out of the data registered using the previously described digital cassette recorder system, automatization of a fast rabbit system, construction of a low count-rate PHA system coupled to the PDP-11.

2.3. Study of the photofission of ^{235}U and ^{238}U

2.3.1. *The photofission of ^{235}U and ^{238}U with 25 MeV bremsstrahlung*

For these experiments the bremsstrahlung was produced by 25 MeV electrons in a 0.5 mm thick tungsten target followed by 10 cm graphite. We studied the kinetic energy distribution of the fragments and the provisional and post neutron mass distributions. From independent yield measurements we deduced most probable charges and from measured isomeric ratios, average primary fragment spins were calculated (see annual report 1975).

Starting from the measured provisional and post neutron mass distributions, the neutron emission curve, $\nu(m^*)$, is calculated by applying a method similar to the method described by J. Terrell [Phys. Rev. 127, 880(1962)]. As a test of the procedure the provisional and post neutron mass distributions for the spontaneous fission of ^{252}Cf and for the thermal neutron induced fission of ^{235}U were measured with the same experimental set-up and procedure as for the photofission of ^{235}U and ^{238}U . The neutron emission curve is calculated and compared to the directly measured curves. In fig.3 the obtained neutron emission curve, $\nu(m^*)$, as a function of the pre-neutron mass for ^{252}Cf s.f. and $^{235}\text{U}(n_{\text{th}}, f)$ is compared to the results of other authors [Bowman et al., Phys. Rev. 129, 2133 (1963); Signarbieux et al., in Proceedings of the Symposium on Physics and Chemistry of Fission, Rochester 1973- IAEA, Vienna 1974, Vol II p.179; Apalin et al., Nucl. Phys. 55, 249(1964); Maslin et al., Phys. Rev. 164, 1520 (1967)]. In fig.4 the neutron emission curve as a function of the pre-neutron fragment mass, for the photofission of ^{235}U and ^{238}U with 25 MeV bremsstrahlung, is shown. In both figures the full circles indicate the error bars on the calculated $\nu(m^*)$ values.

The $\nu(m^*)$ curves show the typical saw-tooth structure, indicating that fragment shell effects play an important role in the photofission of

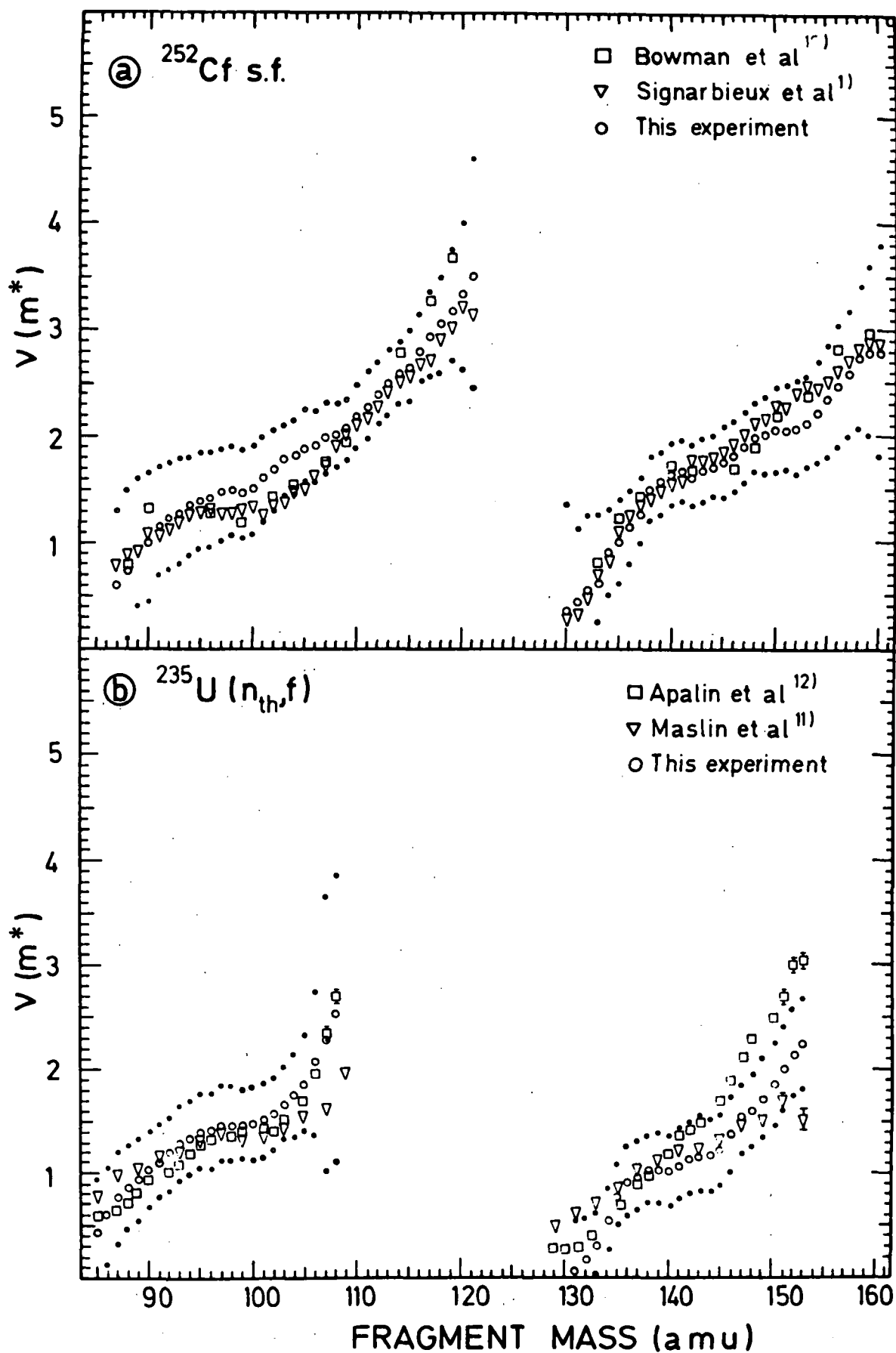


Fig.3. Neutron emission curve $v(m^*)$, as a function of the pre-neutron mass for (a) $^{252}\text{Cf s.f.}$ and (b) $^{235}\text{U}(n_{th}, f)$. The full circles indicate the error bars on the calculated $v(m^*)$ values.

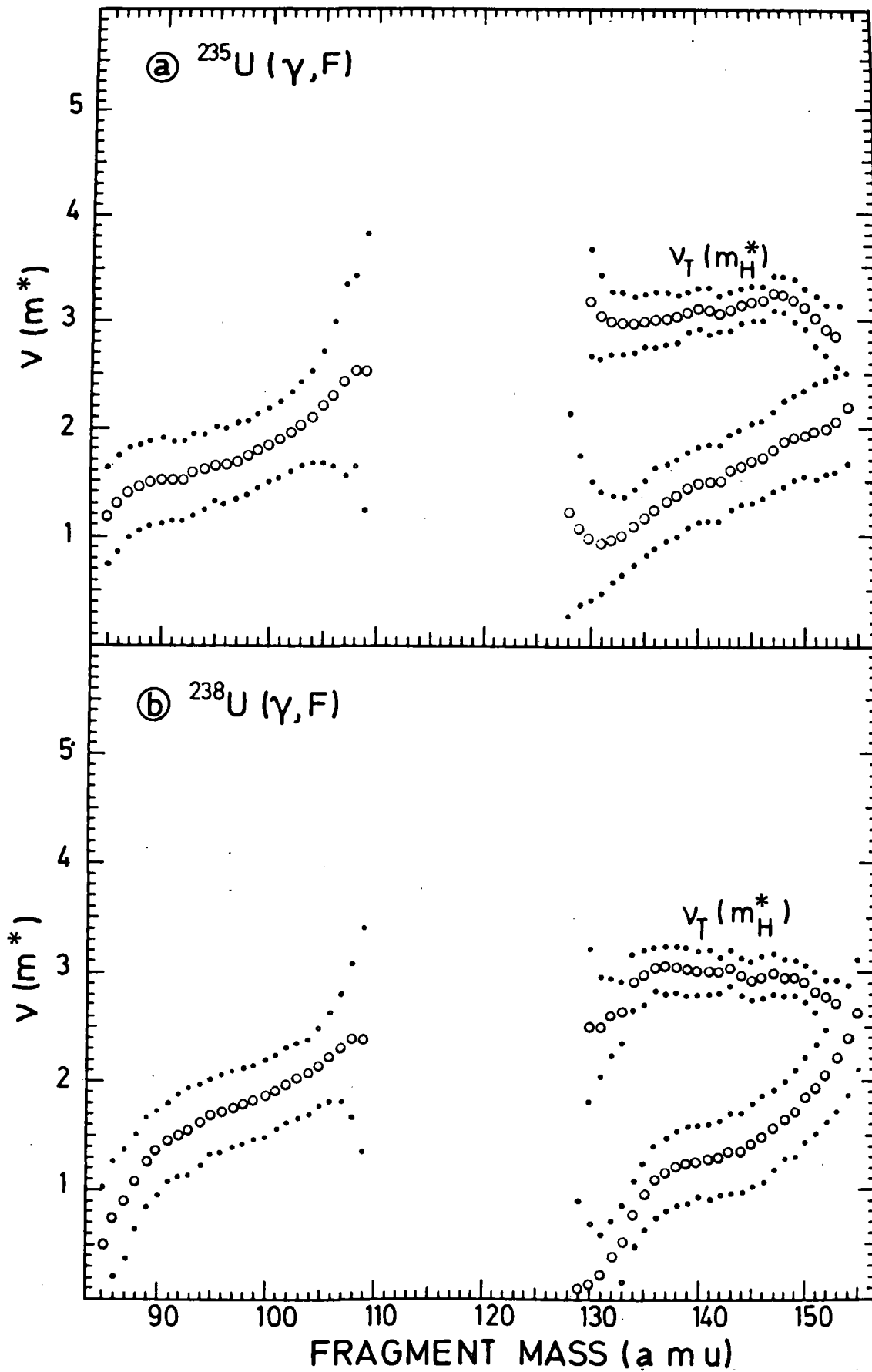


Fig.4. Neutron emission curve $v(m^*)$, as a function of the pre-neutron fragment mass for the photofission of (a) ^{235}U and (b) ^{238}U with 25-MeV bremsstrahlung. The full circles indicate the error bars on the calculated $v(m^*)$ values.

^{235}U and ^{238}U with bremsstrahlung in the mentioned energy region.

2.3.2. Photofission of ^{235}U and ^{238}U at different excitation energies of the compound nucleus

In order to have the possibility to calculate the average excitation energy of the compound nucleus one must know the shape of the bremsstrahlung spectrum for a given energy of the incident electrons. For this purpose we use in these experiments a 0.1 mm thick gold target, followed by a cleaning magnet, to produce the bremsstrahlung. The deflected electrons are caught in a watertank (see annual report 1975).

In these experiments we intend to study the variation of the different fission characteristics mentioned in 2.3.1. (kinetic energy of the fragments, mass distribution, independent yields, isomeric ratios) for photofission induced by bremsstrahlung with different end-point energies. Catcher foil measurements were performed for 12, 15, 20, 30 and 70-MeV bremsstrahlung. The fission product yield for photofission induced with 10-MeV bremsstrahlung is too low in our experimental conditions to obtain a reliable result. These results are not yet fully analyzed.

2.4. Measurement of short-lived fission products produced in photofission

Assuming that the charge distribution for a given mass chain has the form,

$$P(Z) = \frac{1}{\sqrt{\pi c}} e^{-\frac{(Z - Z_p)^2}{c}}$$

not only the most probable charge (Z_p) for this mass chain, but also the width parameter (c) of the charge distribution can be calculated if one knows the fractional independent yield for at least two different isotopes of this mass chain. By studying short-lived fission products together with the longer-lived products (as done in our previous studies - see e.g. 2.3.1. and annual report 1975) the fractional independent chain yields for two or more different isotopes in a given mass chain can be obtained.

An ^{238}U target, followed by a catcher foil was irradiated during 5 min with 25 MeV bremsstrahlung. Starting 2 min and 7 min after the end of the irradiation two successive γ -ray spectra of the Al foil are measured

during 5 min each. For example the independent yield of ^{136}I is obtained from this experiment, while the independent yield of ^{136}Cs can be obtained from previous measurements. However, until now only very preliminary results from this experiment are available.

2.5. Study of long-range α 's emitted in ternary fission

From previous tests concerning the study of photon induced ternary fission we observed that the long-range α spectrum is deformed by the presence of protons produced by (γ, p) reactions (see annual report 1974). To distinguish between protons and α particles we intend to use a $\Delta E - E$ particle identification system.

As a preliminary test the light particles emitted in the spontaneous fission of ^{252}Cf were studied, using a 50 μm thick ΔE detector followed by a 500 μm thick E detector. Three groups of light particles (^6He , ^4He and a light group including protons) could easily be identified.

Further development of the method will make possible to identify the different light particles, emitted in ternary fission.

2.6. β -decay of ^{118g}In and ^{118}Sb to excited states of ^{118}Sn

(In collaboration with K. Heyde)

The ^{118g}In activity was obtained by chemical separation of the parent nucleus ^{118}Cd from an $\text{UO}_2(\text{NO}_3)_2 \cdot 6\text{H}_2\text{O}$ sample, irradiated with 25 MeV and 50 MeV bremsstrahlung. Two successive Ge(Li) γ -ray spectra were measured. Several new γ -rays were found and the relative intensities of the known γ -lines are compared and discussed with respect to the existing data. Levels in ^{118}Sn at 0, 1229.64, 1757.8, 2043.1, 2056.5, 2326.5, 2402.5 and 3137.2 keV were found to be fed in the β^- decay of ^{118g}In . Based on the measured post neutron yields of the masses 111, 112, 113, 115, 117, 123 and 125 for the photofission of ^{238}U with 25 MeV and 50 MeV bremsstrahlung, the post neutron yield of mass 118 was obtained by interpolation, assuming a smooth behaviour of the mass distribution in this region. Herefrom the absolute intensity of the observed γ -lines could be determined. Intensities for all β branches and corresponding logft values were calculated. In fig.5 we show the decay scheme of ^{118g}In according to our experimental results. The γ -ray intensities are given

$1 + 0.0 \ 505$
 $^{118}_{49}\text{In}$
 $Q^- = 4.200$

$1 + 0.0$
 $^{118}_{51}\text{Sb}$
 $Q^+ = 3695$

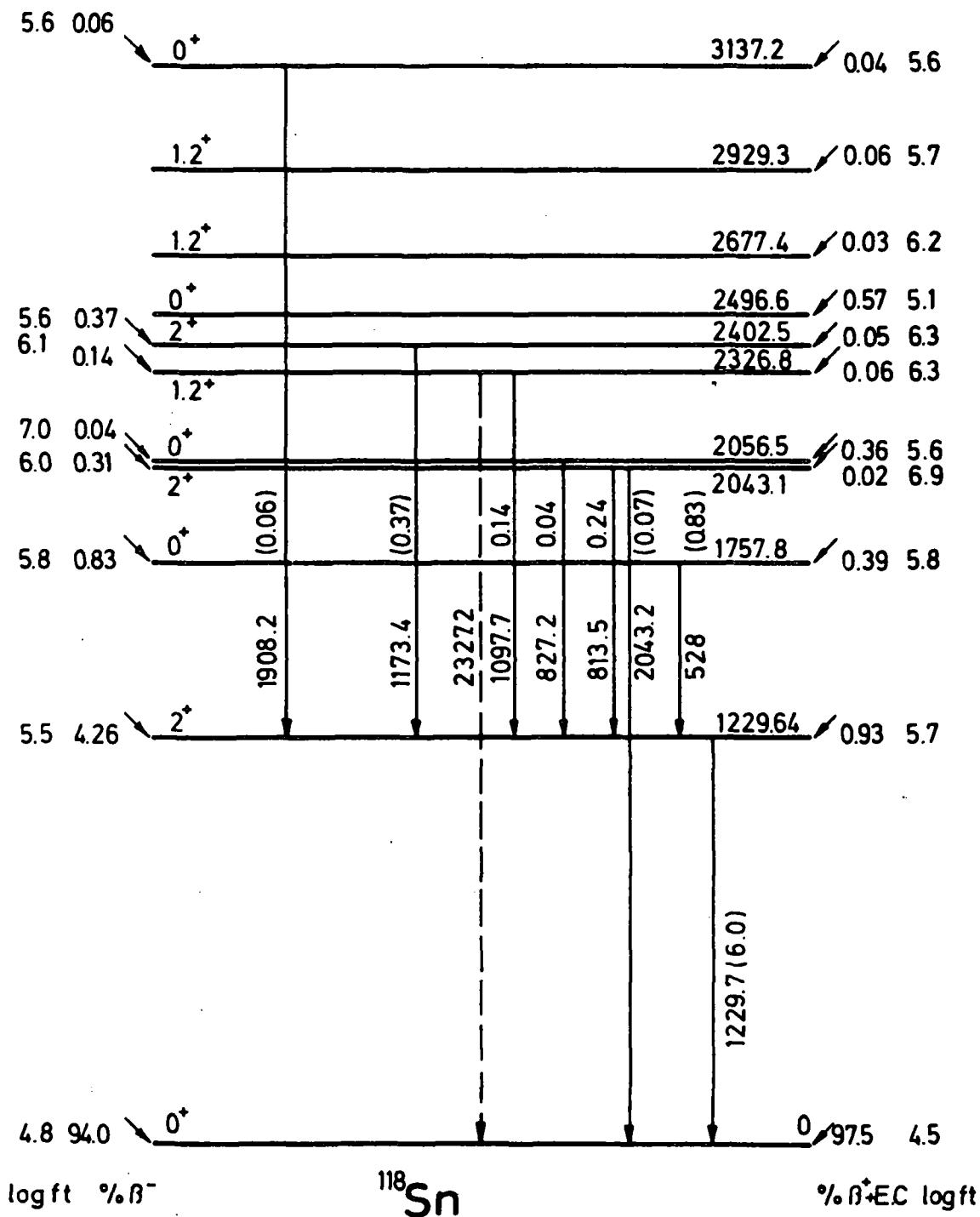


Fig. 5. Decay scheme of ^{118g}In . The γ -ray intensities are given per hundred ^{118g}In decays.

per one hundred ^{118g}In decays. The level energies, the I^π values and the β decay data for ^{118}Sb are taken from Carlson et al. [Nuclear Data Sheets 17, 1 (1976)].

The results of this study differ considerably from those known from the literature. The β -decay rates for ^{118g}In and ^{118}Sb are compared with results of nuclear structure calculations. The systematics of $\log ft$ values for the $1g_{9/2} \rightarrow 1g_{7/2}$ Gamow-Teller β -decay is correlated with the filling of the $1g_{7/2}$ neutron single particle orbit for increasing A.

2.7. Short-lived isomers (micro-and millisecon) in fission products

(In collaboration with J.Uyttenhove and B.Proot)

Using the apparatus developed by J.Uyttenhove for studying micro-and millisecond isomeric states produced in (γ, n) and (γ, p) reactions (see e.g. annual report 1974) preliminary tests were performed to observe isomers in the products of the photofission of ^{238}U with 50 and 70 MeV bremsstrahlung. Indications of isomers with a half-life of the order of 100 μs were obtained.

2.8. Study of some characteristics of the thermal neutron induced sub-barrier fission of ^{231}Pa , ^{232}Th and ^{237}Np

(Experiments by C.Wagemans and P.D'hondt at the ILL-Grenoble)

Some characteristics of the thermal neutron induced fission of ^{231}Pa , ^{232}Th and ^{237}Np were studied using a highly pure thermal neutron beam of the Grenoble High Flux Reactor. Thermal neutron induced fission cross-sections of (20 ± 4) mb for ^{237}Np , (19 ± 4) mb for ^{231}Pa and smaller than 2.5 μb for ^{232}Th were obtained. This is in agreement with calculations based on a double humped fission barrier. Also a mean total fission fragment kinetic energy of (172.8 ± 2.5) MeV was determined for ^{237}Np , which fits into the semi-empirical systematics of \bar{E}_K versus $Z^2/A^{1/3}$, as illustrated in fig.6. The indicated errors are relative for the data of Unik et al. [in Proc. 3rd Symp. on Physics and Chemistry of Fission, Rochester 1973 (IAEA-Vienna, 1974) p.19] and absolute for ours.

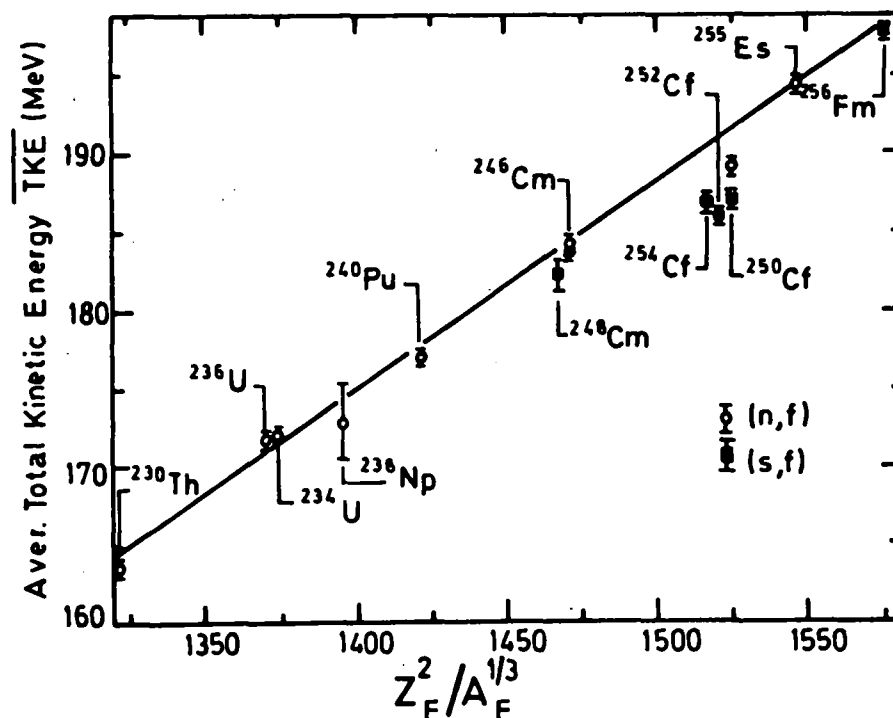


Fig.6. Average total fission fragment kinetic energy \bar{E}_K as a function of $Z_F^2/A_F^{1/3}$. The indicated errors are relative for the data of Unik et al. and absolute for ours.

Finally, we determined $LR\alpha/B$ ratios of $(1.94 \pm 0.17) \cdot 10^{-3}$ for ^{237}Np and of $(1.67 \pm 0.11) \cdot 10^{-3}$ for ^{231}Pa , in disagreement with the theoretical predictions of N:Feather [Proc.R.S.E.(A) 69, 335(1972)], but consistent with the semiempirical systematics of I.Halpern [Ann. Rev. of Nucl.Sc.21,245(1971)]. The $LR\alpha$ yields can be discussed in terms of the sub-barrier superfluid and above-barrier viscous fission modes.

2.9. Scattering of fission fragments

(Experiments by C.Wagemans and G.Coddens at the SCK/CEN-Mol)

The experimental set-up to investigate the scattering of fission fragments (produced by the reaction $^{235}\text{U}(n_{\text{th}}, f)$ at BR2) on different scatter-

ring materials, was constructed. Eight 50 mm² Si-Au surface-barrier detectors were mounted in a vacuum reaction chamber at different angles (θ). The eight pulse height spectra are simultaneously detected and registered. Fig.7 shows the experimental set-up.

This experimental arrangement enables the measurement, with good resolution, of the angular distribution and the energy distribution of the fission fragments (scattered fragments as well as direct ones) as a function of the Z-value of the scattering material. In a scattering experiment (respectively a direct measurement) the ²³⁵U layer is turned to the scattering material (respectively to the detectors).

In preliminary measurements the background was minimized and the most favourable geometry and reproducibility were selected.

A first series of experiments with gold as a scattering material yielded interesting results. The total fraction of scattered fission fragments was about 1%. It appears that the scattering is strongly angular dependent. In addition an important energy loss was observed at small scattering angles.

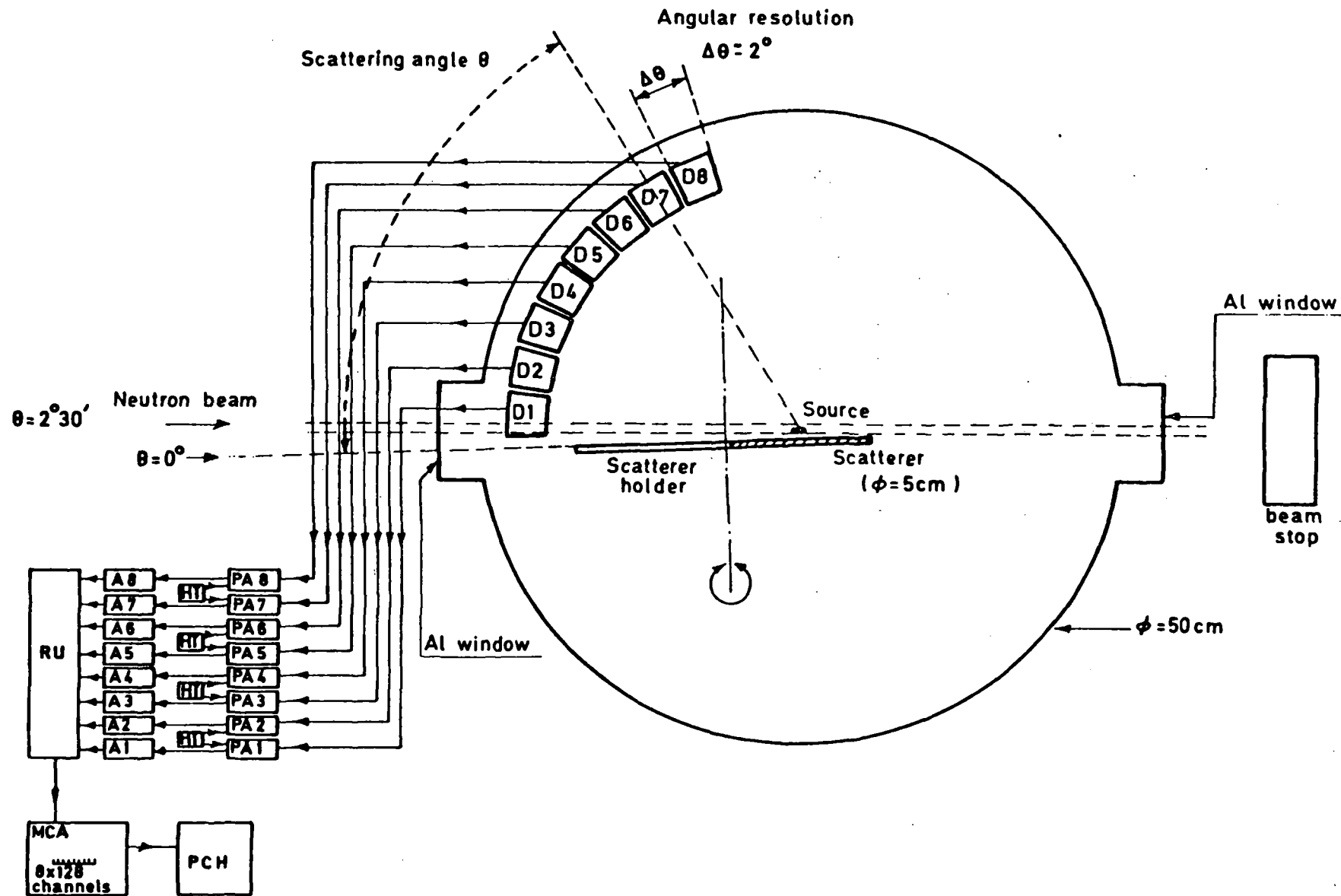


Fig.7. General view of the experimental set-up for the study of the scattering of fission fragments.

3. PHOTONUCLEAR REACTIONS

3.1. Introduction

As the experimental set-up used for the study of photonuclear reactions was rebuilt and is now fully operational, we were able to perform photoproton- and photoneutron spectra measurements simultaneously, using the same bremsstrahlung photon beam.

In order to verify the accuracy of our proton energy calibration procedure we determined the total $^{16}\text{O}(\gamma, p)$ cross section between 20 and 26 MeV, where several prominent resonances are located of which the excitation energies are well-known from the literature. However, by far the largest amount of machine time was devoted to an experimental study of the energy spectra and angular distributions of the photoprotons emitted from ^{89}Y . Apart from a verification of the location of isobaric analogue states, the aim is to determine the (γ, p_0) and eventually the (γ, p_1) cross section, and to look for the E2-component in the absorption mechanism. Some preliminary runs on the $^{19}\text{F}(\gamma, p)$ reaction were performed whereby the attention was focused on the existence of structure in the cross section.

With the recoil-type neutron spectrometer, photoneutron spectra at 90° with respect to the incident photon beam were determined for ^2D , ^{89}Y and ^{19}F at various bremsstrahlung endpoint energies, to complement our information obtained in the (γ, p) experiments.

Some effort was also spent on the study of the rather exotic reaction $^{12}\text{C}(\gamma, n\alpha) ^7\text{Be}$ in the energy range around 30 MeV.

The positron production facility is not operational yet as there was an appreciable delay in the delivery of the cobalt-steel parts, necessary for the construction of new pole pieces that now have been installed in the electron-positron converter lens.

3.2. The total $^{208}\text{Pb}(\gamma, n)$ cross section

(R. Van de Vyver, J. Devos, R. Carchon, E. Van Camp & H. Ferdinande)

Last year we reported on the measurement of the total (γ, n) cross section for ^{208}Pb , whereby the significance of the observed structure was discussed.

If we assume that the triplet at 10.25, 10.8 and 11.45 MeV is riding on a

smooth background E1 cross section, we find for these 3 peaks an integrated photoneutron cross section value between 41 and 83 MeV.mb (both values representing the extremes and depending on the type of near-Lorentzian E1-background curve that has been accepted). On the other hand, for this same triplet one can deduce from (e,e') experiments a weighted mean value for the reduced electric transition strength $\overline{B}(E2)$ of 5000 fm^4 ; this value corresponds to an integrated photo absorption cross section of about 19 MeV.mb. However, one can also interpret this triplet as being due to E1 excitations; this results in a $\overline{B}(E1)$ -value equal to 15 fm^2 , i.e. an integrated photo cross section of about 650 MeV.mb. Consequently, this comparison suggests that the discussed structure is mostly of E2 nature, although some E1 components might also be present.

A similar discussion can be held for the apparent resonance around 9 MeV. Our data yield an integrated photoneutron cross section value of 7 to 12 MeV.mb (above the E1 "background") for the energy region between 8.65 and 9.35 MeV. Recent (e,e') experiments report for this peak a $B(E2)$ -value of $3100 \pm 1200 \text{ fm}^4$, corresponding to an integrated photo absorption cross section of about $7 \pm 2.5 \text{ MeV.mb}$. This agrees quite well with our estimate and seems to confirm the E2 assignment. The results of this $^{208}\text{Pb}(\gamma,n)$ experiment are being presented for publication to the Phys.Rev.C.

3.3. Photoneutron Energy Spectra Experiments

3.3.1. Bremsstrahlung Spectra at 17 and 18 MeV endpoint energy

(J.Devos, R.Van de Vyver, R.Carchon, E.Van Camp, H.Ferdinande)

In order to test the Schiff formula for the bremsstrahlung intensity spectrum used in the conversion of (γ,p) spectra into differential cross sections, we have measured the photoneutron energy spectra (using our recoil-proton type spectrometer) from the reaction $^2\text{D}(\gamma,n)$ at an angle of 90° , at endpoint energies E_0 of 17 and 18 MeV. The target used in this experiment consisted of D_2O with a thickness of about 15 mm, placed at an angle of 45° with respect to the γ -beam. Using the theoretical expression for the differential cross section of this reaction $\frac{d\sigma}{d\Omega}(\theta, E_\gamma)$ as calculated by Partovi, one can derive out of the experimental neutron spectrum the photon intensity distribution $\phi(E_0, E_\gamma)$ using the following expression :

$$\phi(E_\alpha, E_\gamma) = \frac{1}{c} \frac{A-1}{A} \frac{\Delta N(\theta, E_n)}{\Delta E_n} \frac{1}{\frac{d\sigma(\theta, E_\gamma)}{d\Omega} \Delta\Omega}$$

wherein $\frac{\Delta N(\theta, E_n)}{\Delta E_n}$ represents the measured neutron spectrum, A is the mass of the target nucleus while c is a (known) constant.

The results are shown in figure 8. The full line shows the theoretical Schiff-integrated-over-angles spectrum, normally used for thin bremsstrahlung converter targets. The agreement between theory and experiment is remarkable.

3.3.2. The $^{19}\text{F}(\gamma, n)$ Reaction

(J.Devos, H.Ferdinande, R.Carchon, E.Kerkhove, E.Van Camp & R.Van de Vyver)

Simultaneously with the $^{19}\text{F}(\gamma, p)$ experiment, discussed in section 3.4.3, a ^{19}F photoneutron spectrum was recorded at 90° with respect to the direction of the bremsstrahlung beam of which the endpoint energy was 20 MeV. As a target a Teflon TFE[®] disk with a diameter of 9 cm and a thickness of 6 mm was used.

The result is shown in fig.9 (no background subtracted); resonance structure is observed at 15.3, 16.7, 17.8 and 18.9 MeV. The peaks at 15.3 and 16.7 MeV are present in most of the earlier fluorine (γ, n) and (γ, p) measurements, while both the others have rarely be seen before.

3.3.3. Study of the 90° photoneutron spectrum from ^{89}Y .

(J.Devos, E.Van Camp, R.Van de Vyver, R.Carchon, H.Ferdinande & E.Kerkhove)

Together with the current $^{89}\text{Y}(\gamma, p)$ experiment, we have measured the energy spectrum of the photoneutrons from the same element, produced at 90° by 21 MeV bremsstrahlung. This experiment was performed with the aim of checking the possibility for measuring (γ, n) spectra simultaneously with photoproton spectra at a relatively high gamma-beam intensity. The result looks very hopeful. Structure in the neutron spectrum is observed at 4.4, 6.0, 6.7 and 8.0 MeV. If this structure is due to ground state transitions in the residual nucleus, the corresponding excitation energies are : 16.0, 17.6, 18.3 and 19.6 MeV, the peaks at 16.0, 18.3 and

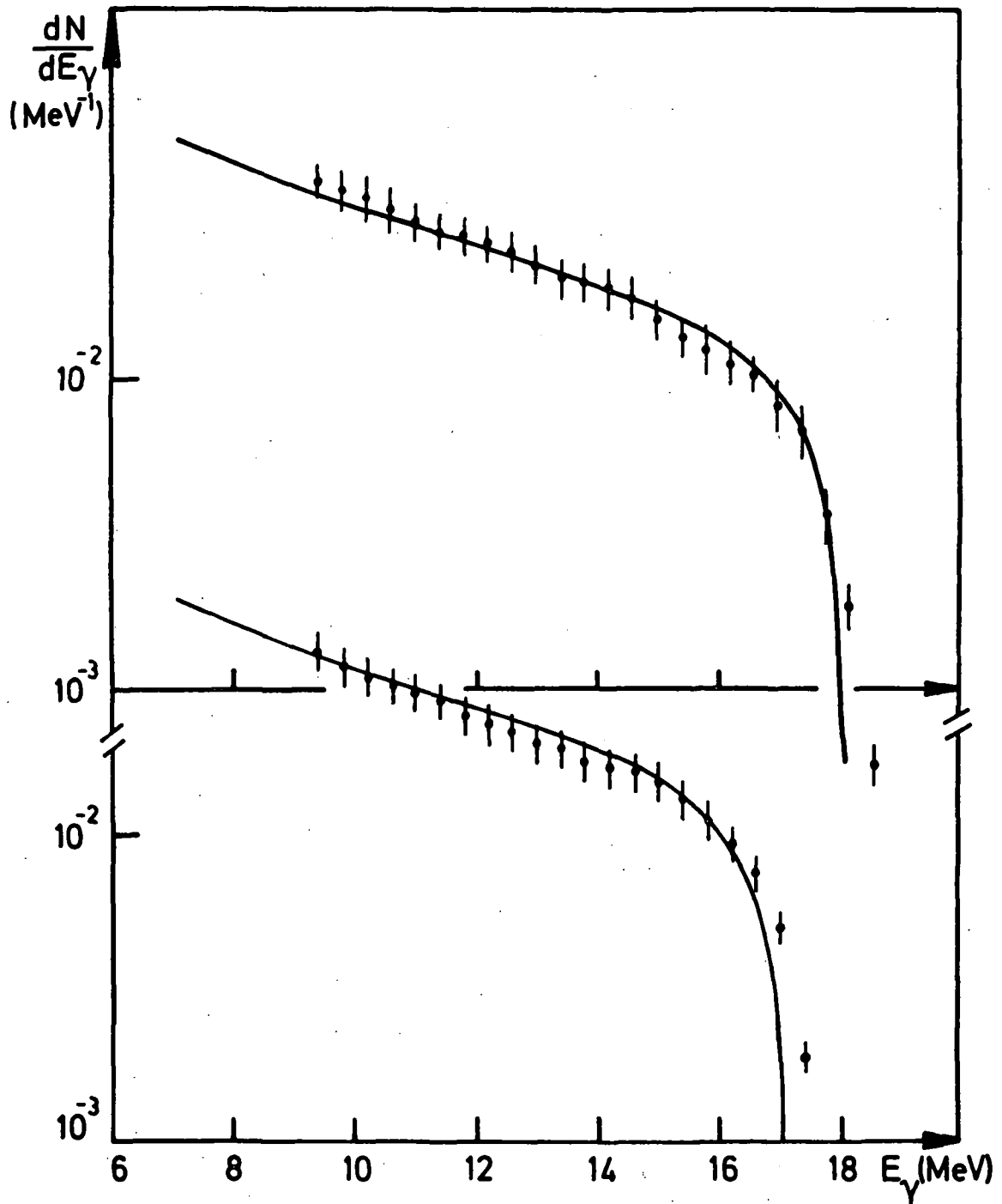


Fig.8. Experimental bremsstrahlung intensity distributions, produced by 17 and 18 MeV electrons; the full lines represent the theoretical Schiff integrated-over-angles spectra.

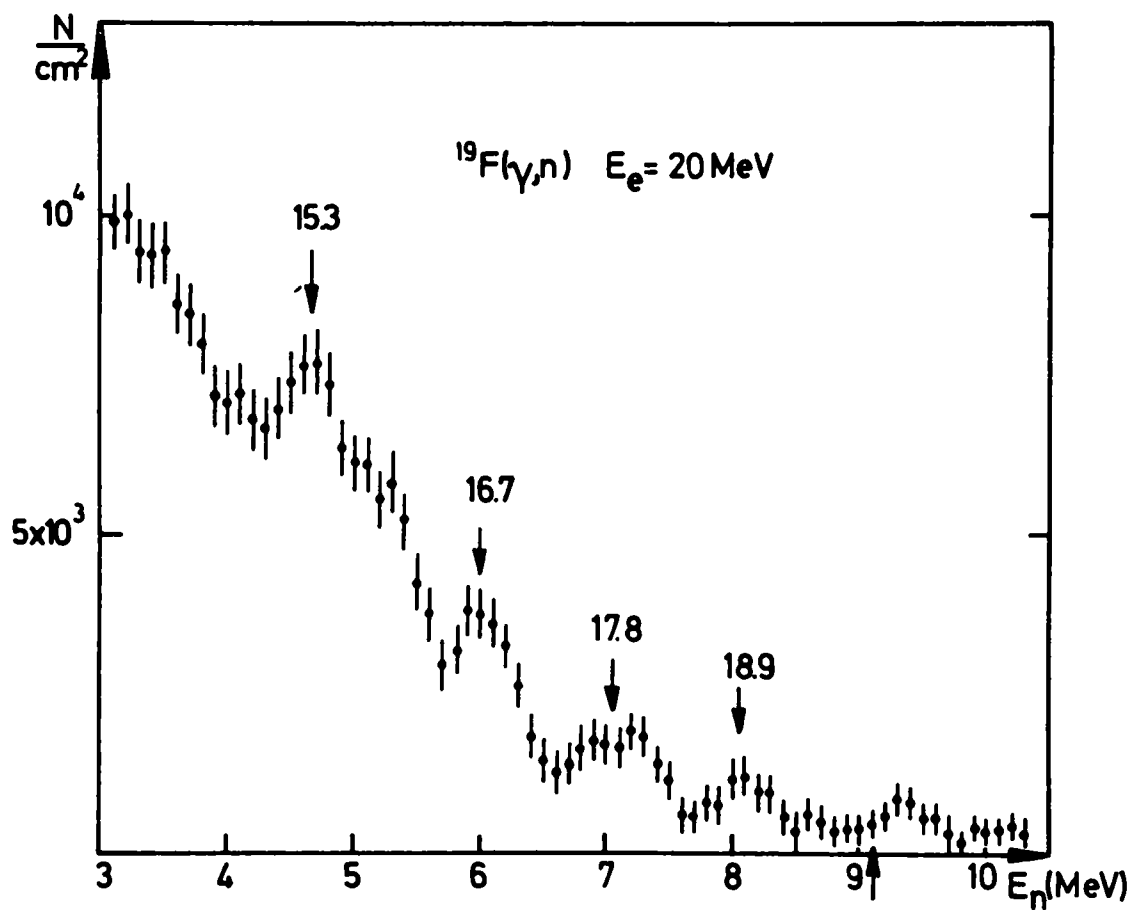


Fig.9. The 90° photoneutron spectrum from ^{19}F ; the indicated values represent pseudo-ground state excitation energies.

19.6 MeV correspond to the resonances observed in the available total (γ, n) cross section data. The 17.6 MeV peak is nowhere else detected; this suggests that the neutrons with 6 MeV energy are not leaving ^{88}Y in its ground state.

Similar measurements at different bremsstrahlung endpoint energies will be undertaken during the coming year, using our recoil-proton type neutron spectrometer.

3.3.4. Photoneutron angular distributions for $^{208}\text{Pb}^*$

(H.Ferdinande, R.U.G.

C.Ross, K.Lokan, N.Sherman, Division of Physics, NRCC, Ottawa,
J.Woodworth, Department of Physics, University of Toronto, Toronto,
J.Jury, Department of Physics, Trent University, Peterborough)

Photoneutron energy spectra from ^{208}Pb have been measured (simultaneously at eight laboratory angles θ_{LAB} ranging from 48° to 138°) by time-of-flight methods for bremsstrahlung end-point energies of 9.6 and 10.6 MeV. In order to avoid measuring the efficiencies of the eight photoneutron detectors in an absolute way, the photoneutron angular distributions for ^{208}Pb were measured relative to the ones for deuterium, which were considered to be well-known theoretically [F.Partovi, Ann.Phys. 27 (1964)79]. Therefore, together with the lead target (enriched to 91% in ^{208}Pb), a D_2O and an H_2O target were mounted on a rotating wheel while being irradiated alternately for some periods in precisely the same circumstances. Preliminary analysis of the data results in angular distributions for the 9.03 MeV and 10.05 MeV resonances in the ground state cross section region, (fig.10), which show that the former would be mostly of E1 nature, while the latter could be an E1-E2 mixture.

* Work performed by H.Ferdinande as a summer guest worker at the Division of Physics of the National Research Council of Canada, (NRCC), Ottawa, Ontario

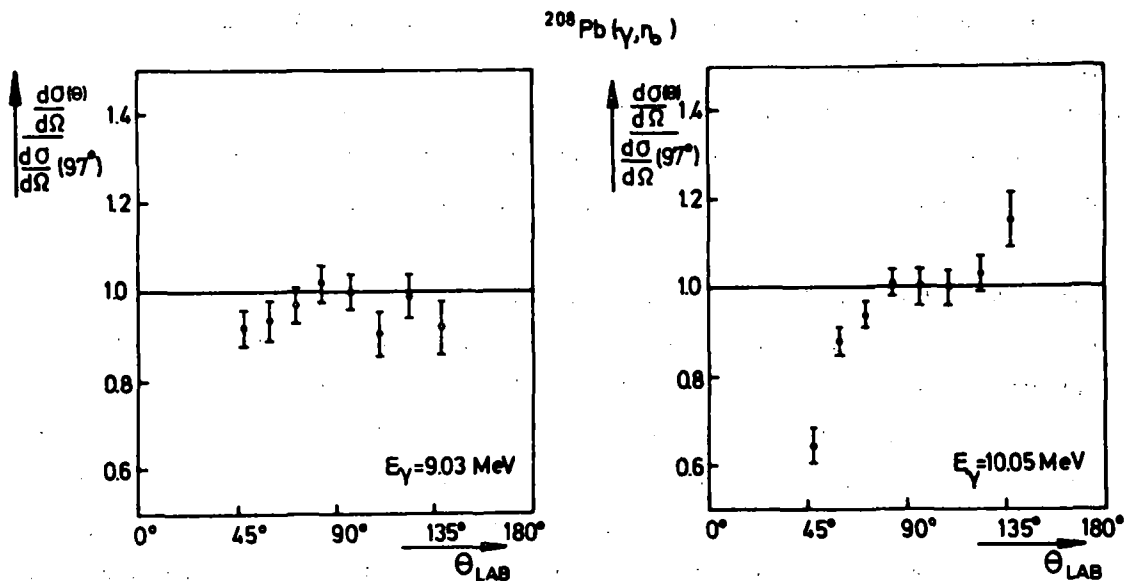


Fig.10. Experimental angular distributions for the 9.03 and 10.05 MeV resonances in the $^{208}\text{Pb}(\gamma, n)$ cross section.

3.4. Photoproton Spectra and Angular Distributions

3.4.1. The $^{12}\text{C}(\gamma, p)$ reaction

(R.Carchon, R. Van de Vyver, H. Ferdinande, J. Devos & E. Van Camp)

From our $^{12}\text{C}(\gamma, p)$ experimental data, obtained with 30 MeV end-point bremsstrahlung, we concluded that the argument developed by Dixon and Thompson [Austr.J.Phys.27(1974)301] on the effect of excited state decay on the measured angular distributions and total cross section for the $^{12}\text{C}(\gamma, p)$ reaction, was overestimated. Based on the fact that there exists a distinct difference between the $^{12}\text{C}(\gamma, p)$ cross section as measured by Frederick and Sherick [Phys.Rev.176(1968)1177] and the cross section as derived from the inverse reaction [Allas et al., Nucl.Phys.58(1964)122], especially in the energy region between 24.2 and 25.5 MeV, Dixon and Thompson proposed the existence of photoproton cross sections for decay to the 4.44 and 5.02 MeV states in ^{11}B . Such cross sections should have a non-negligible magnitude around 29 and 30 MeV respectively, and reach a maximum value of about 1.5 mb.

The fact now that our ^{12}C photoproton cross section around 25 MeV is in good agreement with the one deduced from the (p, γ_0) reaction suggests that

the effect of excited-state decay is certainly less pronounced than was originally believed.

However, the phenomenon discussed by Dixon and Thompson was based on the comparison of (p, γ_0) data with (γ, p) results taken at a bremsstrahlung endpoint energy of 32.1 MeV, while ours were performed with 30 MeV bremsstrahlung.

In order to check whether this differences could have a visible effect, we remeasured the $^{12}\text{C}(\gamma, p)$ cross section with 33 MeV bremsstrahlung; photo-proton energy spectra were taken at 7 angles simultaneously. A sum of Legendre polynomials was fitted to the experimental data, and a very good agreement with our previous results was obtained. Consequently, our conclusion that the effect of excited-state decay in ^{12}C on the angular distribution and on the total cross section was overestimated, remains valid.

We also made a search for collective E2 strength in the $^{12}\text{C}(\gamma, p)$ cross section, above the giant dipole resonance. Frederick [Nucl.Phys. A101 (1967)250] has shown that

$$\frac{\sigma(E2)}{\sigma(E1)} = K \cdot a_1^2$$

wherein $a_1 = A_1/A_0$ (A_1 are the coefficients of the Legendre polynomial expansion) and K represents a rather complicated function of the transition amplitudes. If, for simplicity, one puts $K = 1$, one can obtain a pseudo E2 cross section $\sigma^*(E2) = 4\pi A_0 a_1^2$, as presented in fig.11. This result does not display a strong resonance behaviour, and the strength has a nearly constant value beyond 25 MeV. However, such spreading of the E2 strength is not inconsistent with recent (α, α') data [K.Knöpfle et al., Phys.Lett. 64B (1976)263] where the isoscalar giant quadrupole resonance exhausts about 10% of the energy-weighted sum rule (EWSR) in the same energy region. Further photoproton experiments on ^{12}C are planned to clarify this point.

3.4.2. Structure in the photoproton cross section of ^{16}O

(R.Van de Vyver, R.Carchon, E.Van Camp, H.Ferdinande, J.Devos and E.Kerkhove)

The photonuclear cross section of ^{16}O has been the subject of an extensive experimental study; in the 20 to 25 MeV energy range resonances are located at 21.0, 22.2, 23.0 and 24.3 MeV (this numbers are mean values taken from the literature).

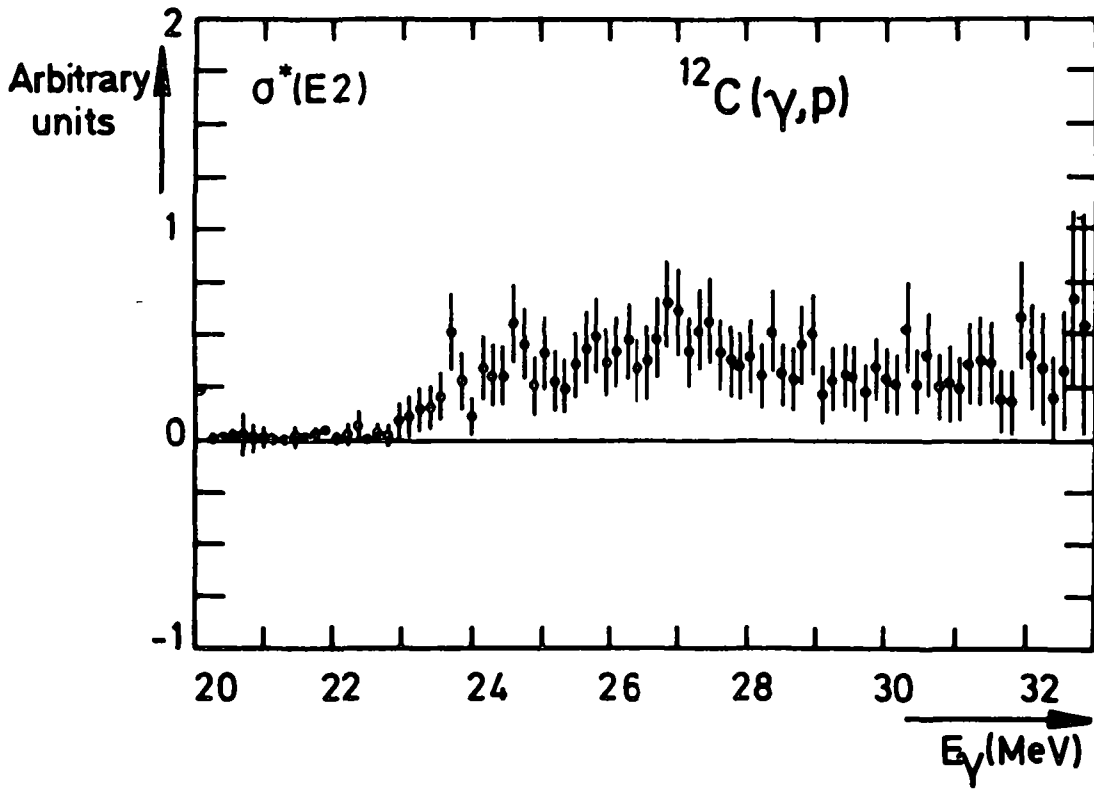


Fig.11. Pseudo-E2 cross section observed in the $^{12}\text{C}(\gamma,p)$ reaction.

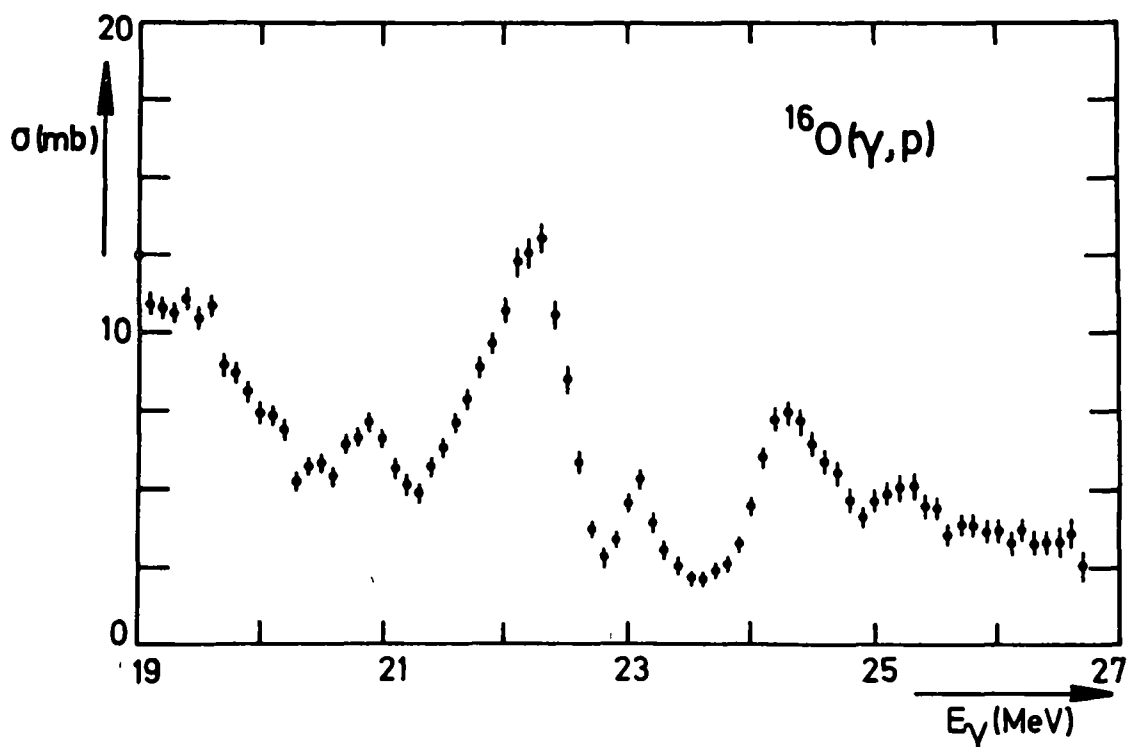


Fig.12. The total $^{16}\text{O}(\gamma,p)$ cross section obtained with 27 MeV bremsstrahlung (no background subtraction).

The aim of the present experiment was to check the energy calibration procedure (based upon 3 alpha-particle energies, in the 5-6 MeV range) of our photoproton detection system. An 18 μm cellophane[®] sample containing 7% H_2O and 93% $\text{C}_6\text{H}_{10}\text{O}_5$, was irradiated with 27 MeV bremsstrahlung. Photoprotons were detected at 7 angles simultaneously (between 37° and 143°) using 2 and 3 mm thick Si(Li) solid detectors. A Legendre polynomial expansion was fitted to the experimental differential cross sections. The total cross section $4\pi A_0$ is shown in fig.12. (no background subtraction). Within our energy resolution the observed resonance energies coincide with the above mentioned values; however, to reach this, the curve which describes the relationship between pulse height and energy has to be slightly parabolic above 6 MeV. Further analysis of the data is still in progress.

* We are indebted to Dr. Bontinck from SIDAC-Research/Ghent for providing the samples.

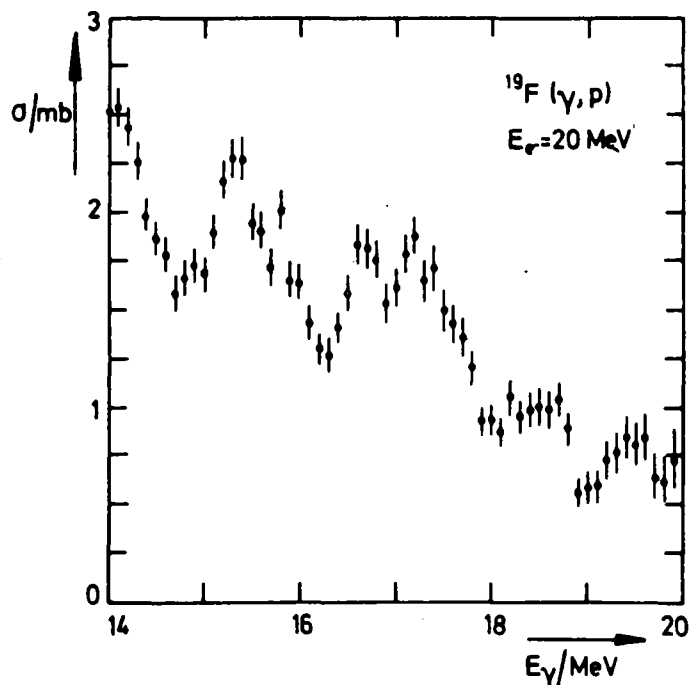


Fig.13. Pseudo ground state cross section for the $^{19}\text{F}(\gamma,p)$ reaction at 20 MeV endpoint bremsstrahlung.

3.4.3. Preliminary results on the $^{19}\text{F}(\gamma,p)$ reaction

(H.Ferdinande, R.Carchon, J.Devos, E.Kerkhove, E.Van Camp & R.Van de Vyver)

A photoproton test experiment was performed on the target nucleus ^{19}F . A 25 μm thick TEFLON FEP[®]* foil was irradiated with bremsstrahlung of which the endpoint energy was 20 MeV. The photoprotons were detected with our standard set-up [Phys.Rev.C14(1976)456]. From the recorded proton energy spectra the differential, pseudo ground state cross sections were extracted assuming a Schiff bremsstrahlung distribution. In the excitation energy region $E_x = 18\text{-}20$ MeV these were real ground state ones. The results were fitted with the conventional sum of Legendre polynomials up to the order 4. In fig.13 and 14 are plotted the total pseudo ground state ^{19}F photo-

* Du Pont's Registered Trademark for completely fluorinated ethylene-propylene copolymer.
Kindly put at our disposal by Du Pont de Nemours Int.S.A.Fluorocarbons Division.Geneva.

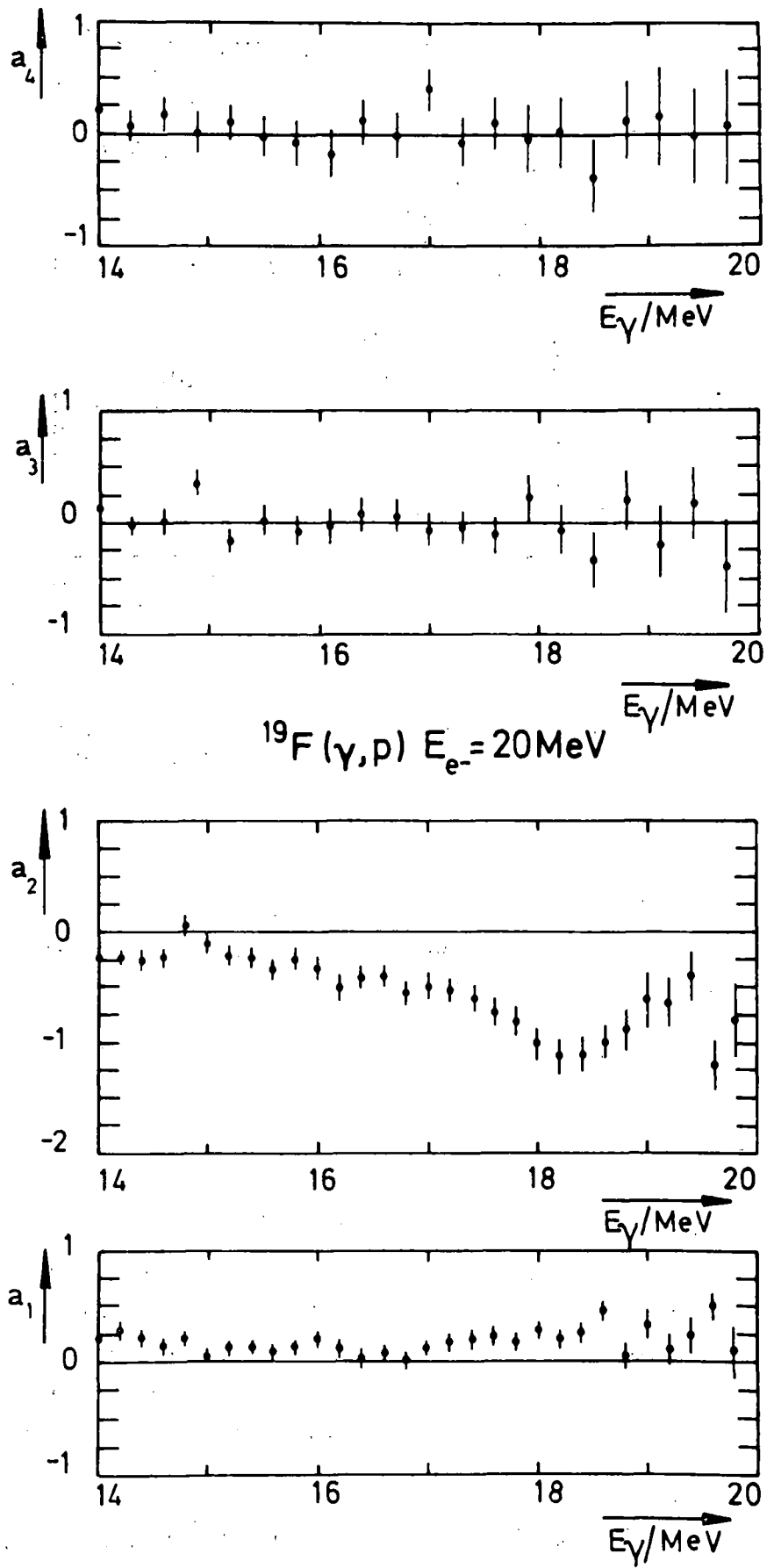


Fig.14. (Preliminary) angular distribution coefficients for the photoprotons from ^{19}F .

proton cross section and the relative coefficients a_i ($i=1, \dots, 4$) from the polynomial expansion as a function of the excitation energy.

Resonance structure was found at 15.4, 15.8, 16.7, 17.2, 18.5 and 19.4 MeV. Due to better energy resolution we were able to split clearly the unresolved resonance, seen at 17.0 MeV in a recent 90° electroproton experiment [H.Tsubota, et al., J.Phys.Soc.Jap.38 (1975)299]. In the region [$E_\gamma = 18-20$ MeV] where the residual nucleus is left in the ground state the coefficients a_3 and a_4 are essentially zero. In the channel spin formalism, considering only E1 and E2 radiation being present, $a_4 = 0$ could mean a zero $d_{5/2}$ (E2) transition matrix element. A zero a_3 coefficient could result from a phase angle ($p_{3/2}$ (E1), $d_{3/2}$ (E2)) = 90° . The values $a_1 \approx 0.25$ and $a_2 \approx -0.8$ in the ground state interval could, along the same lines, be explained if one accepted an almost equal $p_{1/2}$ (E1) and $p_{3/2}$ (E1) contribution and an 8% $d_{3/2}$ (E2) intensity. It would be interesting to investigate in more detail the rich structure in the GR region and the E2 contribution in the region around 23 MeV, where recent (p,p') experiments on the neighbouring nuclei ^{20}Ne and ^{22}Ne [K.Knöpfle et al., Phys.Lett.64B (1976)2] have found an isoscalar GQR. The results could then possibly be interpreted, in a similar way as for these two other (sd)-shell nuclei, with the help of an excited core model [W.Knüpfer, K.Knauss & M.Huber, to be published].

3.4.4. Study of the $^{89}\text{Y}(\gamma, p)^{88}\text{Sr}$ reaction in the G.R. region

(E.Van Camp, R.Carchon, J.Devos, H.Ferdinande, R.Van de Vyver & E.Kerkhove)

In order to investigate the giant resonance of ^{89}Y , the photoproton energy spectra from the $^{89}\text{Y}(\gamma, p)^{88}\text{Sr}$ reaction have been measured at seven angles (from 37° to 143°) and at bremsstrahlung endpoint energies ranging in 1 MeV steps from 15 to 21 MeV. The energy loss of the emitted protons in the 9.45 mg/cm^2 thick ^{89}Y target foil mainly determines the energy resolution which is about 400 keV for 8 MeV protons.

As the energy difference between the ground and first excited state in ^{88}Sr equals 1.836 MeV, one can extract the photoproton cross section for protons leaving the residual nucleus in its ground state. The differential cross sections can be expanded in the usual manner :

$$\frac{d\sigma}{d\Omega}(E_Y, \theta) = \sum_{i=0}^4 A_i(E_Y) P_i(\cos \theta)$$

in which the energy-dependent coefficients $A_i(E_Y)$ contain the nuclear structure information that can be deduced from the experiment. Since the residual nucleus ^{88}Sr has a $J^\pi = 0^+$ ground state spin, the expression of the A_i coefficients in function of electromagnetic multipole transition matrix elements is rather simple, so that we should be able, with some assumptions, to obtain these matrix elements.

Our preliminary results, shown in fig.15, indicate a ground state cross section magnitude of about 3.82 ± 0.13 mb at 17 MeV; this is rather close to the value as obtained by detailed balance from the (p, γ_0) reaction. Some structure is observed which can be interpreted as isobaric analogue resonances. We also have strong indications that the A_3/A_0 coefficients are near zero in the energy region investigated; consequently, if we assume that only E1 and E2 matrix elements contribute to the cross section, the emission of f-wave protons (E2 absorption) seems unlikely. Under these assumptions further analysis shows that the E2 contribution to the $^{89}\text{Y}(\gamma, p_0)$ G.R. may be of the order of 1% of the E1 cross section. The experiment is still in progress because a higher statistical accuracy is required to draw definite conclusions.

3.5. The $^{12}\text{C}(\gamma, \alpha) ^7\text{Be}$ reaction

(E.Kerkhove, R.Van de Vyver & E.Van Camp)

In the $^{12}\text{C}(\gamma, xn)$ reaction cross section, a resonance is observed around 30 MeV for which no theoretical explanation has been given. Direct comparison of the (γ, xn) cross section magnitude with the available (γ, n) cross sections suggests that this structure might be due to a less common reaction type. Owen and Spicer [Phys.Lett.30B(1969)242] have measured the $^{12}\text{C}(\gamma, \alpha) ^7\text{Be}^*$ reaction cross section in the energy range between threshold (26.3 MeV) and 30 MeV using the method of induced activity. They observed a peak at about 29.7 MeV with a cross section value of 0.8 mb; this state was discussed in terms of particle-hole configurations.

In a preliminary attempt to examine the possibilities for studying this same reaction, we have bombarded several ^{12}C targets with a bremsstrahlung beam from our linac; photon endpoint energies were varied between 27 and 33 MeV in 1 MeV steps. The yield of $^7\text{Be}^*$ nuclei was determined by counting its 477.6 keV residual activity ($T_{1/2} = 53.44$ days) using a large(5"x5")

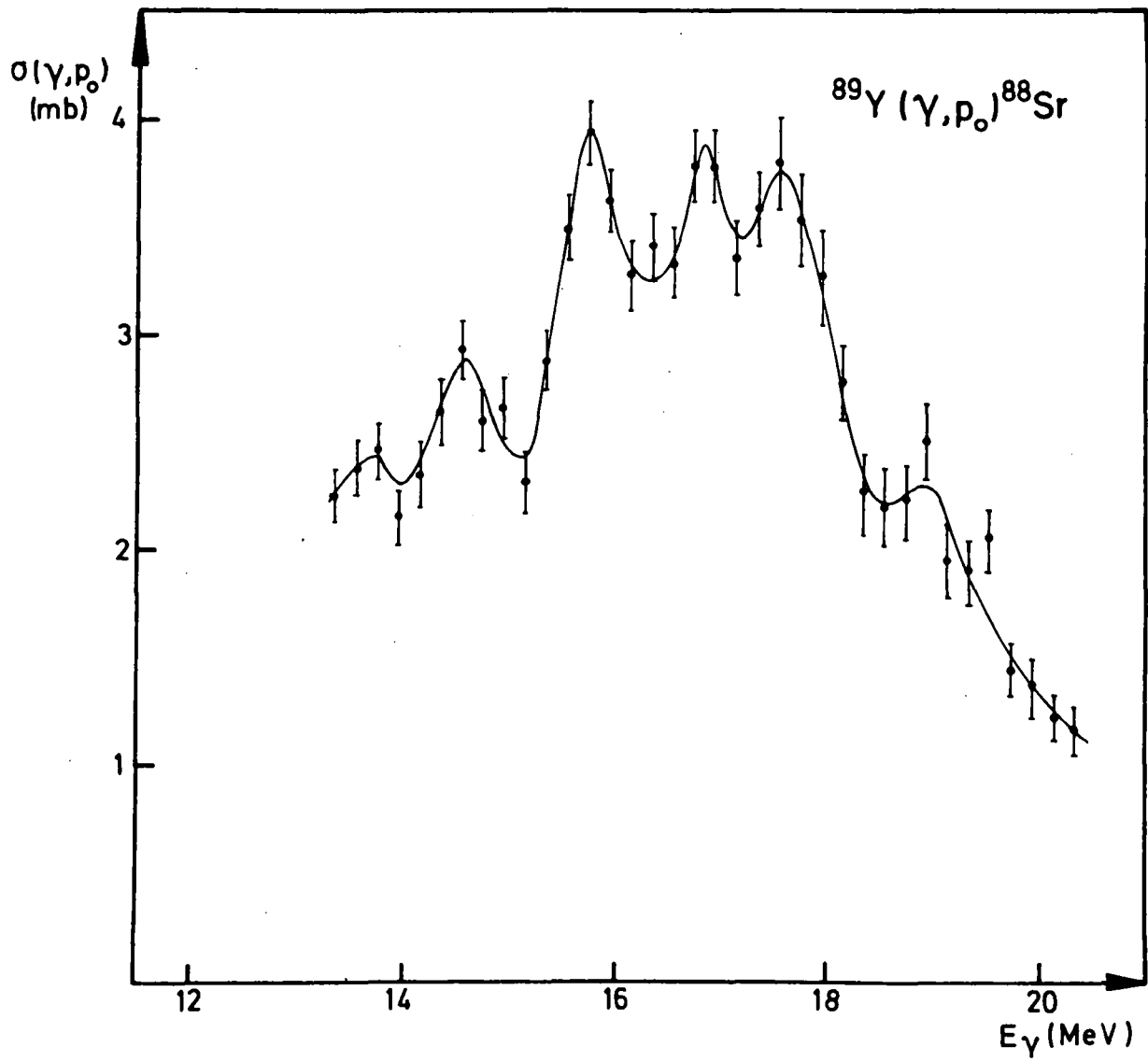


Fig.15. The $^{89}\text{Y}(\gamma, p_0)$ cross section between 13 and 20.5 MeV.

NaI-scintillation spectrometer (with anti-coincidence background shield).

This yield curve was then analysed by means of the Penfold & Leiss unfolding technique. The resulting cross section is double-peaked (at 29.5 and 31.5 MeV) and shows a maximum magnitude of about 0.3 mb. This is in direct contrast to the data obtained by Owen and Spicer.

Further experiments will be necessary to clarify this conflicting situation, although the existence of a resonance around 30 MeV in the $^{12}\text{C}(\gamma, \text{xn})$ cross section—partly due to the $(\gamma, \text{n}\alpha)$ reaction—seems now to be established beyond any doubt.

3.6. Positron production and acceleration

(R. Van de Vyver, H. Ferdinande, E. Van Camp & K. Kiesel)

As stated in last year's report, we planned to modify and replace the pole-pieces of the magnetic electron-positron converter lens. Due to an (unexpected) exceptionally long delivery time, the necessary cobalt-steel pieces were only obtained at the end of September 1976. Presently, these pieces have been machined to the correct geometry and new copper windings (pancakes) have been installed. The converter is now being re-assembled and will be ready for testing by the end of January 1977. It is hoped that the converter assembly will be installed in between both linac sections in the first half of 1977.

4. NUCLEAR SPECTROSCOPY AND POSITRON ANNIHILATION

(M.Dorikens, L.Dorikens-Vanpraet, D.Segers and J.Uyttenhove*)

4.1. First test on the anti-compton spectrometer

A new instrument, i.e. an anti-compton shield was installed and tested. It consists of a split-annulus of NaI(Tl) (12"Ø x 10" thick) and a 3"Ø x 5" end crystal. The anti-compton shield is designed for one of the 50cc custom-series Ge(Li) detectors in the laboratory, but can also be used for other Ge(Li) detectors. A lead collimator for the source was designed and constructed. Special preamplifiers were built for the NaI(Tl) detectors suited for high count rates and severe overload. All 7 photomultipliers were carefully adjusted to have the same gain. The information of the 7 preamplifiers is summed in linear summing networks. The coincidence electronics is based on zero strobe fast timing. Resolution is $2\tau = 100$ ns for an energy range from 100 keV up to 5 MeV.

The first measurements show that the instrument is very well suited to distinguish between gamma transitions that are coincident with one another, and non-coincident ground-state transitions. The best peak-compton ratio obtained was 60:1, which means an improvement of about a factor 3.

Test measurements are in progress on the catcher foil spectra from the gamma induced (25 MeV) fission products from ^{238}U and natural fission products from ^{252}Cf . The influence of the catcher foil source surface on the compton suppressed spectrum will be subjected to a systematic investigation.

4.2. Measurement of the angular shapefactor in deformed copper

During the test runs with the "windowed angular correlation" set-up (described in annual report 1975), it became clear that stabilization of the plastic-scintillator measuring chain was necessary. Light pulses of a green LED were fed into each photomultiplier; they give rise to a peak at the high-energy end of each plastic scintillator spectrum, far beyond the actual spectrum. On this peak a window is set to drive the stabilization chain, with feedback to the voltage divider of the photomultipliers.

* Laboratorium voor Natuurkunde, Groep II, R.U.G.

With this "windowed angular correlation" set-up, the angular shapefactor in deformed copper was measured as a function of the degree of thickness reduction. The measurements are illustrated in fig. 16.

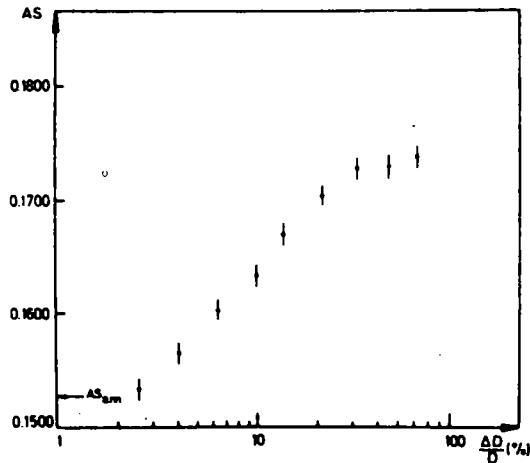


Fig.16

The influence of the deformation is clearly seen as an increase in the angular shapefactor AS from a value AS_{ann} , which corresponds to the well annealed sample, to a saturation value, corresponding to high deformations. At these high deformations all the positrons are trapped by dislocations. The general trend of the curve is the

same as obtained from Doppler broadening S-factors or positron lifetime measurements [C.Dauwe et al., Appl.Phys. 5,117(1974)]. The shape of the curve can be described with the help of the well-known trapping model, in which the trapping of positrons by dislocations is taken into account. From these measurements on deformed copper, some interesting conclusions can be drawn, concerning the propagation regime or the diffusion regime of positrons. Our measurements seem to indicate that the interaction of the positron with dislocations can be better described with the help of the propagation model. This conclusion agrees with the results of B.T.McKee (paper E33, Fourth International Conference on Positron Annihilation, 1976) but disagrees with the interpretation of positron trapping results in terms of the diffusion model as stated by Brandt et al. [Phys.Letters 48A,480(1974)].

4.3. Measurement of the Doppler-broadened positron annihilation lineshape in Indium

It was recently experimentally demonstrated by Lichtenberger et al. [Appl.Phys. 6 305(1975)] that in metals the temperature dependence of the positron annihilation parameters below the vacancy trapping threshold, cannot be solely attributed to thermal expansion. This so called "pre-vacancy effect"

was theoretically interpreted by Seeger [Appl. Phys. 7 85 (1975)] as an effect of self-trapping of positrons. Seeger's theory predicts the shape of the lineshape factor versus temperature curve in the intermediate temperature range: at the low temperature end all positrons are free, and a saturation of the lineshape factor occurs; for increasing temperatures an increase in the lineshape factor is expected up to a saturation value, corresponding to the state where all the positrons are self-trapped. At this high temperature end, the effect of vacancy trapping is superimposed on this "self-trapping" curve.

We measured the temperature dependence of the lineshape factor in Indium between 74°K and the melting point. The measurements are shown in fig.17. The data follow exactly the theoretical curve as predicted by

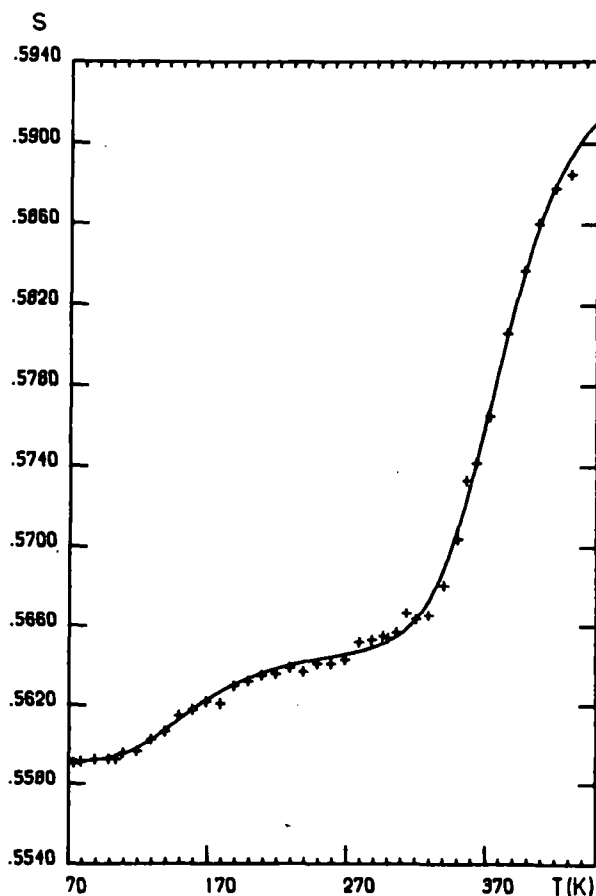


Fig.17. Temperature dependence of the lineshape factor S in Indium.

Seeger. Indium is the first example where the saturation of the self-trapping effect at the high temperature end can be actually seen. Also the non-linear behaviour between $T=100^{\circ}\text{K}$ and $T=280^{\circ}\text{K}$ emerges very clearly. This gives evidence to the fact that the intermediate temperature effect is not due to thermal expansion. The classical trapping model was extended for the case of self-trapping and fitted to the data. A value for the mono-vacancy formation enthalpy of (0.48 ± 0.03) eV was obtained. This value agrees very well

with the range of previously obtained values with the positron annihilation technique (ranging from 0.39 eV to 0.55 eV), and is also quite compatible with the activation energy for self-diffusion of $(0.81 \pm 0.015)\text{eV}$.

4.4. The effect of thermal expansion on the Doppler-broadened positron annihilation lineshape factor

From a Doppler broadened positron annihilation lineshape factor study in solid Gallium as a function of temperature (see annual report 1975), it followed that no effect of thermally induced vacancies and no "pre-vacancy effect" could be detected (see also measurements in Indium). In order to investigate the influence of thermal expansion of the Gallium lattice on the lineshape factor, and to reduce the statistical uncertainties, more accurate measurements of the lineshape factor as a function of temperature were performed, and this for a larger set of temperatures. The results are shown in fig.18. A straight line was fitted through the data

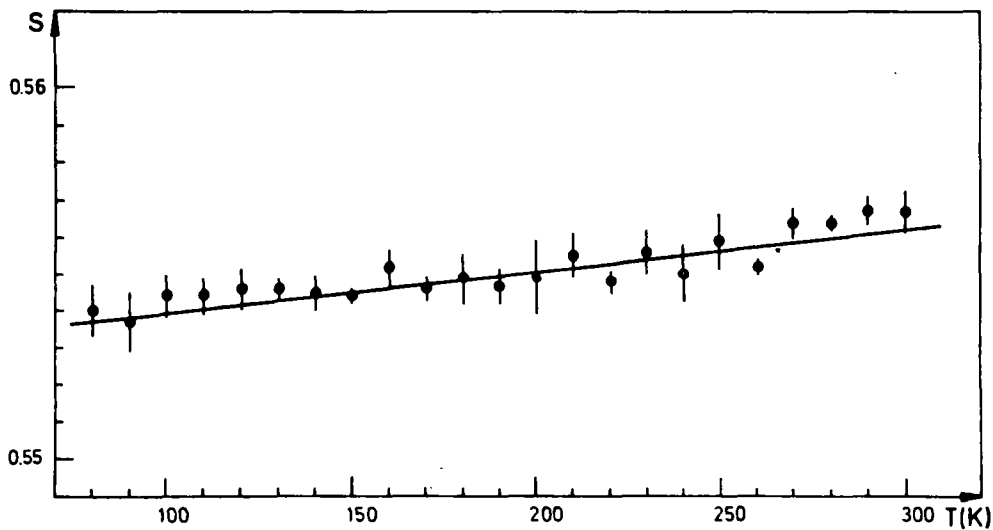


Fig.18. Lineshape factor S for solid Gallium as a function of temperature.

and is represented by :

$$S = (0.5528 \pm 0.0002) + (1.1 \pm 0.1) 10^{-5} T$$

Thermal expansion affects the measurements in two ways :

- 1) through the effect of the lowering of the Fermi surface and
- ii) through the decrease in the number of annihilations with core electrons.

On the basis of these two principles and using the free electron approxi-

mation of metals, an expression for the lineshape factor as a function of temperature was obtained. The influence of instrumental resolution was included in the model by convoluting the intrinsic lineshape with the experimental resolution function of the Ge(Li) detector, approximated for this purpose by a Gaussian distribution. Some relevant parameters of the model (i.e. P_0 = the Gaussian fraction of the annihilation lineshape at a reference temperature $T_0 = 293^\circ\text{K}$, and S_1 = the lineshape factor associated with this Gaussian) could be estimated in two independent ways : i.d. through the temperature effect of the lineshape factor, and by a curve fitting to the total line at $T_0 = 293^\circ\text{K}$. Within the statistical uncertainties the results agree quite well and confirm in this way the interpretation of the measurements in terms of thermal expansion effects.

4.5. Electro-optical stabilization of the positron annihilation life-time equipment

The formerly used stabilization system(see annual report 1974), though an improvement on non-stabilization, was not perfect since it included only the electronic circuitry of the positron annihilation life-time set-up, but not the detectors, photomultipliers, bases and high-voltages. A new stabilization system was therefore designed; it includes the whole timing system from the photomultiplier up to the ADC. Red LED's (RL50) are mounted in front of the plastic scintillators of the start and the stop chains. An avalanche pulser triggered by another dual avalanche pulser was built and drives the Litronix RL50 LED's, in forward direction. The pulse-form as obtained with this avalanche pulser has a risetime of less than 1 ns and a FWHM of about 1 ns. By using appropriate cable lengths, from these light pulses, two peaks in the timing spectrum can be derived; one in the beginning of the spectrum and one at the end, used respectively for digital stabilization of zero and gain.

In order to separate the stabilization spectrum from the real life-time spectrum, routing is performed. The block diagram of the complete set-up is shown in fig.19. To test the stability of the equipment, we measured the time spectrum of ^{60}Co , which results in a prompt curve at $t=0$. The reproducibility of the peak position of this prompt curve gives an idea of the stability of the system. This peak position was obtained by fitting a sum of three Gaussian curves, all centred at the same peak position, to the prompt curve. The result of the test run is shown in fig.20. The rms on the peak position of the prompt curve is 3 ps.

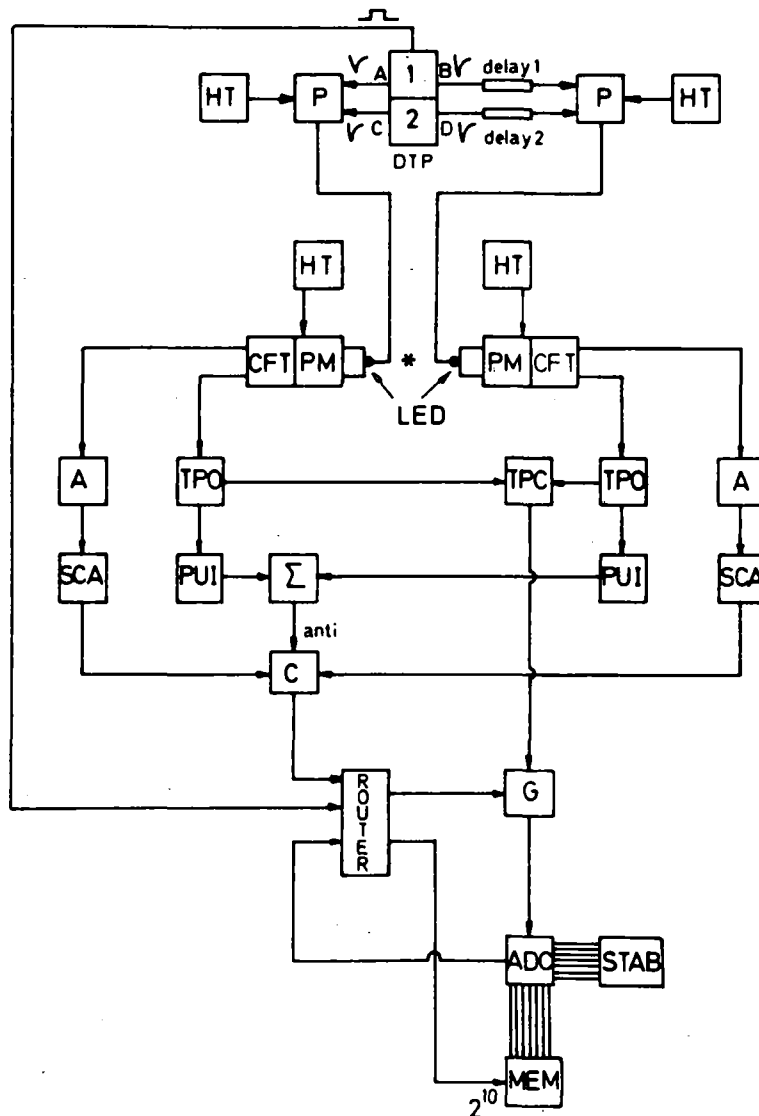


Fig.19. Block diagram of the electro-optical stabilization set-up for the positron annihilation life-time measurements.

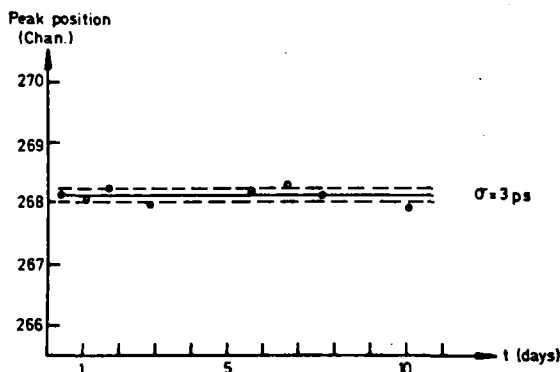


Fig.20. Reproducibility of the peak position of the prompt curve as measured with ^{60}Co .

4.6. Positron annihilation study of neutron-irradiation induced voids in Aluminium

(in cooperation with S.C.K.-Mol)

The trapping of positrons by vacancies or vacancy-like defects is a well established fact. In order to perform a systematic study of positron trapping by voids, 6N Al samples were irradiated with fast neutrons in the BR2 reactor (Mol, Belgium) to five different fluences ranging from $1.21 \cdot 10^{19}$ up to $8.76 \cdot 10^{19}$ n/cm². Positron annihilation lifetime measurements and Doppler-broadened annihilation lineshape measurements were performed for the different samples. The results are presented in table 2.

Table 2

Fluence (n/cm ²)	Lifetime results			Lineshape results
	τ_1 (psec)	τ_2 (psec)	I_2 (%)	S
$1.21 \cdot 10^{19}$	135 ± 4	281 ± 6	31.3	0.5692±0.0005
$1.72 \cdot 10^{19}$	136 ± 4	286 ± 6	36.5	0.5709±0.0002
$1.70 \cdot 10^{19}$	138 ± 4	293 ± 6	35.7	0.5699±0.0002
$1.94 \cdot 10^{19}$	140 ± 4	303 ± 6	28.2	0.5694±0.0005
$8.76 \cdot 10^{19}$	125 ± 4	320 ± 6	41.0	0.5749±0.0005
annealed 6N Al	: $\tau = (167 \pm 4)$ psec			S=0.5662±0.0005
strongly deformed(60%) 5N Al.	: $\tau = (246 \pm 4)$ psec			S=0.5801±0.0007

For comparison we also measured the lifetime and lineshape factor in well annealed and strongly deformed Aluminium samples.

From the measurements it follows that for the irradiated samples τ_1 decreases below the value of the well annealed sample, and an intense second component emerges. These results can be described with the help of a simple two-state trapping model in which we assume the voids to be the trapping centres.

Some preliminary measurements were carried out on the annealing of voids; the "lowest dose sample" was heated to different temperatures, then slowly cooled to room temperature and the positron annihilation lifetime and lineshape factor measured. The results for τ_1 and S are represented in fig. 21. For T = 540°K all the voids are annealed out and the posi-

tron parameters revert to the same values as for the well-annealed sample. Annealing studies for the samples irradiated to higher fluences are still in progress.

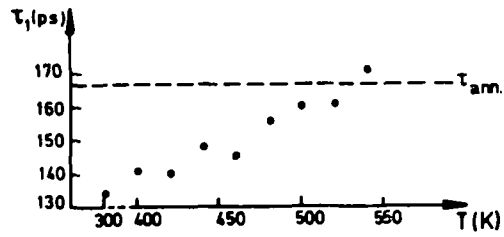


Fig.21 a. Recovery of τ_1 as a function of annealing temperature in neutron irradiated aluminium.

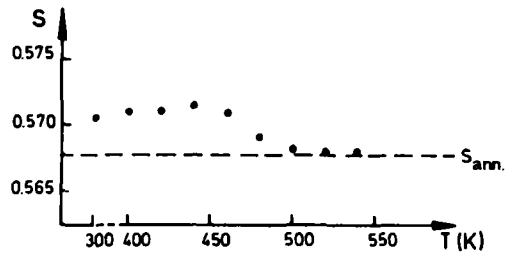


Fig.21 b. Recovery of S as a function of annealing temperature in neutron irradiated aluminium.

5. DOSIMETRY

(G.Eggermont, A.Janssens, J.Buysse

in cooperation with R.Jacobs^{*}, E.Cottens^{**} and G.Thielens^{***})

5.1. Cavity theory and related transport problems

The fundamental concepts of the cavity theory remained unchanged. Some secondary aspects of the application of the surface model have been investigated, such as :

- the integration of the weighting function over the entire Compton spectrum of secondary electrons.
- the integration of the weighting function over the distribution of chordlengths in specific geometries, in particular a parallel plate and a sphere.
- the inhomogeneous term in the surface method and the modified two-step model, in comparison with the Spencer-Attix theory.

The computational method for the calculation of the energy-distributions of the equilibrium fluences, and of the stopping powers, has been improved, such that an accuracy of a few % was reached.

The theory for the calculation of the build-up of fluorescence photons in an attenuating plane-parallel body, has been extended with a general method for the numerical computation of the fluence of secondary photons(both fluorescence-and Compton-scattered photons), for a cylindrical body. This method has been applied to the standard ionisation chamber of the Bureau International des Poids et des Mesures,Paris(BIPM) for ⁶⁰Co radiation. Our calculations have shown that the extrapolation method applied at the BIPM, underestimates the dose deposited by secondary photons by an amount of about 1% of the dose deposited by primary photons.

The fluence of secondary photons has also been calculated for the high pressure ionisation chamber, to be used for the experimental determination of the weighting function in the cavity theory. In order to design this chamber such that all error contributions are optimally reduced,theoretical calculations have been performed of :

- the optimal dimensions of the chamber for comparison with the theory.
- the recombination of the ions in the chamber(mainly initial recombination).
- the sidewall contribution and the radial homogeneity of the X-ray beam.

* Centrale Dienst voor Fysische Controle-RUG(Director Prof.Segaert)

** Laboratorium voor Natuurkunde groep II-RUG(" " ")

*** Dienst voor Veiligheid en Hygiëne - RUG

- the contribution of secondary electrons from the lucite supports of the wall materials.

The final design of the set-up is shown in figure 22.

The construction of the pressure vessel and of the ionisation chambers is almost complete. An appropriate technique for the coating of the reference chamber with a 15 μm thick carbon layer was developed. Considerable difficulties in the stretching of the lucite plates and in the measurement of the plate separation have been overcome.

The effective energy of the X-ray beam, and the attenuation in the entrance window of the vessel, the lucite plates and the gold foils, have been measured by means of energy independent thimble ionisation chambers. In order to obtain a better reproducibility, the hardening filters have been placed in front of the monitoring chamber. The distance between the beam collimator and the target has been modified, in order to obtain an optimal focussing of the beam. The homogeneity and the centering of the beam have been verified by means of X-ray films. The actual measurements with the experimental chamber will start in the beginning of 1977. (The cavity theory, the theory for the transport of secondary photons and for the corrections to the experiment, form part of the doctoral thesis of A.Janssens).

5.2. Calorimetry

The measuring and control circuit of the calorimeter has been designed and partly constructed.

(This is a part of the doctoral thesis of E.Cottens).

5.3. Film dosimetry

The results of the CEC intercalibration program on film dosimetry (1975) were published and used to evaluate the AERE-RPS personal dosimetry system of the CDFC.

5.4. Chemical Dosimetry

Since lucite irradiation cells were preferred to glass for in-phantom irradiation and for absolute comparisons with calorimetry, the interaction of Fricke solution with lucite has been studied. The evolution of Fricke characteristics in contact with lucite was looked for in standar-

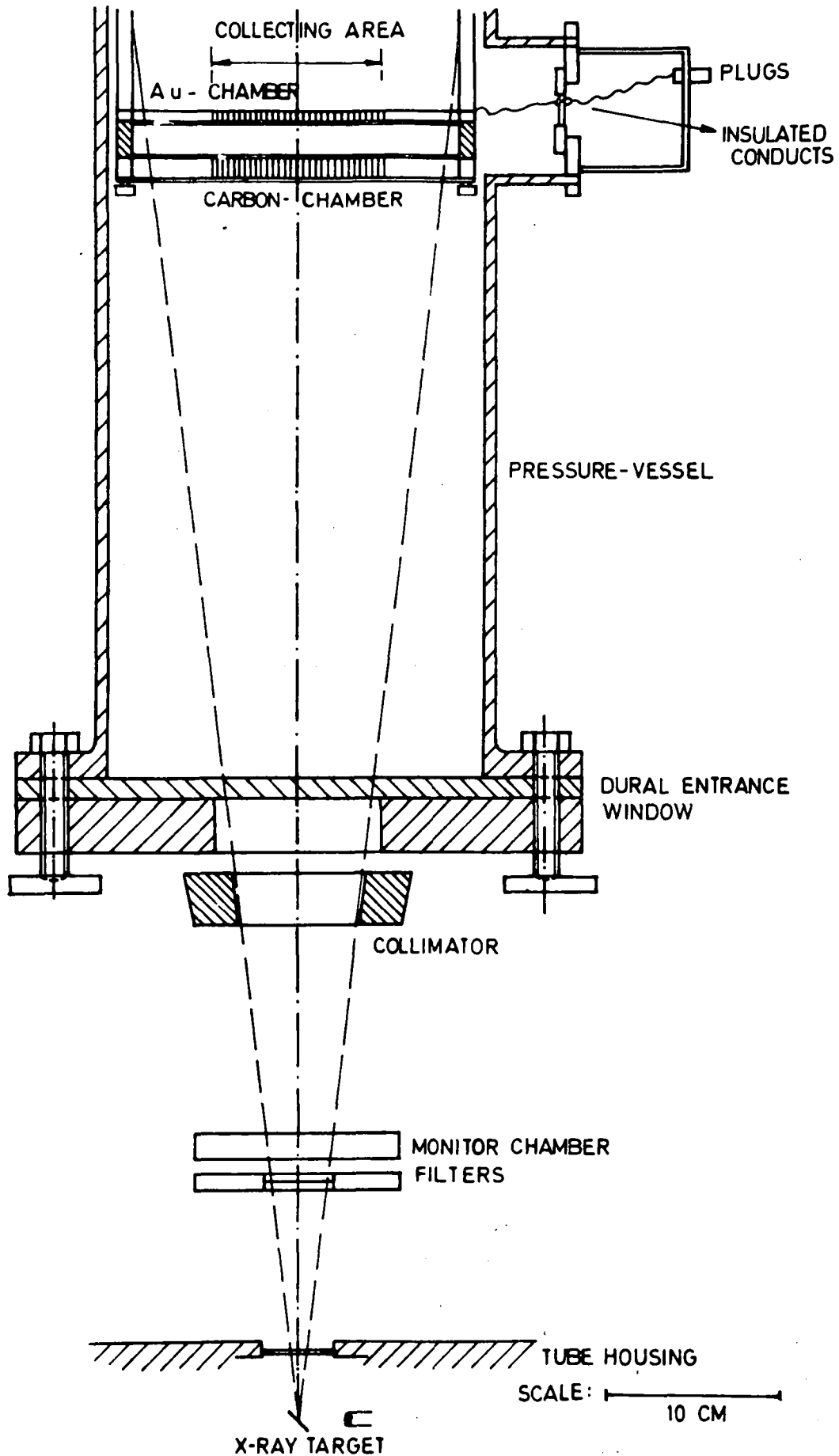


Fig.22. General lay-out of the high pressure ionisation chamber.

dized conditions without irradiation. The increase in optical density was of the order of $2 \cdot 10^{-4}$ OD units/h. Further research is in progress to determine an accurate correction for the cell history. The individual cell reproducibility is acceptable (2.5%).

The absorption spectrum of an irradiated Fricke solution has been measured and analysed.

Standard solutions were prepared to calibrate the optical density scale of the spectrophotometer. Spectral measurements on $K_2Cr_2O_7$ illustrated a small wavelength shift of the spectrum as compared to published data, whereas measurements at the absorption peaks were in agreement. The wavelengths have been carefully calibrated using a mercury arc. The difference at 302 nm was only .09 nm as compared to an instrumental tolerance of .5nm. The comparison for $K_2Cr_2O_7$ was not conclusive considering the accuracy of the available standard data. Alternatively, research was performed to improve the behaviour of an other standard solution, KNO_3 . Different KNO_3 solutions were prepared, with varying origin and grade of purity. The measurements were performed at 302 nm, the same wavelength region as for the Fe^{3+} peak.

As illustrated in figure 23, the concentration dependence of the molar extinction coefficient, ϵ , discussed in the literature, was confirmed. The error discussion, however, shows that the systematic decrease of ϵ with concentration is only slightly larger than the accuracy of our measurements. We decided to use the KNO_3 measurements as instrument calibration at a fixed concentration based upon the data of the National Physical Laboratory. Our measured value of the Fe^{3+} molar extinction coefficient corrected in this way was found to be consistent with the agreed standard value for Fricke dosimetry.

5.5. Atmospheric Pollution of ^{85}Kr

- Atmospheric measurements : An experimental set-up has been developed to separate krypton gas from air samples by an selective absorption technique.

Activity measurements and calibrations have still to be performed.

- Pollution calculations : New detailed estimates of ^{85}Kr pollution during the next 25 years have been made, based on recent prognoses and using actual atmospheric activity data. This resulted in a mean global atmospheric activity of 1. to $1.8 \cdot 10^{-9}$ Ci/m³ in the year 2000, with

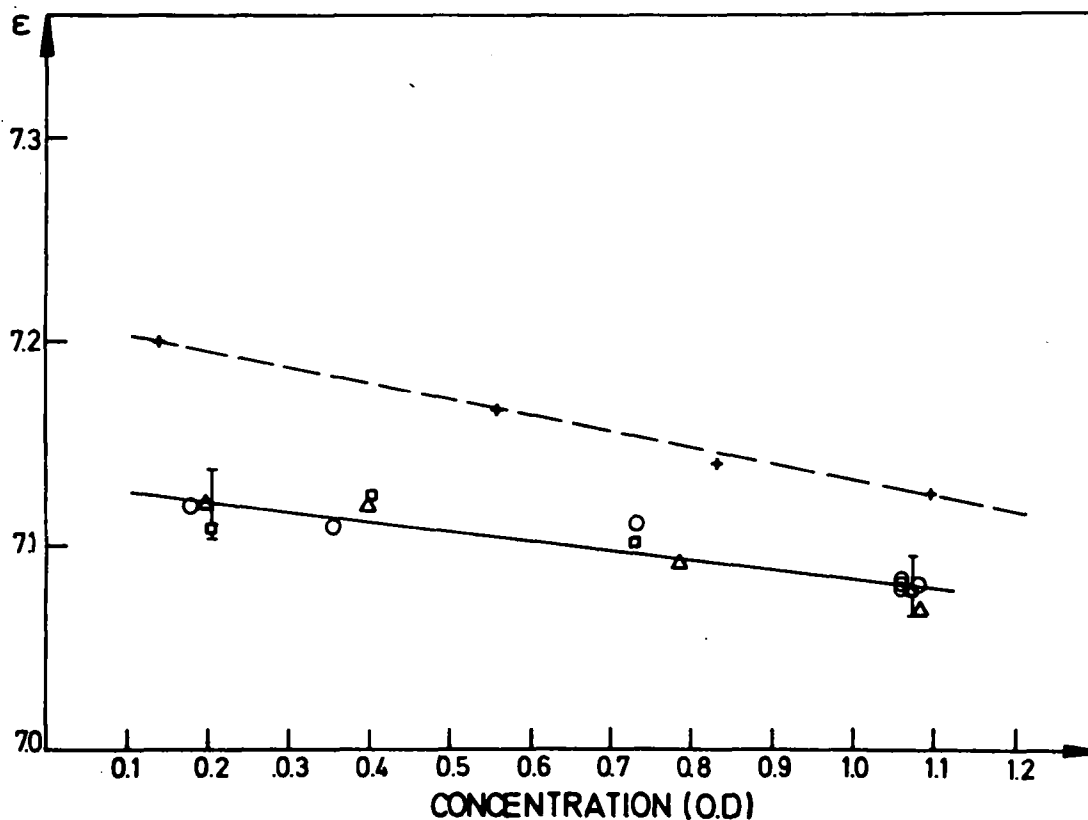


Fig.23. Dependence of the molar extinction coefficient ϵ of KNO_3 - solutions on the concentration (optical density OD)

- + : NPL (S.C.Ellis, in "Problems in Spectrophotometry and their influence in Radiation Measurements")
- ⊙ : KNO_3 pro analyse / U C B -Ghent
- ▲ : KNO_3 "Baker analyzed" /Baker - Ghent
- ◻ : KNO_3 "Suprapur" / Merck -Ghent

higher concentrations in the northern troposphere and especially around reprocessing centers. Dose calculations were performed as well. An atmospheric activity of $3 \cdot 10^{-7} \text{ Ci/m}^3$ yields values of 609 mrad/y at the skin surface, which is the most critical organ; 426.mrad/y for the epidermis; 10.8 mrad/y for the lungs and 6.5 mrad/y for the whole body dose. In our country a maximum of 20 mrad/y in the year 2000 and 60 mrad/y in 2010 are to be expected when all krypton is further released.

An optimal time program implying retention techniques mainly in reprocessing centres, has been derived in curve 3 of figure 24.

A cost-benefit analysis proved the cost-effectiveness of the proposed retention scheme, as far as the whole body equivalent skin risk of the global pollution is taken into account. Curves 1 imply 4190 to 7750 victims from which 48% should occur later than 2000. The pollution stabilisation represented in curve 3 reduces the number of victims to 300 (18% after 2000). The derived cost for the Belgian reprocessing plans should be less than .0005 BF/kwh. Alternatively the treatment of the gaseous waste creates other risks which were calculated for the Belgian nuclear program up to 1990 assuming the Kr-85 control to start in 1980. The Kr-85 waste disposal could increase up to 34 MCi in 1992. The consequences of an accidental dispersion of this quantity is calculated, at different distances, for some weather categories; the results are shown in table 3.

Table 3

Consequences in rem(maximal integrated dose equivalent)of an accidental release of 34 MCi in different Pasquill weather categories for a realistic unfavourable windspeed of 1m/s assuming continuous residence during release.

weather category	release height (m)	lateral distance (m)	axial distance (km)			
			.1	1.	3.	10.
F	0	0	($1.8 \cdot 10^6$)	950	220	50
F	0	50	0	520	200	50
F	20	0	0	250	160	45
A	0	0	1300	13	1.7	.18

The study of eventual synergistic effects of Kr-85 pollution and chemical pollution has been started.

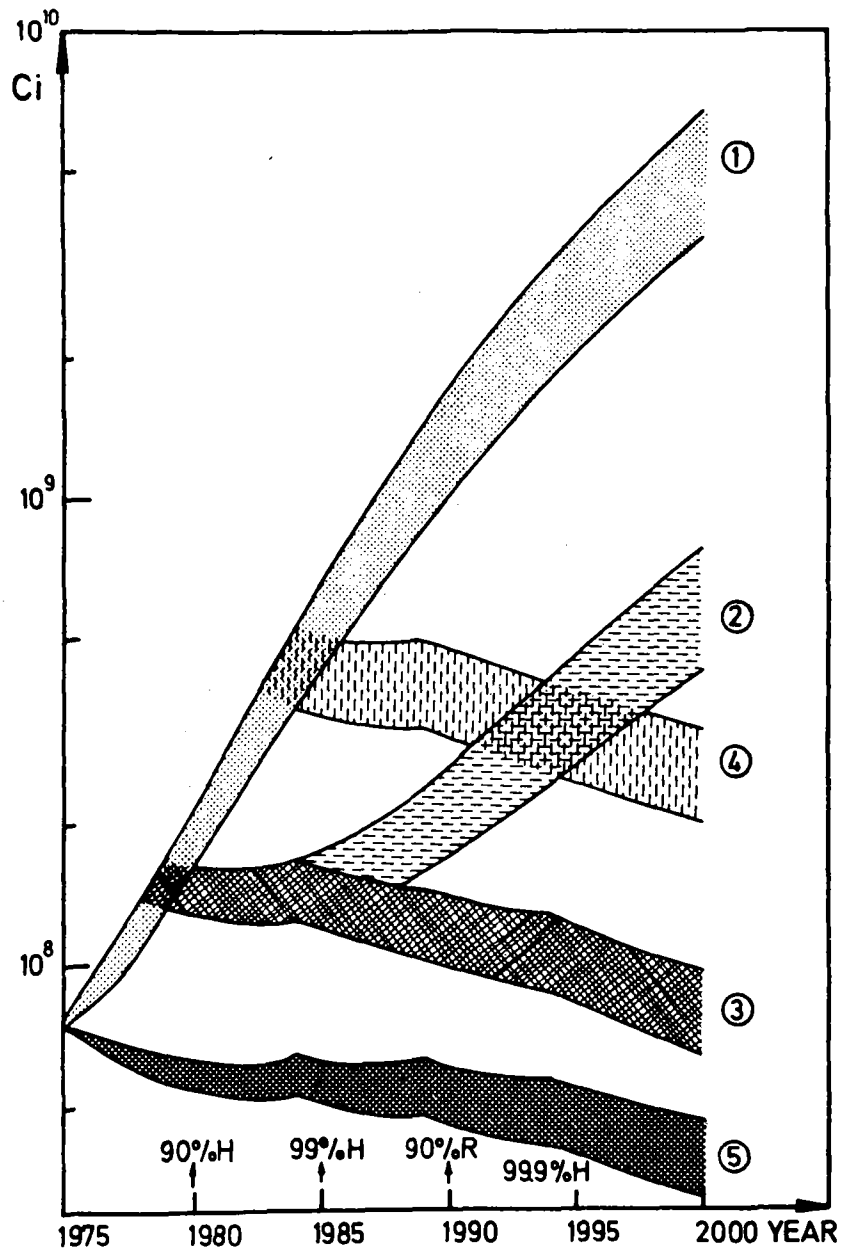


Fig.24. Cumulated ^{85}Kr activity in the atmosphere due to nuclear energy production (minimum and maximum prognoses) :

- curve 1 : total release (actual philosophy)
- curve 2 : 90% retention at reprocessing, starting in 1980
- curve 3 : 90% retention at reprocessing, starting in 1980
99% in 1985, 99.9% in 1995, and at reactorparcs,
90% in 1990
- curve 4 : same retention program as for curve 3, but started
5 years later
- curve 5 : same retention program as for curve 3, but with 5
years delay in reprocessing.

5.6. Nuclear Energy

The technical reports of the Governmental Commission dealing with the total impact of the nuclear energy development in Belgium have been studied. We attended conferences and public debates on nuclear energy problems.

The radiological consequences of radium and radon pollution by the nuclear and fossil fuel cycles for electricity production have been compared. The radium-activity released through 1000 MWe electricity production is of the same order for both energy sources. The radon -and daughter pollution, however, is essentially located at the tailing piles of uranium mines and contributes orders of magnitude more than the amount released in coal electricity plants. The radon emanation remains constant for thousands of years unless expensive sand covering is applied.

6. NUCLEAR THEORY

(K.Heyde, M.Waroquier, H.Vincx and P.Van Isacker

in collaboration with

* D.Fossan, R.Shroy, M.Gai, SUNY, Stony Brook, New York

* D.Meyer, Lawrence Livermore Laboratory, Univ. of California

{ S.Gales, M.Vergnes, IPN, Orsay

* P.Glaudemans, J.Koops, Fysisch. Laboratorium, Utrecht

{ V.Paar, Institute Ruder Boskovic, Zagreb

6.1. Coexistence of spherical and deformed states near closed shells

6.1.1. *Unified description of odd-mass In nuclei*

Many difficulties occurred up to now in trying to explain the nuclear structure of the odd-mass In isotopes in either spherical hole-core coupling or deformed (Nilsson model) descriptions. According to the hole-core coupling calculations, the single-hole excitations $1g_{9/2}^{-1}$, $2p_{1/2}^{-1}$, $2p_{3/2}^{-1}$ as well as the one quadrupole phonon multiplet $|1g_{9/2}^{-1} 2_1^+, JM\rangle$ can be well understood, and several attempts have been performed with considerable success. Additional experimental evidence, however, opposes a complete understanding on the basis of hole-core coupling calculations i.e.

- i) rather strong $B(M1)$ transitions to the $J^\pi = 9/2^+$ groundstate,
- ii) the existence of low-lying ($E_x \approx 1$ MeV) $J^\pi = 1/2^+, 3/2^+, \dots, 9/2^+$ levels in the energy region corresponding with the $|1g_{9/2}^{-1} 2_1^+, JM\rangle$ multiplet,
- iii) the strongly enhanced $B(E2; 1/2_1^+ \rightarrow 3/2_1^+)$ (≈ 100 W.U.) and $B(E2; 7/2_1^+ \rightarrow 3/2_1^+)$ (≈ 55 W.U.) values in ^{115}In .
- iv) the large quadrupole moment of the $J^\pi = 3/2^+$ level,
- v) reaction studies $^{112,114,116}\text{Cd}(\tau, d)^{113,115,117}\text{In}$ clearly indicate the population of states being due mainly to 1p-2h excitations through the $Z=50$ proton closed shell.

Quite some attempts have been made to incorporate these extra states in the hole-core coupling calculations in a rather ad hoc way as being due to rotational excitations built on the $1/2^+ [431]$ Nilsson orbital.

Therefore, we have performed a unified-model calculation for the description of the odd-mass In isotopes (especially ^{115}In) without the introduction of rotational states and the particle-core (Cd) coupled configurations as unspecified states. All single-hole ($1g_{9/2}^{-1}$, $2p_{1/2}^{-1}$, $2p_{3/2}^{-1}$, $1f_{5/2}^{-1}$) as well as 1p-2h states (seniority $\nu=1$ and $\nu=3$ with $p\pi$ ($2d_{5/2}$, $1g_{7/2}$, $3s_{1/2}$, $2d_{3/2}$, $1h_{11/2}$) are considered together with the collective excitations of the

underlying Sn-core (quadrupole as well as octupole phonons). We perform the calculation, however, in a two-step procedure in which first the Cd nuclei are treated in a hole-core (Sn) coupling calculation. Afterwards, the hole-core (Sn) as well as particle-core (Cd) configurations are treated simultaneously, thereby knowing the precise structure of the Cd-core state and their relation with the hole-core (Sn) configurations. The simplification towards the numerical simpler phenomenological hole-core (Sn) + particle-core (Cd) calculation is discussed and the limited validity of the assumptions for these calculations, as performed by Abecasis et al., is pointed out. Detailed results for ^{115}In concerning energy spectra (fig.25), electromagnetic properties, spectroscopic factors for both stripping and pick-up reactions are obtained and have been compared with the experimental data and with earlier calculations. Comparison with a rotational explanation for the $J^\pi = 1/2^+, 3/2^+$ sequence of states is also made and its strong resemblance with the unified-model calculations pointed out. We also performed calculations in a deformed basis (Nilsson-model) in order to look for an alternative description for the "intruder" states. A complete bandmixing calculation for all $N=4$ harmonic oscillator Nilsson orbitals, corresponding with the equilibrium deformation for the $1/2^+ [431]$ orbital, is performed (fig.26) and compared with the experimental results and with earlier attempts of describing these low-lying ($0.5 < E_x < 1.5$ MeV) positive parity states as members of a pure rotational band on top of the $1/2^+ [431]$ Nilsson orbital.

Calculations for all other odd-mass In nuclei with mass number $107 \leq A \leq 119$ have been performed within the same model as discussed above.

Some of the pertinent results from these extensive calculations have already been presented at the Fall Meeting of the American Physical Society [East-Lansing, Michigan] and will be published in more detail (manuscripts are being prepared), partly in collaboration with D. Meyer [Lawrence Livermore Laboratory, University of California].

The β -decay from the odd-odd ^{118}In nucleus towards the ground state and collective excited states (one and two quadrupole phonon vibrations) has been studied, stimulated by the experimental work of H. Thierens et al. In this calculation, the wavefunction obtained for the $J^\pi = 9/2^+$ ground state of ^{117}In has been used as a description of the odd proton system. The β -decay mainly concerns the Gamov-Teller $1g_{9/2} \rightarrow 1g_{7/2}$ matrix element. Also the systematics of the odd-odd to even-even nuclei β -decay as well as β -decay within the odd-mass chain has been studied and correlated with

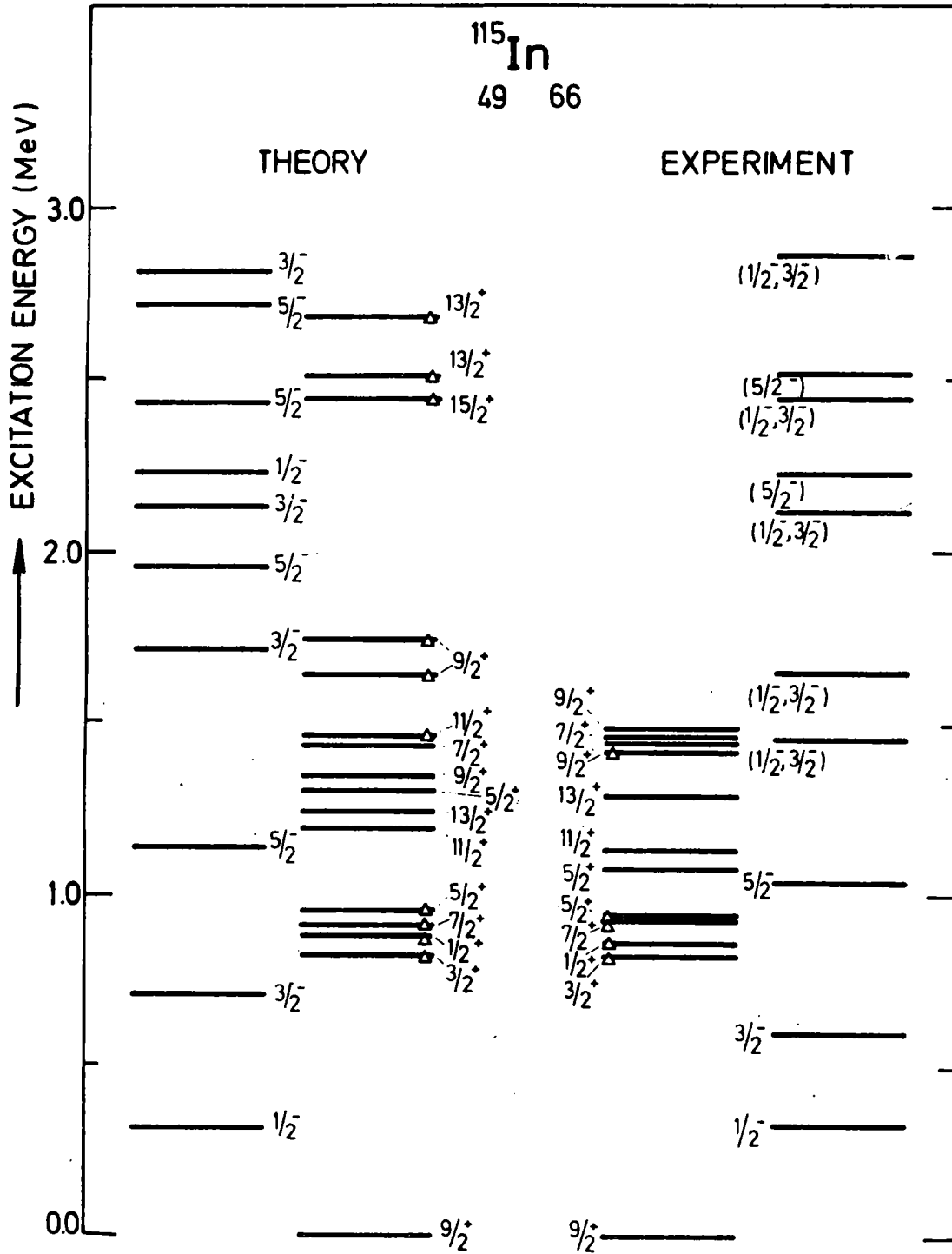


Fig.25. The negative as well as positive parity levels,calculated in a unified-model,are compared with the experimental data.Levels marked with a triangle mainly consist of particle-core(Cd) coupled configurations.

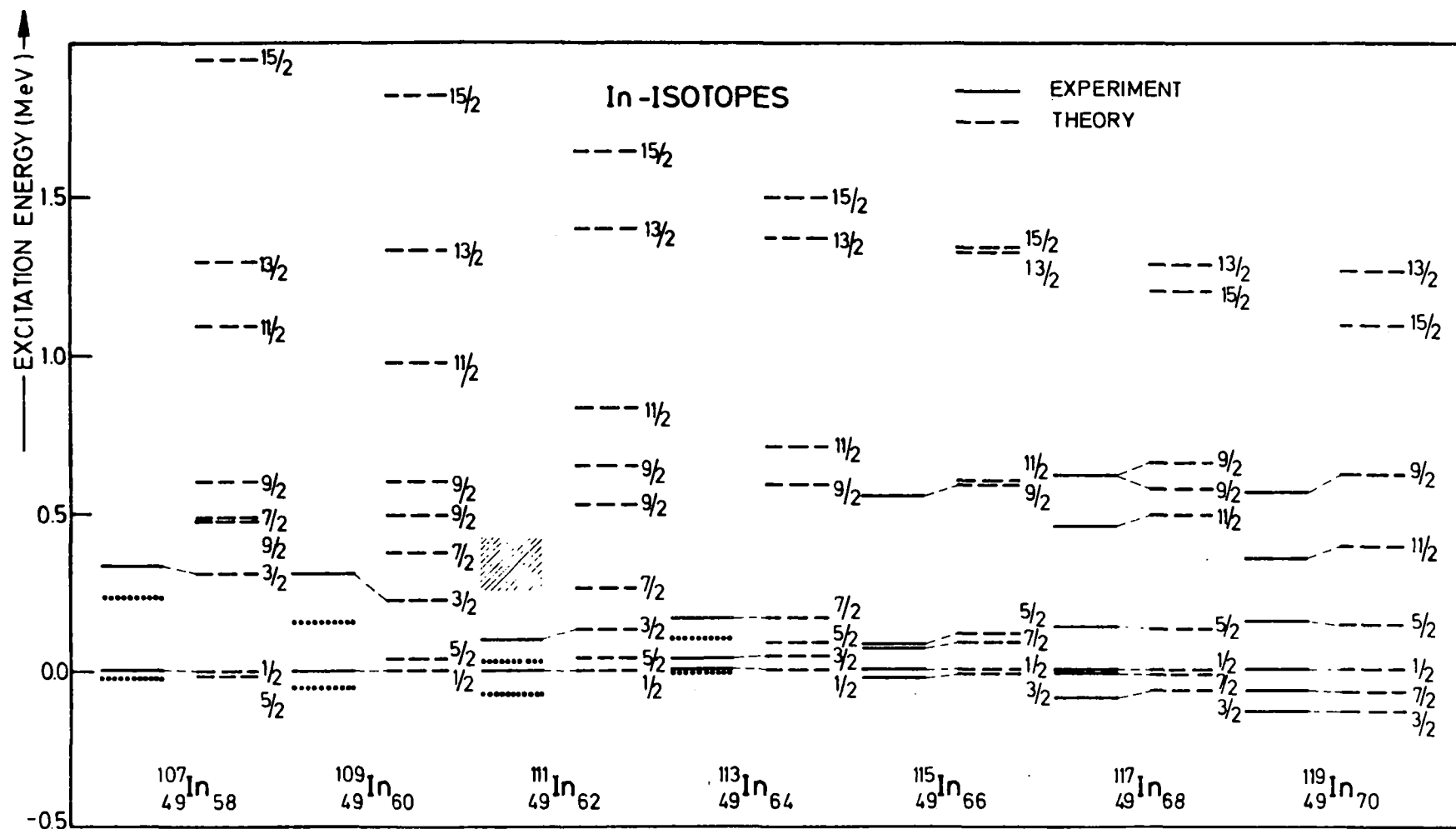


Fig.26. The results from the band-mixing calculation (full $N=4$ harmonic oscillator shell) are compared with the experimental positive parity, rotational-like levels in $^{107-119}\text{In}$. The calculation is normalized to the energy position for the $J^\pi = 1/2^+$ level. The dotted line indicates possible fragmentation for the $J^\pi=5/2^+$ levels whereas the hatched region indicates the expected position for the $J^\pi=7/2^+$ level.

$v^2_{1g_{7/2}}$, the filling of the neutron $1g_{7/2}$ single-particle state. This study, together with the results from the experimental study, has resulted in a manuscript to be published in Phys.Rev.C.

6.1.2. $J^\pi = 9/2^+$ deformed states in odd-mass Sb, I nuclei

(This work has been performed in collaboration with D.Fossan, R.Shroy and M.Cai from SUNY; Stony Brook (New-York))

The occurrence of low-lying $J^\pi = 9/2^+$ states in the odd-mass Sb, I nuclei and also of well developed rotational $\Delta J=1$ bands on top of this state has made the explanation in terms of a unified-model calculation very difficult if not impossible.

Within our systematic study of coexistence of spherical and deformed states near closed shells and by use of the macroscopic-microscopic Strutinsky renormalisation method, total potential energy (TPE) curves have been calculated for the odd-mass Sb isotopes ($113 \leq A \leq 133$) and the odd-mass I isotopes ($111 \leq A \leq 131$). In all cases, well developed minima occur for prolate quadrupole deformations ($0.15 \leq \epsilon_2 \leq 0.25$), thus giving a simple physical interpretation for the low excitation energy of these "intruder" states (1p-2h like microscopic configurations).

Also, the systematic changes of E_x with mass number is qualitatively explained for the odd-mass Sb and I isotopes.

The higher spin members of the rotational-like band structure $9/2^+ \leq J^\pi \leq 21/2^+$ have also been calculated by means of extended Coriolis coupling calculations performed at the equilibrium deformation corresponding with the $\Omega=9/2^+$ intrinsic orbital. We have taken into account all Nilsson orbitals, originating from the $N=4$ harmonic oscillator shell. As a result, a good overall reproduction of the $\Delta J=1$ rotational bands is obtained in all cases (see fig.27).

Our aim is also to calculate electromagnetic (static and dynamic) properties such as $Q, \mu, B(E2), B(M1)$, mixing ratio's, spectroscopic factors, etc. By transforming the strong coupling wave functions as obtained in a basis where the core angular momentum is a good quantum number,

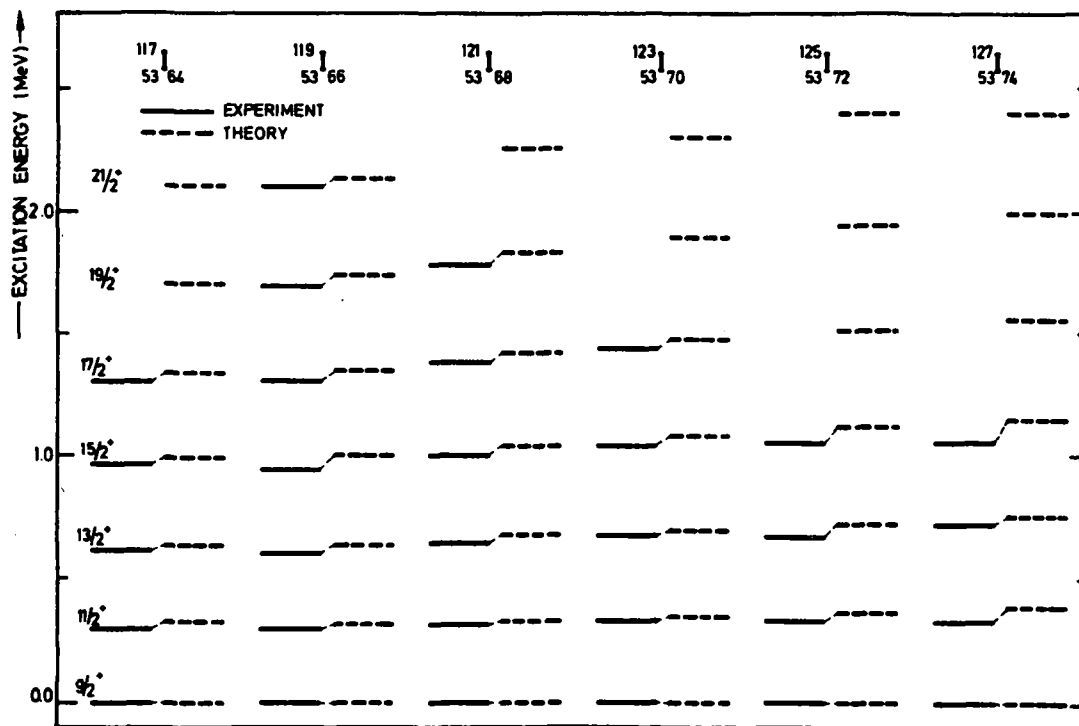


Fig.27. Comparison of experimental and theoretical band energies (relative to the band head) for the $\Delta J=1$ bands observed on the $9/2^+$ proton-hole states in odd-A I nuclei.

$$\left(|jJ_c, JM\rangle = \sum_m c_j^m \frac{M-mM}{J_c J} \left(\frac{2J_c+1}{8\pi^2}\right)^{1/2} \eta_{J_c}^{l-m,0}(\omega) \alpha_{j,m}^+ | \phi(\text{core}) \rangle \right)$$

we understand clearly why a simple unified-model calculation truncating the configuration space at 3 quadrupole phonon states fails (by transforming, core states with $J_c = 12^+, 14^+$ occur). The manuscript is being prepared for publication in Phys.Rev.C.

Calculations, in order to understand the connection with anharmonic core coupling in a schematic model (exactly solvable in perturbation theory) will be started.

6.1.3. Anharmonicities in N=81,83 isotones

A complete Hamiltonian for describing nuclei with N=81,83 neutrons and $52 < Z < 66$ has been derived. This Hamiltonian should give a good description of the

- i) collective motion of the nuclear core,
- ii) neutron excitations for the N=83 neutron particle (or N=81 neutron hole) configuration,
- iii) the modes of motion for the extra protons (protons moving outside the Z=50, N=82 core) in a quasi-particle description,
- iv) all possible interactions between modes(i),(ii) and (iii).

As possible basis states we consider up to 3 quadrupole phonon, up to 2 octupole phonon and mixed 1 quadrupole-1 octupole phonon excitations. The proton-neutron interaction, as a vital element for a good description of these nuclei, has been studied separately. A schematic δ -function force has been used for the description of proton-neutron p-p and p-h matrix-elements. The strength and the exchange mixture

$V = -V_{\text{eff}} [(1-\alpha) + \alpha \vec{\sigma}_1 \cdot \vec{\sigma}_2] \delta(\vec{r}_1 - \vec{r}_2)$, have been determined by a fit to the low-lying levels of the odd-odd nucleus $^{132}_{51}\text{Sb}_{81}$, with as a result $V_{\text{eff}} = 519.8 \text{ MeV}$, $\alpha=0.21$.

Detailed calculations have started for the nucleus $^{143}_{60}\text{Nd}_{83}$ in order to study in detail the influence of proton-neutron and quasi-particle proton core coupling interactions on the results as obtained already in a pure core-coupling description of the same nucleus (as well as for other N=83,81 isotones). Especially the redistribution of the single-particle configurations will be studied. Also, the observation of low lying ($E_x \approx 2 \text{ MeV}$) high-spin states ($15/2^- \leq J^\pi \leq 21/2^-$; $13/2^+ \leq J^\pi \leq 25/2^+$) is already noticed, as well as the very large level density above $E_x = 2 \text{ MeV}$. More detailed calculations on ^{143}Nd as well as on other N=83 isotones are in progress.

6.2. Magnetic moment of the isomeric $J^\pi = 6^+$ level in ^{134}Te

In a recent Phys.Rev.Lett. article [36 (1976)1072], Wolf and Cheifetz were able to measure the magnetic dipole moment of the $J^\pi = 6^+$ isomeric level in ^{134}Te . The value of $g_{\text{exp.}}(6_1^+) = 0.846 \pm 0.025$ can be reproduced with an effective spin gyromagnetic factor for the $1g_{7/2}$ proton single-particle orbit $g_s(1g_{7/2}) = 2.5$, a value close to effective g_s factors used for the description of N=82,81 nuclei.

Wolf and Cheifetz point out that in order to understand the quenching from the free nucleon value $g_{s,p}(1g_{7/2})$, core-polarization corrections and configurations admixtures still leave a discrepancy of 42%, when using our earlier published $J^\pi_1 = 6_1^+$ wave function.

We have shown that by taking into account in a concise way

- i) core polarization effects (proton $1g_{9/2}^{-1} 1g_{7/2}$, neutron $1h_{11/2}^{-1} 1h_{9/2}$),
- ii) modifications of the M1 operator through the velocity dependence of the average one-body potential into

$$\delta \mathcal{H}(M1, \mu) = \left(\frac{e}{4\pi}\right)^{1/2} g_l \left\{ -\frac{4\pi}{3\hbar^2} \tau^2 f(\tau) \left[(2\pi)^{1/2} [\vec{Y}_2 \otimes \vec{J}]_{\mu}^1 + \sigma_{\mu} \right] \right\}$$

$$\text{with } f(\tau) \equiv -V_{1s} \frac{\hbar^2}{4} \frac{1}{\tau} \frac{d}{d\tau} (V_{\text{WOODS-SAXON}})$$

iii) the complete wave function describing the $J_1^\pi = 6_1^+$ level in a two particle calculation,

one is able to reproduce $g_{\text{exp.}}(6_1^+)$ within the experimental error and obtain a theoretical value $g_{\text{theor.}}(6_1^+) = 0.828$.

In table 4, all separate contributions to $g_{\text{theor.}}(6_1^+)$ are given, calculated with our wavefunction and with wavefunctions as obtained by H. Wildenthal.

Table 4

Contributions	Wildenthal		This work	
(1) $g(1g_{7/2})$	0.491		0.491	
(2) $\Delta g(1g_{7/2})$ core pol.	0.223		0.223	
(3) $\Delta g(1g_{7/2})$ vel.dep $ (1h_{11/2})^2, 6^+_{\text{adm.}}\rangle$	0.060		0.060	
(4) $\Delta g(6_1^+)$ $ 2d_{5/2}1g_{7/2}, 6^+_{\text{adm.}}\rangle$	0.002		0.002	
(5) $\Delta g(6_1^+)$ (diag.)	0.043		0.027	
(6) $\Delta g(6_1^+)$ (non-diag.)	0.025	0.030	0.021	0.025
$g(6_1^+)$ (total)	0.844	0.849	0.824	0.828

6.3. Study of isobaric analog resonances (IAR) in fp-shell nuclei

[In collaboration with S.Gales, M.Vergnes (IPN, ORSAY),
P.Glaudemans, R.Koops (Fysisch Laboratorium, Utrecht) and V.Paar
(Institut Ruder Boskovic, Zagreb)]

A systematic study of the $2p_{3/2}$, $1f_{5/2}$, $2p_{1/2}$, $1g_{9/2}$ ($2d_{5/2}$) IAR has been undertaken. Part of this study i.e. the experimental work was performed at Orsay (IPN), whereas the study within the framework of the core-coupling model was started at Gent.

The nuclei considered are $^{49}_{20}\text{Ca}_{29}$, $^{51}_{22}\text{Ti}_{29}$, $^{53}_{24}\text{Cr}_{29}$, $^{55}_{26}\text{Fe}_{29}$, $^{57}_{28}\text{Ni}_{29}$ and $^{59}_{28}\text{Ni}_{31}$. In nearly all cases (except for ^{59}Ni), by coupling the neutron single-particle states outside the $Z, N=28$ core, to the low-lying quadrupole and octupole excitations, a good description of not only the energy

but also of the most important components of the wavefunctions (single particle $|2^+ @ j, J\rangle$ and $|3^- @ j, J\rangle$ amplitudes) are reproduced. In the particular case of ^{59}Ni , exact neutron 3 particle shell-model calculations have been performed by P. Glaudemans and J. Kooops at Utrecht, and 3 particle-core coupling calculations by V. Paar at Zagreb. A comparison of the results from the three calculations clearly indicates the limitations of the 1 particle-core coupling and shows the importance of the 3 particle correlations in order to reproduce the low-lying $J_1^\pi = 3/2_2^-, 5/2_2^-$ and $1/2_1^-$ levels. A general observation for the $9/2^+$ IAR is the fact that the $|3^- @ 2p_{3/2}; 9/2^+\rangle$ configuration constitutes the major component of the wavefunction. This result is also in agreement with experiment.

6.4. Microscopic nuclear structure calculations with effective three-body forces

6.4.1. *Removal of shortcomings of the Skyrme force by addition of a momentum dependent three-body interaction*

The use of Skyrme forces has become popular during the last years. Since Vautherin and Brink [Phys.Rev.C5(1972)626] have performed successfully self-consistent HF calculations on spherical doubly-closed shell nuclei with the Skyrme force as effective interaction, many investigators take the opportunity to make use of it in all possible applications: - study of spherical and deformed nuclei through the whole mass region,

- derivation of deformation ,
- energy curves (application also for fission),
- generator coordinate calculations for monopole and quadrupole vibrations,
- RPA-calculations, -etc..

It is indeed interesting to look for an effective interaction to describe both ground and excited states.

The Skyrme force in its original form exhibits some shortcomings : spin-instability, overbinding of odd-mass and odd-odd nuclei, small reduced mass, antipairing, large incompressibility. These limitations can be removed by addition of a momentum dependent three-body interaction. This addition leaves the characteristic analytical structure of the HF equations unchanged. Moreover, it gives a supplementary force parameter, of which one can dispose to vary the incompressibility and the effective mass ratio independently. It removes the shortcomings

of the original Skyrme force in the reproduction of all nuclear matter quantities. An investigation of the spin-stability in a nuclear matter model leads to a stability condition which is less severe than originally, and which is satisfied for each suitable interaction parameter choice. Difficulties concerning antipairing effects are also removed, since large repulsive t_3 - pairing matrixelements are mainly compensated by the strong attractive momentum-dependent three-body parts.

An application of a suitable parametrisation of the extended Skyrme force is represented in table 5 and figures 28 & 29. They show the results obtained after an exact self-consistent Hartree-Fock calculation on spherical double-closed shell nuclei. At any time a comparison with the best VB-parametrization (Sk III) is given. The obtained results clearly demonstrate the favourable influence arising from the addition of a momentum dependent three-body term to the original Skyrme-force: good reproduction of nuclear matter quantities, binding energies, r.m.s.-radii, nucleon density functions, level densities at the Fermi surface, etc.

6.4.2. Self-consistent treatment of pairing correlations with effective three-body forces

In nearly all calculations performed self-consistently with Skyrme interactions, pairing correlations have not been taken into account. In the few cases where they are included, one has treated them by introducing a constant pairing-force, resulting in an additional constant pairing energy contribution to the HF ground state energy. The correct way is, however, to carry out complete HFB calculations. In this spirit, we have extended the HFB-formalism with explicit inclusion of three-or more-nucleon interactions. Since these interactions contain implicitly the nucleon density information, it constitutes a method of treating density-dependent forces in microscopic calculations.

In the development of the extended HFB-formalism the three-body interaction introduces additional energy contributions to the self-consistent HF-potential and to the pairing energy. The pairing effect can be studied separately in the HF-BCS procedure, consisting in a two-step minimization. Besides an additional three-body contribution to the BCS-selfenergies, the single-particle energies are supplementary corrected by a specific three-body pairing energy term. It is obvious, that in view of this extension, the BCS-quantities establish a nucleon density-dependence. The Skyrme-force in its original form cannot be used for a self-consistent

I	t_0 [MeV fm ³]	t_1 [MeV fm ⁵]	t_2 [MeV fm ⁵]	t_3 [MeV fm ⁶]	t_4 [MeV fm ⁶]	x_0	W_0 [MeV fm ³]		
Sk III	-1128.75	395	-95	14000	0	0.45	120		
SkE1	-1272.76	806.08	-3040	15065.68	-11727.51	0.158	120		
	K [MeV] incompressibility	$\frac{E}{A}$ (nucl matt) [MeV]	k_F [fm ⁻¹]	$\frac{m^*}{m}$ reduced mass ratio	a_T [MeV] spin sym- metry energy	α [MeV] spin stability coefficient	$\frac{E}{A}$ (HF) [MeV] ¹⁶ O	$\frac{E}{A}$ (HF) [MeV] ⁴⁰ Ca	$\frac{E}{A}$ (HF) [MeV] ²⁰⁸ Pb
Sk III	356	-15.87	1.29	0.76	28.2	36.8	-8.03	-8.57	-7.87
SkE1	230	-16.00	1.33	0.61	29.0	15.9	-7.95	-8.55	-7.86
Exp.							7.98	-8.55	-7.87

Table 5. The parameters for Skyrme III and the extended Skyrme(SKE1) interactions. Nuclear matter quantities as well as the binding energy for finite nuclei, calculated with both parametrizations, are compared with each other and with the experimental data.

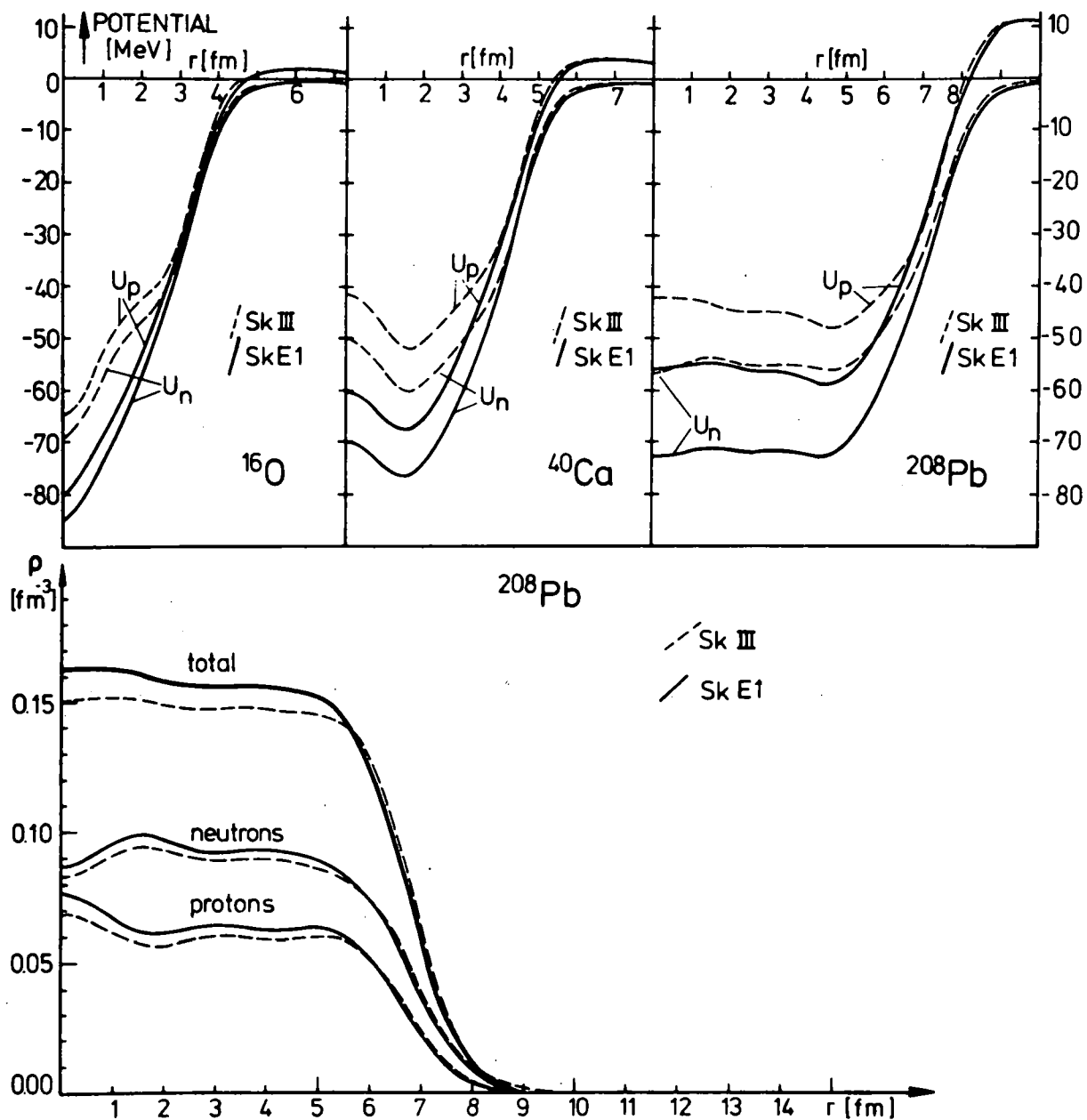


Fig.28. The self-consistent proton and neutron potential (U_p , U_n) as determined with the Skyrme III and with the extended Skyrme interaction (SKE1). For ^{208}Pb also the self-consistent proton, neutron and total densities are given.

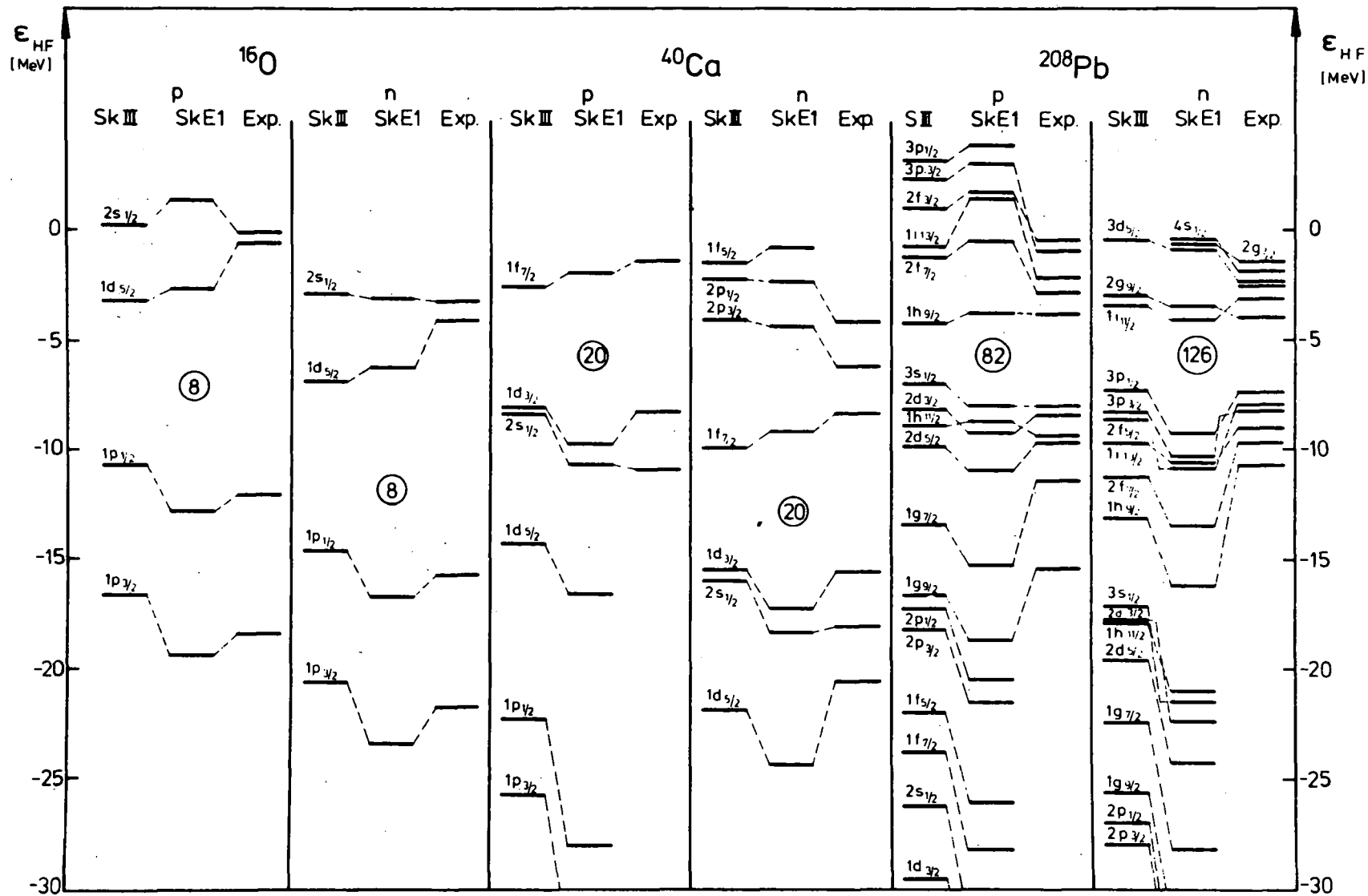


Fig.29. The Hartree-Fock energies (ϵ_{HF}) for proton (p) as well as neutron (n) orbits, as determined with the Skyrme III and extended Skyrme interactions(SKE1)are compared with the Hartree-Fock energies determined from experiment.

treatment of pairing correlations, as it exhibits antipairing effects due to strong repulsive pairing matrixelements from the three-body part. An extension of the force, as proposed in 6.4.1., removes this restriction: the strong attractive contributions from the momentum-dependent three-body force make the pairing matrixelements realistic and allow us to perform self-consistent HF + BCS calculations with the use of the same effective interaction. It opens the way to describe ground and excited states with the same effective nucleon-nucleon force.

6.5. Dissipation in quantum mechanical systems with inclusion of collective motion

The study of dissipative phenomena in nuclei has been continued. We have concentrated mainly on dissipative effects in nuclear collective motion due to the coupling between intrinsic and collective degrees of freedom. Especially, we have studied unbound collective motion, i.e. the collective motion to which a continuous energyspectrum is associated (this occurs for heavy ion collisions, in nuclear fission where the distance between both fragments is interpreted as the collective coordinate). We make use of a set of basis states, characterized by the collective coordinate and a quantum number specifying the intrinsic structure of the nucleus. As the collective coordinate acts as a continuous variable, the energy spectrum associated with the set of basis states will also be continuous. Also, the basis states are chosen to be smooth functions of the collective coordinate.

Within this particular representation, a Hamiltonian results which consists of a potential (local and non-local) energy term, a kinetic energy contribution for the different intrinsic states of the nucleus as well as residual interactions (local and non-local) between the different intrinsic states. The zero-order eigenvectors have been determined and contain information about the collective motion whereas the higher mentioned basis states contain information about the intrinsic motion of the nucleus for each value of the collective coordinate. Making use of an expansion for the total wavefunction in a series of products of intrinsic and collective basis states, the evolution of the system is formulated by making use of the time-dependent Schrödinger equation. This leads to a description within the Hilbert space. In order to make comparisons possible with a statistical-kinetic description (by means of transport equations), the evolution of the system

has been formulated within the Liouville-space. Therefore, the density matrix of the system has been expanded in a basis obtained by constructing the appropriate tensorproducts of the higher mentioned basis states and the adjoint basis. Use has been made of generalized Zwanzig-projection operators, chosen in order to separate phase differences between different intrinsic states, from phase differences within the same intrinsic state. This choice implies a clear difference in treating the collective "ordered" motion and the "not ordered" evolution of intrinsic phase correlations. Eliminating the intrinsic phase correlations, a generalized transport equation for the local (statical) and non-local (kinetic) occupation probabilities for the intrinsic motion is obtained. Within this approach, collective and intrinsic motion are treated in a unified way. Dissipation now occurs because of the fact that the coupling between the intrinsic states of motion within the generalized transport equation is determined by a generalized non-Hermitean collision operator (up to second order). Time irreversible dissipation is warranted because of the continuous spectrum, associated with the unbound collective motion, and not because of the infinite number of degrees of freedom (which is the case in many other systems).

Moreover, the density matrix has been transformed to a new representation in which the general dynamical effects of the residual interaction have been taken into account. This transformation has been chosen such that for a discrete spectrum an exact equivalence occurs with the transformation that diagonalises the Hamiltonian. For a continuous spectrum the transformed Liouvillian is not exactly diagonalised but already exhibits a non-zero transformed collision operator (with a more symmetric structure than before the transformation). Such transformation is (most generally) not unique. For the determination, dynamic-collective as well as statical-collective arguments can be used, giving rise to simple results (physical interpretation) in the limit of weak and strong coupling respectively. At this moment, it is not exactly clear whether a connection exists between both transformations or if a generalization exists, implying a reduction of the separate transformations in the limit of weak and strong coupling.

PUBLICATIONS BY MEMBERS OF THE LABORATORY-1976

1. Normalisation of the ^{241}Pu fission cross section
A.J.Deruytter
Proceedings of an Advisory Group Meeting on Transactinium Isotope Nuclear Data, IAEA (Vienna 1976), Transactinium Isotope Nuclear Data (TND) IAEA-186-Vol.II p.77
2. The ^{241}Pu neutron induced fission cross-section from 0.01 eV to 50 eV and its normalisation
C.Wagemans and A.J.Deruytter
Nuclear Cross Sections and Technology, National Bureau of Standards Special Publication, NBS SP 425 Vol.II (1975) p. 603-606
3. Measurement and normalization of the relative Plutonium - 241 fission cross section in the thermal and low resonance energy region
C.Wagemans and A.J.Deruytter
Nucl.Science and Eng., 60 (1976) 44
4. Fragment mass and kinetic energy distribution for the photofission of ^{235}U and ^{238}U with 25-MeV end-point bremsstrahlung
A.De Clercq, E.Jacobs, D.De Frenne, H.Thierens, P.D'hondt and A.J. Deruytter
Phys.Rev. C13 (1976)1536
5. Study of the catcherfoil technique with the aid of ^{252}Cf s.f. and $^{235}\text{U}(n_{\text{th}},f)$
H.Thierens, D.De Frenne, E.Jacobs, A.De Clercq, P.D'hondt and A.J. Deruytter
Nucl.Instr. 134 (1976) 299
6. Product yields for the photofission of ^{235}U and ^{238}U with 25-MeV bremsstrahlung
H.Thierens, D.De Frenne, E.Jacobs, A.De Clercq, P.D'hondt and A.J. Deruytter
Phys.Rev. C14 (1976)1058
7. Neutron emission in the photofission of ^{235}U and ^{238}U with 25-MeV bremsstrahlung
E.Jacobs, H.Thierens, A.De Clercq, D.De Frenne, P.D'hondt and A.J. Deruytter
Phys.Rev. C14 (1976) 1874
8. The thermal neutron induced fission cross section of ^{232}Th
C.Wagemans, P.D'hondt, A.J.Deruytter, M.Asghar and A.Emsalleem
Nucl.Phys. A259 (1976) 423
9. The $^{238}\text{U}(n,\alpha)^{235}\text{Th}$ reaction with thermal neutrons
M.Asghar, A.Emsalleem, R.Chery, C.Wagemans, P.D'hondt and A.J.Deruytter
Nucl.Phys. A259 (1976) 429

10. Mesure et calcul de la section efficace de fission induite par neutrons thermiques en-dessous du seuil pour quelques noyaux lourds
C.Wagemans, P.D'hondt, A.J.Deruytter, M.Asghar et A. Emsalleem
Rapport BLG-514(1976)
11. An absolute recoil-proton photoneutron spectrometer using a Monte Carlo calculated efficiency
J.Devos, R.Van de Vyver, E.Van Camp, R.Carchon & H.Ferdinande
Nucl.Instr. & Meth.135(1976)395
12. Photoproton cross section and angular distributions for ^{12}C in the giant dipole resonance region
R.Carchon, R.Van de Vyver, H.Ferdinande, J.Devos & E.Van Camp
Phys.Rev.C14 (1976)456
13. Ground state transitions from the giant dipole resonance
N.K.Sherman, K.H.Lokan, C.K.Ross & H.M.Ferdinande
Bull.Am. Phys.Soc.21 (1976)517
14. Ground and first excited state transitions in the $^{208}\text{Pb}(\gamma, n)$ reaction
N.K.Sherman, K.H.Lokan, C.K.Ross & H.M.Ferdinande
Bull.Am. Phys.Soc.21 (1976)777
15. Ground state transitions from the giant dipole resonance
K.H.Lokan, N.K.Sherman, C.K.Ross & H.M.Ferdinande
Bull.Am. Phys.Soc.21(1976)777
16. Temperature Dependence of Positron Annihilation Parameters in Solid Gallium
D.Segers, C.Dauwe, M.Dorikens and L.Dorikens-Vanpraet
Applied Physics 10 (1976) 121
17. Recent developments in general cavity theory
A.Janssens, G.Eggermont and R.Jacobs
Proc. of 5th Sympos. on Microdosimetry, EUR5452 II(1976)1067
18. De Kr-85 pollutie door de nucleaire industrie
G.Eggermont
Technisch Rapport, Commissie van Beraad inzake Kernenergie, Min.Ekon.Zak., groep VI Gezondheid, Deel 1 (1976)360
19. Ongevalsrisico's bij drukwaterreactoren
G.Eggermont
Technisch Rapport, Commissie van Beraad inzake Kernenergie, Min.Ekon.Zak., groep VI, Gezondheid, Deel 2 (1976)568

20. Antisymmetry in the three body interaction matrix elements
M.Waroquier, K.Heyde and H.Vincx
Phys.Rev.C13(1976)1664
21. On the systematics of the $1i_{13/2}$ single-particle state in
N=83 isotones
K.Heyde, M.Waroquier and H.Vincx
Int.Symp.on Nuclear Structure, Proceedings (Budapest 1976)
Vol.II, p.557
22. Microscopic structure from scattering through isobaric analogue
resonances
K.Heyde, M.Waroquier and H.Vincx
Physics Reports 26C(1976)229
23. Coexistence of spherical and deformed states near closed shells
K.Heyde, M.Waroquier, P.Van Isacker and H.Vincx
Phys.Lett.64B (1976)135
24. On the equivalence of vibrational and rotational descriptions of
odd-mass In isotopes
K.Heyde, M.Waroquier, P.Van Isacker and H.Vincx
BAPS 21 (1976)1003
25. Unified description of odd-mass In nuclei
K.Heyde, M.Waroquier, P.Van Isacker and H.Vincx
BAPS 21(1976)1002
26. De atmosferische pollutie van ^{85}Kr door de nucleaire energie
G. Eggermont, R. Jacobs and A. Janssens
Annalen van de Belgische Vereniging voor Radioprotectie 1 (1976) 275

PUBLICATIONS IN PRINT

1. The neutron induced fission cross-section of ^{235}U in the energy region from 0.008 eV to 30 keV
C.Wagemans and A.J.Deruytter
Annals of Nuclear Energy (1977)
2. Study of the fission products of $^{235,238}\text{U}$ by irradiation with 25-MeV bremsstrahlung
H.Thierens, D.De Frenne, E.Jacobs, A.De Clercq, P.D'hondt and A.J.Deruytter
Proceedings of the conference on the physics of tandem, Triëste (27-30 april 1976)
3. A versatile camac based linear PHA system
A.De Clercq, E.Jacobs, D.De Frenne, H.Thierens, P.D'hondt and A.J.Deruytter
Nucl.Instr.(submitted for publication)
4. Study of the excited states in ^{118}Sn by the β^- decay of $^{118\text{g}}\text{In}$
D.De Frenne, H.Thierens, E.Jacobs, P.D'hondt, A.De Clercq, K.Heyde and A.J.Deruytter
Phys.Rev.C. (submitted for publication)
5. Study of some characteristics of the thermal neutron sub-barrier fission of ^{231}Pa , ^{232}Th and ^{237}Np
C.Wagemans, M.Asghar, P.D'hondt, A.J.Deruytter and A.Emsallem
Nucl.Phys.(1977)
6. Photoneutron cross sections in ^7Li
H.Ferdinande, N.K.Sherman, K.H.Lokan & C.K.Ross
Can.J.Phys. 55 (1977)
7. Fine Structure in the $^{208}\text{Pb}(\gamma, n)$ Cross Section
R.Van de Vyver, J.Devos, H.Ferdinande, R.Carchon & E.Van Camp
Phys.Rev.C (1977)
8. Positron trapping in Indium
D.Segers, L.Dorikens-Vanpraet and M.Dorikens
Applied Physics
9. On the Effect of Thermal Expansion on Positron Annihilation Lineshape Factors
D.Segers, C.Dauwe, M.Dorikens and L.Dorikens-Vanpraet
Phys.Stat.Sol.(a)
10. W.A.C.:an alternative Method to measure Positron Annihilation Parameters
M.Dorikens, C.Dauwe, D.Segers and L.Dorikens-Vanpraet
Nucl.Inst. and Meth.

11. Electro-Optical Stabilization of a subnanosecond Lifetime Spectrometer
J.Uyttenhove, D.Segers, M.Dorikens and L.Dorikens-Vanpraet
Nucl.Inst. and Meth.
12. The hazards of particle fluence to current conversion
A.Janssens
Health Physics
13. On pollution hazards
G. Eggermont
Physics To-day (1977)
14. A unified description of odd-mass In isotopes
K. Heyde, M. Waroquier, P. Van Isacker and H. Vincx
Submitted to Nuclear Physics
15. Deformed $9/2^+$ proton-hole states in odd-A I nuclei
D.B. Fossan, M. Gai, A.K. Gaigalas, D.M. Gordon, R.E. Shroy, K. Heyde,
M. Waroquier, H. Vincx and P. Van Isacker
Phys. Rev. C (1977)
16. Removal of shortcomings of the Skyrme force by addition of a momentum dependent three-body interaction
M. Waroquier, K. Heyde, P. Van Isacker and H. Vincx
Phys. Lett. (1977)
17. Magnetic moment of the $J^\pi=6^+$ isomeric level in ^{134}Te
K. Heyde, M. Waroquier, P. Van Isacker and H. Vincx
Phys. Rev. C (1977)

CONFERENCE OR SYMPOSIA CONTRIBUTIONS

1. Conference on the physics of tandem, Triëste (27-30 April 1976)
Study of the fission products of ^{235}U , ^{238}U by irradiation with 25-MeV bremsstrahlung
H.Thierens, D.De Frenne, E.Jacobs, A.De Clercq, P.D'hondt and A.J. Deruytter
2. Journées d'études sur la fission, Aussois (24-26 Mai 1976)
La fission de ^{235}U et ^{238}U par photons de bremsstrahlung avec une énergie maximale de 25 MeV
E.Jacobs, D.De Frenne, A.De Clercq, H.Thierens, P.D'hondt et A.J. Deruytter
3. Journées d'études sur la fission, Aussois (24-26 Mai 1976)
Mesure et calcul de la section efficace de fission induite par neutrons thermiques en-dessous du seuil pour quelques noyaux lourds
C.Wagemans, P.D'hondt, A.J.Deruytter, M.Asghar et A.Emsalleem
4. Algemene Wetenschappelijke Vergadering van de B.N.V., Louvain-La-Neuve (3-4/6/1976)
Neutronenemissie $\bar{\nu}$ (m^*) voor de fotofissie van ^{235}U en ^{238}U met 25 MeV bremsstrahlung
E.Jacobs, H.Thierens, A.De Clercq, D.De Frenne, P.D'hondt en A.J. Deruytter
5. Algemene Wetenschappelijke Vergadering van de B.N.V., Louvain-La-Neuve (3-4/6/1976)
Studie van het β^- verval van ^{118g}In via de fotofissie van ^{238}U
D.De Frenne, H.Thierens, E.Jacobs, P.D'hondt, A.De Clercq en A.J.Deruytter
6. Algemene Wetenschappelijke Vergadering van de B.N.V., Louvain-la-Neuve (3-4/6/1976)
Onderzoek van door thermische neutronen in ^{237}Np geïnduceerde fissie
C.Wagemans, P.D'hondt, A.J.Deruytter, M.Asghar en A.Emsalleem
7. Algemene Wetenschappelijke Vergadering van de B.N.V., Louvain-la-Neuve (3-4/6/1976)
Studie van de reacties $^{237}\text{Np}(n,\alpha)$ en $^{238}\text{U}(n,\alpha)$
P.D'hondt, C.Wagemans, A.J.Deruytter, M.Asghar, A.Emsalleem en R.Chery
8. Seminarium Fysika SCK/CEN-Mol (6/5/1976)
Photofission studies on ^{235}U and ^{238}U with 25-MeV bremsstrahlung
E.Jacobs, D.De Frenne, A.De Clercq, H.Thierens, P.D'hondt and A.J.Deruytter

9. Spring Meeting of the American Physical Society-Washington D.C.
(26-29/4/76)
Ground state transitions from the giant dipole resonance
N.K.Sherman, K.H.Lokan, C.K.Ross & H.M.Ferdinande

10. CAP-APS-SMF Joint Congress - Laval University, Québec(14-17/6/76)
Ground and first excited state transitions in the $^{208}\text{Pb}(\gamma, n)$
reaction
N.K.Sherman, K.H.Lokan, C.K.Ross & H.M.Ferdinande

11. CAP-APS-SMF Joint Congress-Laval University, Québec(14-17/6/76)
Ground state transitions from the giant dipole resonance
K.H.Lokan, N.K.Sherman, C.K.Ross & H.M.Ferdinande

12. Algemene Wetenschappelijke Vergadering van de BNV, Louvain-la-Neuve
(3-4/6/76)
Calculation of the neutron efficiency of an organic scintillator
using a Monte Carlo method
J.Devos, R.Van de Vyver, E.Van Camp, R.Carchon & H.Ferdinande

13. Algemene Wetenschappelijke Vergadering van de BNV, Louvain-la-Neuve
(3-4/6/76)
Fine structure in the total (γ, n) cross section for ^{208}Pb
R.Van de Vyver, J.Devos, R.Carchon, E.Van Camp & H.Ferdinande

14. Algemene Wetenschappelijke Vergadering van de B.N.V., Louvain-la-Neuve
(3-4/6/76)
Meting van Positron annihilatie levensduren en lijnvormfactoren
in neutronen-bestraald Aluminium
D.Segers, M.Dorikens, L.Dorikens-Vanpraet, C.Dauwe, A.Deruytter
J.Cornelis, J.Nihoul, J.Roggen en L.Stals

15. Algemene Wetenschappelijke Vergadering van de B.N.V., Louvain-la-Neuve
Positron annihilatie lijnvormfactormetingen in Indium
D.Segers, M.Dorikens en L.Dorikens-Vanpraet

16. Fourth International Conference on Positron Annihilation, Helsingør,
Denmark (23-26/8/76)
Positron Annihilation study of neutron-irradiation induced voids
in Aluminium
D.Segers, M.Dorikens, L.Dorikens-Vanpraet and C.Dauwe

17. Fourth International Conference on Positron Annihilation, Helsingør,
Denmark(23-26/8/76)
W.A.C.: an alternative method to measure positron annihilation
parameters
M.Dorikens, C.Dauwe, D.Segers and L.Dorikens-Vanpraet

18. Fourth International Conference on Positron Annihilation
Helsingør, Denmark (23-26/8/76)
On the evidence of positron self-trapping in Indium
D.Segers, M.Dorikens and L.Dorikens-Vanpraet

19. Belg.Veren.Stralingsbescherming, IRE, Fleurus (1976)
De atmosferische pollutie van ^{85}Kr door de nucleaire energie
Eggermont G, Jacobs R. and Janssens A.

20. VIII Congrès Intern.de la Société Franc. de Radioprotection
Saclay(1976)
Cavity theory, a general formulation of the problem and a proposal
for practical application
A.Janssens, G.Eggermont and R.Jacobs

21. VIII Congrès de la Soc.Franc.Radioprot., Saclay (1976)
Dosimetry of high energy electrons and X-rays at the linear accelerator
in Ghent
R.Jacobs, E.Cottens, G.Eggermont, A.Janssens and G.Thielens

22. Algemene Wetenschappelijke Vergadering van de B.N.V., Louvain-la-Neuve
(3-4 juni 1976)
Aequivalentie van vibrationele en rotationele beschrijvingen der In-
isotopen
K.Heyde, M.Waroquier, P.Van Isacker en H.Vincx

23. Algemene Wetenschappelijke Vergadering van de B.N.V., Louvain-la-Neuve
(3-4 juni 1976)
Coexistentie van sferische en gedeformeerde toestanden
K.Heyde, M.Waroquier, H.Vincx en P.Van Isacker

24. Réunion du Comité Scientifique du Tandem d'Orsay(4-5 mai 1976)
Isobaric analogues resonances in fp-shell nuclei
K.Heyde

25. Fall Meeting of the American Physical Society, East Lansing(Michigan)
(28-30 October 1976)
Unified description of odd-mass In nuclei
K.Heyde, M.Waroquier, P.Van Isacker and H.Vincx

26. Fall Meeting of the American Physical Society, East Lansing(Michigan)
(28-30 October 1976)
Equivalence of vibrational and rotational descriptions of odd-mass
In isotopes
K.Heyde, M.Waroquier, P.Van Isacker and H.Vincx

27. SUNY, Stony Brook, New York (26 October 1976)
Unified description of spherical and deformed states near closed shells
K.Heyde

NOT FOR PUBLICATION

INDC (Can)-18/G

PRIVATE COMMUNICATION ONLY

Not to be quoted, abstracted, reproduced or transmitted to libraries. The information contained, which may be only of a preliminary nature, should be used with discretion.

ATOMIC ENERGY OF CANADA LIMITED
CANADIAN PROGRESS REPORT TO THE INDC
(October, 1975 to April, 1977)

Compiled by
W.G. Cross

Chalk River, Ontario

April 15, 1977

NOT FOR PUBLICATION

ATOMIC ENERGY OF CANADA LIMITED
CHALK RIVER NUCLEAR LABORATORIES

Thermal Neutron (n, α) Reactions

D.C. Santry and R.D. Werner

Confirmation of our measurements of the $^{59}\text{Ni}(n,\alpha)$ thermal neutron cross section (INDC(Can)-14/G) has been made recently by McDonald and Sjöstrand ¹. In their work, two additional peaks were observed in the charged particle spectrum. One peak at 1.82 MeV was assumed to be due to proton emission and was assigned a cross section value of ~ 5 barns*. Another peak at 0.9 MeV was unassigned.

We have repeated our measurements using a " ^6Li -free" surface barrier α detector and were unable to confirm the presence of additional peaks. However, the low-energy background continuum observed with the α detector made it difficult to resolve statistically low-intensity peaks at energies below 2 MeV. We were able to show that the source of the background continuum was γ rays from neutron capture in surrounding materials. A better signal to background ratio could be obtained using an external neutron beam from the NRU crystal spectrometer.

(1) J. McDonald and N.G. Sjöstrand, Bull. Am. Phys. Soc. 20,
168 (1975)

Thermal Neutron Cross Section for ^{125}I

D.C. Santry and R.D. Werner

The ^{126}I contaminant, formed by neutron capture during production of ^{125}I , restricts the usefulness of ^{125}I in diagnostic medicine. A more accurate value of the capture cross section would help in keeping the contamination level within acceptable limits.

The activity depletion method was used to measure the

* 1 barn = 10^{-28} m²

thermal neutron capture cross sections for ^{125}I and ^{131}I , ion-implanted into super-pure Al foils. ^{131}I was chosen as an experimental control because it should show little activity depletion (capture cross section estimated as ~ 0.7 barns¹). The integrated neutron flux was determined by measuring the ^{60}Co production in 0.1% Co in Al wires. Gamma-ray counting rates of the iodine samples were measured before and after neutron irradiations, using high resolution photon detectors. The 35-keV gamma ray of ^{125}I was measured with an intrinsic Ge X-ray detector, while the 364-keV gamma ray of ^{131}I and 1.33-MeV gamma ray of ^{60}Co were measured with a Ge(Li) detector.

Irradiations in the NRU reactor for about 33 days gave an integrated flux of 7.3×10^{20} neutrons/cm² with depletion ratios of 2.2 for ^{125}I and 1.037 for ^{131}I . Calculated cross sections based on these depletion ratios are 1030 ± 300 barns for ^{125}I and 85 ± 50 barns for ^{131}I .

The depletion rate for ^{125}I should have enabled the cross section to be measured to approximately 5%. An observed scatter in results of 15 to 25% was traced to instabilities in the data acquisition system. The measurements will be repeated using an improved system.

(1) J. Halperin and R.E. Druschel, ORNL-3488 (1963) 15.

Measurement of the $^{176}\text{Yb}(p,\gamma)^{177}\text{Lu}$ Cross Section

D.C. Santry and E.D. Earle (CRNL); B. Pålsson (University of Lund)

This experiment, described in INDC(Can)-14/G, was designed as a check on discrepant values of 14-MeV neutron capture cross sections, on the assumption that capture mechanisms for neutrons and protons are similar. The results support the (lower) neutron cross section values obtained by observing capture gamma rays, rather than those from earlier activation measurements. Our measurements have now been repeated at 0.5 MeV intervals from $E_p = 13.5$ to 24 MeV and confirm our previous results.

As a check on the activation measurement techniques used, a thick target of Cu was irradiated and the amount of 244-day ^{65}Zn was determined. Our results for the $^{65}\text{Cu}(p,n)^{65}\text{Zn}$ reaction at 13.5 MeV were within 5% of the accepted value, as measured by Colle et al ¹.

- (1) R. Colle, R. Hishore and J.B. Cumming, Phys. Rev. C9, 1819 (1974).

Upper Limit for the $^1\text{H}(n,\gamma\gamma)^2\text{H}$ Cross Section

E.D. Earle, A.B. McDonald and M.A. Lone

This work has been published in the Physical Review C, 14,1298 (1976), with the following abstract:

"A value of $(-0.8 \pm 2.5) \times 10^{-5}$ has been measured for the ratio of double-photon to single-photon emission following neutron capture in hydrogen for $600 \text{ keV} < E_{\gamma} < 1620 \text{ keV}$. The two Ge(Li) detectors used in the experiment subtended an angle of 85° at the H_2O target and were shielded from each other to reduce the background from the cross-registration of single γ rays. The upper limit of the measured two-photon cross section ($-3 \pm 8 \mu\text{b}$) is two orders of magnitude larger than the most recent theoretical predictions ($\sim 0.07 \mu\text{b}$) for this energy range."

Remeasurement of the $^1\text{H}(n,\gamma\gamma)^2\text{H}$ Cross Section

E.D. Earle, S.T. Lim and A.B. McDonald

An examination of the experimental limitations of the $^1\text{H}(n,\gamma\gamma)^2\text{H}$ cross section measurements suggests that a factor of 10 to 20 reduction in the cross section upper limit can be attained by replacing the Ge(Li) detectors with NaI. An experiment is in preparation. The neutron flux has been increased by more than an order of magnitude while the neutron background in the vicinity of the NaI detectors has been reduced. The ^6LiF flight tube will be replaced by ^6LiD . Tests with the NaI detectors show that a time resolution of 1.6 ns (FWHM) per detector can be attained.

Doubly Radiative n,p Capture

H.C. Lee and F.C. Khanna

This work has been published in the Physical Review C (14, 1306 (1976)) with the following abstract:

"The theory of the reaction $n + p \rightarrow d + \gamma + \gamma$ is reviewed with emphasis on the dominant, or (E1,E1), mode. The differences between the length and the gradient electric dipole operators are studied in detail and the two-photon cross section ($\sigma_{2\gamma}$) is calculated using both operators. The length operator yields a very reliable value of $\sigma_{2\gamma} = 0.118 \mu\text{b}$ ($\pm 1\%$). The result obtained with the gradient operator is $\sim 20\%$ smaller and has large uncertainties. Results for other two-photon modes are also presented."

Doubly Radiative Neutron Capture by ^2H , ^3He , ^{16}O and ^{208}Pb

H.C. Lee, F.C. Khanna, M.A. Lone and A.B. McDonald

This work has been published in Physics Letters 65B, 201 (1976), with the following abstract:

" Cross sections for doubly radiative thermal neutron capture on ^2H , ^3He , ^{16}O and ^{208}Pb are calculated to be 21, 1200, 41 and 50 nb, corresponding to branching ratios of $\sigma(n,\gamma\gamma)/\sigma(n,\gamma) = 4.0 \times 10^{-5}$, $\sim 3 \times 10^{-2}$, 2.2×10^{-4} and 1.0×10^{-4} , respectively."

Doubly Radiative Thermal Neutron Capture in ^2H and ^{16}O

A.B. McDonald, E.D. Earle, M.A. Lone, F.C. Khanna and H.C. Lee

In continuing the investigation of the doubly radiative capture processes in nuclei, we have obtained a value of $\sigma_{2\gamma} = 3 \pm 19 \mu\text{b}$ for the $^{16}\text{O}(n,\gamma\gamma)^{17}\text{O}$ reaction for a restricted energy range of $1200 < E_\gamma < 2943$ keV. Recently, Lee et al (previous section) have calculated a value of $\sigma_{2\gamma} = 0.041 \mu\text{b}$ for the total energy range of zero to 4143 keV. According to this calculation the cross section for the restricted energy range is $0.025 \mu\text{b}$.

No previous measurements of the doubly radiative capture cross section in ^{16}O have been reported. The $^{16}\text{O}(n,\gamma)^{17}\text{O}$ cross section, the level scheme and the branching ratios are well known (see following section). The restricted energy range of $1200 \text{ keV} < E_\gamma < 2943 \text{ keV}$ was chosen to eliminate any contributions from two-step cascades via the intermediate states. The probability for triple coincidences summing to 4143 keV in these measurements is negligible.

We also measured $\sigma_{2\gamma} = 8 \pm 15 \text{ } \mu\text{b}$ for the $^2\text{H}(n,\gamma\gamma)^3\text{H}$ reaction for the γ -ray energy range $700 \text{ keV} < E_\gamma < 5550 \text{ keV}$. The cross section for $^2\text{H}(n,\gamma\gamma)^3\text{H}$ is calculated to be $0.021 \text{ } \mu\text{b}$. The double-photon cross sections for H_2O and D_2O were measured relative to the cross section ($156 \pm 16 \text{ } \mu\text{b}$) of the sum peak from the 870.89 and the 1087.88 keV cascade in ^{17}O . The cross section for this cascade is an average of our results (measured relative to the known $\text{D}(n,\gamma)\text{T}$ cross section of $521 \text{ } \mu\text{b}$) and the results of Journey and Motz ¹. This work has been submitted to Nuclear Physics.

- (1) E.T. Journey and H.T. Motz, ANL-6797, Proc. Int. Conf. on Nuclear Physics with Reactor Neutrons, Argonne, 1963, p.236.

Thermal Neutron Capture in ^{16}O

A.B. McDonald, E.D. Earle and M.A. Lone

The thermal neutron capture cross section and the gamma-ray branching ratios for the $^{16}\text{O}(n,\gamma)^{17}\text{O}$ reaction were measured in a coincidence experiment with two Ge(Li) detectors. H_2O and D_2O targets were used. Gamma rays of energies 870.89 ± 0.22 , 1087.88 ± 0.17 , 2184.47 ± 0.12 and $3272 \pm 1 \text{ keV}$ were observed in the singles and the coincidence spectra.

The branching ratios of the M1 transition to the 871 keV $1/2^+$ level and the E1 transition to the 3055 keV $1/2^-$ level were determined to be $(18 \pm 3)\%$ and $(82 \pm 3)\%$ respectively. A total capture cross section of $202 \pm 27 \text{ } \mu\text{b}$ for the $^{16}\text{O}(n,\gamma)^{17}\text{O}$ reaction was determined relative to the cross section ($521 \pm 9 \text{ } \mu\text{b}$) for the $\text{D}(n,\gamma)\text{T}$ reaction ⁽¹⁾.

Our measured branching ratios and the capture cross section for ^{16}O are in good agreement with the M1 branching ratio (19%) and the total capture cross section ($178 \pm 25 \mu\text{b}$) reported by Journey and Motz.

- (1) S. Friarman and S.S. Hanna, Nucl. Phys. A251(1975)1
- (2) E.T. Journey and H.T. Motz, Proc. Int. Conf. on Nuclear Physics with Reactor Neutrons, Argonne, 1963, ANL 6797, 236.

Thick Target Neutron Yields and Spectral Distributions from the $^7\text{Li}(\text{d},\text{n})$ and $^9\text{Be}(\text{d},\text{n})$ Reactions

M.A. Lone, C.B. Bigham, J.S. Fraser, H.R. Schneider, A.J. Ferguson and A.B. McDonald.

This work is described in INDC(Can)-15/G and has been submitted to Nuclear Instruments and Methods. Re-analysis of the data shows that the preliminary 0^0 yields (for $E_n > 2.3 \text{ MeV}$) reported should be increased by 21% but there is no significant change in the average neutron energies.

Observation of Gamma Rays in $^{232,234}\text{U}$ Following $(^4\text{He},\text{xn})$ Reactions

D. Ward, H.R. Andrews, O. Hausser, J.R. Beene and R.B. Walker

In order to study high spin states in actinide nuclei it would be desirable to form them in (heavy ion, xn) reactions. Unfortunately such systems have a high probability of fission and to date it has not been possible to observe discrete gamma-ray transitions because of the very high background associated with prompt gamma rays accompanying fission. We have employed a high geometry gas scintillation counter to provide fast signals when fission fragments are detected in order to reject prompt-fission gamma events observed in a Ge(Li) detector. The success of this technique depends upon detecting fission fragments at a very high count rate with a total efficiency $\gg 90\%$.

The reaction $^{232}\text{Th} + ^4\text{He}$ at 25 - 39 MeV was used. A Th target, 500 $\mu\text{g}/\text{cm}^2$ thick, was positioned relative to the counter in such a way that the calculated geometrical efficiency for detecting at least one fragment was 98%. The counter contains pure nitrogen gas which appears to give the best timing, although pulse amplitudes are smaller than from Ar or Ar-N₂ mixtures. This arrangement reduced the gamma-ray background in the $^{232}\text{Th}(^4\text{He}, 2n)^{234}\text{U}$ (25 MeV) and $^{232}\text{Th}(^4\text{He}, 4n)^{232}\text{U}$ (39 MeV) reactions by about a factor of five, and gamma rays depopulating the ground state rotational bands in $^{232}, ^{234}\text{U}$ were then clearly observable to at least spin $12^+ \rightarrow 10^+$. Improvements to the system are currently being studied.

Contribution of Sub-threshold Fission to the Mean Cross Section of $^{237}\text{Np}(n, f)$ in Various Neutron Spectra

W.G. Cross and H. Ing

While $^{237}\text{Np}(n, f)$ is a particularly useful threshold reaction for neutron dosimetry, its sub-threshold cross section is large enough to affect dose measurements in a spectrum containing a substantial low-energy component. To simplify the correction of measurements in such spectra, the recent cross section data of Plattard *et al*⁽¹⁾ and others, between 1 eV and 200 keV, were fitted by an analytical function of energy, in a manner similar to that used to fit cross sections in the MeV range⁽²⁾. This expression was used to derive mean cross sections for spectra of fission neutrons transmitted by various thicknesses of H₂O, D₂O, Fe, Cu, U and concrete. For most of these spectra, the contribution of sub-threshold fission is less than 3% but, for neutrons transmitted by heavy elements and then moderated by hydrogen, it can exceed 10%. The calculated resonance integral, between 1 eV and 100 keV, is 0.28 barns.

(1) S. Plattard, J. Blons and D. Paya, Nucl. Sci. Eng. 61, 477 (1976).

(2) W.G. Cross and H. Ing, Nucl. Sci. Eng. 58, 377 (1975).

The Neutron Strength Functions and Radiative Widths of ^{206}Tl Resonances

E.D. Earle (CRNL), R.R. Winters (Denison University), J.A. Harvey and R. Macklin (Oak Ridge National Laboratory)

The parameters of ^{206}Tl resonances from 2 to 102 keV have been determined from neutron total cross section measurements (INDC(Can)-15/G) and neutron capture measurements.

The neutron strength function $\Sigma g\Gamma_n^0/\Delta E$ for known s-wave resonances is 0.23×10^{-4} below 40 keV and 0.98×10^{-4} above 40 keV. The strength function $\Sigma g\Gamma_n^1/3\Delta E$ for known p-wave resonances is 0.26×10^{-4} . The contribution to the s-wave strength function of unidentified resonances is too small to modify the conclusion that it exhibits a pronounced change of slope at about 40 keV. This effect could be interpreted as evidence for intermediate structure (as has previously been seen for s-wave resonances in the Pb isotopes).

The radiative widths fall into two groups depending on the parity of the resonances. The s-wave resonances have Γ_γ in the range 0.8 to 6 eV while the p-wave resonances have Γ_γ in the range 0.04 to 0.2 eV. It is suggested that this unusual separation of radiative widths into two families is due to the nature of the low-lying states. Since all known states below 2 MeV have high spin or negative parity there can be no high energy E1 primaries from p-wave resonances whereas many E1 transitions from each s-wave resonance are possible.

The ^{198}Au γ -ray Strength Function Below 9 MeV

E.D. Earle and I. Bergqvist (University of Lund, Sweden) and L. Nilsson (Tandem Accel. Lab., Uppsala, Sweden)

The γ -ray spectra following capture of 0.03, 0.56, 1.2, 1.5, 2.0 and 2.5 MeV neutrons in Au (INDC(Can)-14/G) have been fitted to intensity distributions derived from a single γ -ray strength function according to the spectrum fitting method described by Bartholomew et al. (Advances in Nuclear Physics, eds. M. Baranger and E.W. Vogt (Plenum Press, New York, 1973) Vol. 7, p. 229, AECL-5729).

The shape of the γ -ray spectra at various neutron energies can be described by the statistical model. A γ -ray strength function was found which gives calculated spectra in good agreement with all measured spectra. However, the Lorentz line shape which is frequently used to fit the experimental γ -ray absorption cross section in the giant dipole resonance region does not provide an appropriate description of the average strength in gold at lower γ -ray energies. The observed strength is significantly lower than that estimated from the Lorentzian tail and furthermore does not decrease monotonically with decreasing γ -ray energy. However, the ^{198}Au strength function is consistent in magnitude with that for ^{197}Au above 8 MeV as deduced from (γ, n) measurements by Veyssière et al. (Nucl. Phys. A159 (1970) 561).

Measurements of $\bar{\nu}(E)$ in the Photofission of ^{238}U

S.T. Lim, R.N. King and J.W. Knowles

Preliminary measurements of $\bar{\nu}(E)$, the average number of neutrons emitted per fission in ^{238}U following photo-absorption of radiation of $E = 6$ to 8 MeV, have been made with a resolution of 70 keV, with the Compton scattering facility at NRU. A collimated photon beam passes through six 10-chamber fission counters placed beside one another. These measure, simultaneously, fissions produced by 6 adjacent bands of radiation each 70 keV wide. Surrounding the fission counters and photon beam is a hollow cylindrical array of BF_3 counters enclosed in paraffin, with an internal diameter of 15 cm. The efficiency of this neutron detector was measured, at a mean neutron energy of 2.13 MeV, with a calibrated ^{252}Cf source and at 0.26 MeV with a calibrated $d(\gamma, n)p$ source using the 2.75 MeV γ -rays of ^{24}Na .

The value of $\bar{\nu}(E)$ is derived from the ratio of fission counts to coincidences between the fission and neutron detectors.

Coincidences within 300 μ s, an interval large compared with the slowing down time of neutrons in paraffin, are accepted. Our preliminary result at 8.0 ± 0.15 MeV is $\bar{\nu} = 2.76 \pm 0.10$ in agreement with recent measurements of Caldwell et al.

(IAEA Symposium on the Physics and Chemistry of Fission, 1973, Vol. I, p. 431).

Measurement of the Photofission Spectrum of ^{232}Th

J.W. Knowles (CRNL); T.E. Drake and B.O. Pich (University of Toronto); P. Axel and R. Starr (University of Illinois)

The 5000-wire fission chamber, described in INDC(Can)-15/G, was used at the University of Illinois, with a bremsstrahlung monochromator and CW (40% duty factor) microtron, to measure the photofission yield of ^{232}Th at photon energies between 5.5 and 7.4 MeV. The resolution of 75 keV was set by the monochromator. Well resolved structure in the photofission spectrum was observed at 5.60, 5.95 and 6.30 MeV and partly resolved structure at 6.50, 6.65 and 6.85 MeV. Photofission cross sections, obtained by averaging the present results over 300 keV intervals, agree to within statistical errors with previous measurements.

The prominent structure near 6.30 MeV, observed by others in both photo and transfer reactions with resolutions > 200 keV, has been interpreted as the plateau arising from competition with neutron emission, because of its proximity to the neutron separation energy (6.36 MeV). However, the structure we observed cannot be so interpreted since the fission transmission factor, derived from our photofission cross section, the photoabsorption cross section and gamma-ray and neutron transmission factors⁽¹⁾, has a maximum value much too small (1.5×10^{-2}) compared with unity.

(1) A.M. Khan and J.W. Knowles, Nucl. Phys. A179, (1972) 333.

High Energy Alpha Decay in ^{238}U

S.T. Lim, J.W. Knowles and E.D. Earle

Recent measurements (E. Wolyneć et al, Phys. Rev. Lett. 37 (1976) 585) of the production rate of ^{234}Th following the irradiation of ^{238}U with 10 - 25 MeV electrons indicate an enhancement in the cross section for the $^{238}\text{U}(e, e'\alpha)$ reaction near 9 MeV excitation. This result was interpreted as an indication of E2 strength at this energy.

We have attempted to excite this resonance with 9.0 MeV γ -rays and to observe the 13 MeV α -particles which should follow from the reaction $^{238}\text{U}(\gamma, \alpha)^{234}\text{Th}$. For this purpose we used the 9.0 MeV γ -rays from a nickel source in the NRU reactor. These γ -rays were incident on a 500 $\mu\text{g}/\text{cm}^2$ target of UF_4 placed inside a multiwire gas counter. A 4 mg/cm^2 aluminum foil placed between the target and the counter gas completely absorbed the fission particles and the 4 MeV α -particles from spontaneous decay and the fission particles from the (γ, f) reaction. With this arrangement we measured a pulse-height distribution of events in the gas counter, which we interpreted as arising from highly penetrating α -particles of energy ≥ 8 MeV. The observed counting rate corresponds to a (γ, α) cross section of about 4 mb (0.4 fm^2) in agreement with the photo-cross section calculated from results of the $^{238}\text{U}(e, e'\alpha)^{234}\text{Th}$ measurement.

Measurements of the energy and angular distribution of these penetrating particles, using solid-state charged-particle detectors, are in progress.

Time Evolution of Heavy-ion Induced Fission Studied by Crystal Blocking

J.U. Andersen, E. Laegsgaard and K.O. Nielsen (University of Aarhus); W.M. Gibson (Bell Laboratories); J.S. Forster, I.V. Mitchell and D. Ward (CRNL)

This work, partly described in INDC(Can)-15/G, has been published in Physical Review Letters (37 (1976) 1933) with the following abstract:

"The shapes of crystal blocking angular distributions have been used to study the fission decay of excited compound nuclei produced by the bombardment of tungsten with ^{16}O ions. Two lifetime components have been found. The relative amounts of a "prompt" and a "slow" component and the effective lifetime of the slow component are found to depend on the energy of the incident ion over the energy range 90 to 97 MeV that was investigated."

The Half-life of ^{198}Au

J.S. Merritt and F.H. Gibson

The decay of a sample of ^{198}Au produced by a short irradiation in the NRU rabbit was followed for approximately 14 half-lives by measuring it versus a radium reference source in the 4π ion chamber. No impurities were detectable by Ge(Li) spectrometry either initially or after 14 half-lives had elapsed. A least-squares analysis of the data gave a preliminary half-life value of 2.6937 days with a standard deviation of ± 0.0002 day. It is estimated that the effect on the apparent half-life of a small but undetected ^{199}Au impurity is 0.0001 day. This effect and other possible sources of error will be examined further, because gold is an important neutron-capture standard and this preliminary value is low compared with the accepted ^{198}Au half-life of 2.696 ± 0.002 days (ORNL-5114, 1976).

The Half Lives of ^{85}Sr and ^{113}Sn

J.S. Merritt and F.H. Gibson

Gamma emission rates from sources of ^{85}Sr and ^{113}Sn , made in 1973, have been measured at monthly intervals with a 4π ion chamber. A sealed ^{226}Ra needle was used as reference. The half lives obtained were 64.84 ± 0.03 days for ^{85}Sr and 115.12 ± 0.20 days for ^{113}Sn . The ^{85}Sr sample was followed for 15 half lives, at the end of which small impurities (< 1%) of ^{57}Co and ^{133}Ba were detected by Ge(Li) spectrometry. Corrections for these impurities affect the half life by 0.001 day. Thus the only

significant known source of error is statistical and the quoted error is three times the standard deviation.

The ^{113}Sn decay was followed by about 9 half lives. ^{125}Sb and $^{114}\text{In}^{\text{m}}$ were detected at the beginning of the measurement period and estimated to contribute 0.7% of the ion-chamber response. The systematic uncertainty in half life resulting from this impurity was estimated to be 0.10 days.

These results agree with, but are more precise than, presently accepted values^(1,2).

- (1) Nuclear Data Tables A8 (1970) 150.
- (2) F. Lagoutine, J. Legrand, C. Perrot, J.P. Brethon, J. Morel, Int. J. Appl. Rad. & Isotopes 5 (1972) 225.

Breeding Yields in Spallation Targets

J.S. Fraser, J.C.D. Milton and P.M. Garvey (CRNL); B.P. Pate, I.M. Thorson and F.M. Kiely (Simon Fraser University)

An experimental program to measure yields of fissile materials (^{233}U and ^{239}Pu) produced by the bombardment of target assemblies of fertile materials (^{232}Th and ^{238}U) by high energy protons is in progress at CRNL and Simon Fraser University. It is intended to provide experimental checks of neutron and fissile material production in spallation targets for electro-nuclear breeding.

In the first phase of the program, the neutron production and leakage from targets bombarded by 350 and 480 MeV protons (from the TRIUMF cyclotron) are being measured, by surrounding the target with water and integrating the thermal flux in the water, by self-powered neutron detectors and from measurements on gold foils. The targets used are bundles of rods of Th, depleted U, Pb and UO_2 , up to 23 cm in diameter and 30 cm long. The objective of this phase is to test the accuracy of calculations of neutron production and transport, made using intranuclear cascade and evaporation models for individual

collisions. While the preliminary experimental results show some anomalies in the neutron flux distributions, most measurements of leakage neutrons per incident proton agree with calculations to about 10%.

In the second part of the experiment, yields of fissile isotopes throughout the bundle will be measured by X and gamma-ray spectrometry. Preparations for this phase are under way.

NUCLEAR DATA ACTIVITIES REPORT FOR THE NETHERLANDS OVER 1976

1. Netherlands Energy Research Foundation (ECN), Petten, The Netherlands.

1.1. Neutron cross sections for fission-product nuclides

1.1.1. Evaluation activities (H. Gruppelaar, F.J. Luider)

Documentation of the first part of the RCN-2 evaluation has been prepared |1|. Neutron cross sections (σ_t , σ_{el} , $\sigma_{n\gamma}$, $\sigma_{nn'}$, σ_{n2n}) have been obtained for 24 nuclides (i.e. ^{93}Nb , $^{92,94,95,96,97,98,100}\text{Mo}$, ^{99}Te , $^{101,102,104}\text{Ru}$, ^{103}Rh , $^{102,104,105,106,107,108,110}\text{Pd}$, ^{127}I , ^{133}Cs , ^{139}La and ^{141}Pr).

Details of the evaluation method are given in refs. |1-6|.

New evaluations, to be included in the second part of the RCN-2 evaluation, have been obtained for ^{129}I , ^{107}Ag and ^{109}Ag . The capture cross sections evaluation for ^{127}I and ^{103}Rh have been revised. A discussion on different recent evaluations for fission-product isotopes is given in ref. |5|.

Recently a study has been performed on pre-equilibrium models for the prediction of neutron emission spectra. The results will be published in a forthcoming ECN-report. Further details are given in progress reports |7|.

1.1.2. Adjustment of capture cross sections (J.W.M. Dekker, A.J. Janssen)

The capture cross sections of the RCN-2 library have been adjusted according to a method described in ref. |8| using reactivity worths of isotopic samples measured in five STEK cores |9|. The results of these adjustments have been published in ref. |10|. Comparisons with different evaluations are given in ref. |5|.

Further details are given in progress reports |7|.

References

- | 1 | H. Gruppelaar, Tables of RCN-2 fission-product cross sections evaluation, vol. 1 (24 nuclides), ECN-13 (1977).
- | 2 | H. Gruppelaar, Uncertainty estimates of statistical theory calculations of neutron capture cross sections of fission products, IAEA Consultants meeting on the use of Nuclear theory in neutron data evaluation, Trieste, Dec. 1975, IAEA-190, vol. 2, p. 61, 1976.
- | 3 | G. Reffo, F. Fabbri and H. Gruppelaar, Enhancement of certain non-elastic cross-sections as an effect of the width fluctuations, Lett. al Nuovo Cim. 17 (1976) 1.
- | 4 | H. Gruppelaar and G. Reffo, Some properties of the width fluctuation factor, to be publ. in Nucl. Science and Eng.
- | 5 | H. Gruppelaar, A.J. Janssen and J.W.M. Dekker, Intercomparison of recent evaluations for the capture cross sections of some fission-product nuclides, ECN-12 (1976).
- | 6 | J.W.M. Dekker et al., Fission-product capture cross sections for a fast breeder reactor, Reaktortagung 1977 (Deutsches Atomforum), Mannheim 1977, ZAED Karlsruhe 1977.
- | 7 | E.K. Hoekstra (Comp.), Fast Reactor Programme Quarterly progress reports, RCN-248 (1976), ECN-7 (1976), ECN- (1977).
- | 8 | J.B. Dragt, J.W.M. Dekker, H. Gruppelaar and A.J. Janssen, Methods of adjustment and error evaluation of neutron capture cross sections; application to fission product nuclides, Nucl. Science and Eng. 62 (1977) 117.
- | 9 | J.J. Veenema and A.J. Janssen, Small-sample reactivity worths of fission-product isotopes and some other materials measured in STEK, ECN-10 (1976).
- | 10 | J.W.M. Dekker, Tables and figures of adjusted and unadjusted capture group cross sections based on the RCN-2 evaluation and integral measurements in STEK, vol. 1, ECN-14 (1977).

1.2. Nuclear structure work (FOM-ECN Nuclear Structure Group)

1.2.1. The $^{87,88}\text{Sr}(n,\gamma)$ reactions at 2- and 24-keV* (J. Kopecky, R.E. Chrien[†], R.C. Greenwood[†], and M. Stelts[†])

Energies and intensities of some 95 transitions have been measured for these isotopes for the 2- and 24-keV neutron beams from HFBR. Resonance neutron capture with the HFBR fast chopper time-of-flight facility was used to supplement the filtered-beam results. Thirteen new primary transitions were found, some of which populate $J^\pi = 2^+$ levels. Improved values for level energies were obtained. Of special interest are the particle-hole levels of the type $\{(\ell, j)_n (lgg/2)_n^{-1}\}$ in ^{88}Sr . The averaged intensities for p-wave capture show a striking concentration of radiative strength near the $d_{5/2}$ and $s_{1/2}$ levels near 4.5 and 5.5 MeV excitation. The use of the filtered beams, with their admixtures of $\ell=1$ and $\ell=0$ components, combined with $\ell=0$ resonance data, serves to select spin-parity values for many final states.

No transitions from $^{88}\text{Sr}(n,\gamma)^{89}\text{Sr}$ were seen at 2 keV; however at 24.3 keV primary transitions were observed to the $5/2^+$ gs of ^{89}Sr and to the $1/2^+$ first excited state. This observation strongly suggests that capture from a $3/2^-$ resonance is dominant near 24.3 keV.

* Work performed under the auspices of U.S. ERDA.

† Brookhaven National Laboratory, Upton, New York 11973.

† Permanent address: INEL, Idaho Falls, Idaho.

1.2.2. Simple p-wave neutron states (K. Abrahams, J.B.M. de Haas and R. Vennink)

Spins have been assigned to bound states of nuclei with $N = 29, 33$ and 37 , with the (n,γ) reaction. The nuclear orientation method and the circular polarization method have been used. The $J^\pi = 3/2^-$ states with a high (d,p) strength are indicated by *, and similarly the $J^\pi = 1/2^-$ states by \square in the table below.

^{52}V		^{59}Fe				^{65}Ni			
E_x (MeV)	J^π	E_x (MeV)	J^π	E_x (MeV)	J^π	E_x (MeV)	J^π		
0^*	3^+	0.80^{\square}	3^+	0^*	$3/2^-$	1.92	$3/2^-$	0.06^{\square}	$1/2^-$
0.02^*	$(2)^+$	0.85^{\square}	4^+	0.29	$1/2^-$	1.96	$1/2^-$	0.31	$3/2^-$
0.02^*	$(5)^+$	1.56	4^+	0.73	$3/2^-$	2.44	$3/2$	0.69^*	$3/2^-$
0.15^*	4^+	2.10	3^+	1.16	$3/2^-$			1.42	$1/2^-$

For ^{52}V an $f_{7/2}^-p_{3/2}$ quadruplet ($J^\pi = 2^+, 3^+, 4^+, 5^+$) and an $f_{7/2}^-p_{1/2}$ doublet ($J^\pi = 3^+, 4^+$) have been observed. The corresponding neutron separation energy fits in the proper order at $N = 29$. The following empirical relations have been derived for the energy $E_\gamma(3/2)$ and $E_\gamma(1/2)$ of the primary γ rays to these $l_n = 1$ states with $J^\pi = 3/2^-$ and $1/2^-$ respectively:

$$16 < N \leq 20 \quad E_\gamma(3/2) = .7Z - .35N - .1 \text{ MeV}$$

$$20 < N \leq 29 \quad E_\gamma(3/2) = .7Z - .17N - 4.0 \text{ MeV}$$

$$29 < N \leq 40 \quad E_\gamma(3/2) = .7Z - .66N + 10.2 \text{ MeV}$$

$$\text{If } Z \neq 20-28 \quad E_\gamma(1/2) = .5Z - .17N - 2.1 \text{ MeV}$$

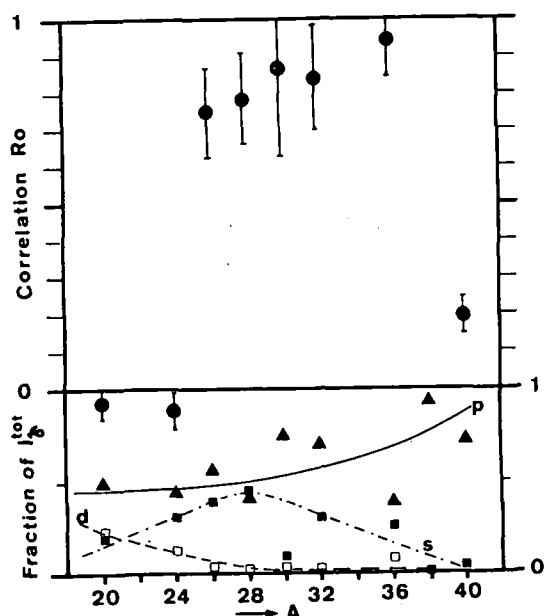
$$Z=20-28, N > 29 \quad E_\gamma(1/2) = .5Z - .5N + 10.2 \text{ MeV}$$

$$Z=20-28, N \leq 29 \quad E_\gamma(1/2) = Z - .17N - 11.9 \text{ MeV}$$

The relations given above fit with an r.m.s. error of about 0.2 MeV, 70 E_γ values ($2 < E_\gamma < 10$ MeV).

1.2.3. Anomalous M1-capture in mass region A = 20-40 (J. Kopecky)

The importance of non-statistical effects has been known for long time in the E1-neutron capture. None of these effects have been expected for M1-primary transitions, since for thermal capture they should be of $3s_{1/2} \rightarrow 2s_{1/2}$ or $1d_{3/2}$ character, and they are both forbidden in single particle model.



The $(n,\gamma)(d,p)$ correlation and a fraction of total I_γ to s, p and d levels for odd targets in $A = 20-40$.

has been found for $3s_{1/2} \rightarrow 1d_{3/2}$ transitions in agreement with the theoretical expectations.

It seems therefore, that a presence of more mechanisms (direct capture and probably a two step process) is needed to explain the simultaneous non-statistical behaviour of E1 and M1 transitions appearing in odd ^{25}Mg , ^{27}Al , ^{29}Si , ^{31}P and ^{35}Cl targets.

The single particle estimate for the $B(M1)/B(E1)$ ratio is ~ 0.035 for the targets with $A = 20-40$. The experimental value for even (odd) targets averaged over 9 (8) nuclei and 55 (147) primary transitions reads as $\langle B(M1)/B(E1) \rangle = 0.025$ (0.463), respectively, which clearly manifests the enhancement of M1-transitions relative to the E1-transitions in odd targets. In recent capture measurements in 400 eV p-wave resonance in ^{35}Cl the value of $\langle B(M1)/B(E1) \rangle = 1.95$ has been found for 23 transitions.

Moreover for some odd targets a significant $(n,\gamma)(d,p)$ correlation exists for $3s_{1/2} \rightarrow 2s_{1/2}$ transitions as displayed in the figure. Remarkable is that this correlation is neither disturbed by a possible multipole admixture nor by the admixture of d-configuration, which is present in 70% of the levels considered. No correlation

1.2.4. Polarized neutron capture in ^{52}V (J.B.M. de Haas)

A 55% V- 45% Fe target was cooled to 40 mK in an external field of 5 T. By means of the γ -intensities as a function of the spin direction (spins parallel and antiparallel) and of the angular distribution with respect to the magnetic field some spin dependent parameters could be deduced [1]. From these parameters and some R values from circular polarization measurements the following spins could be obtained.

line	level	$\ell_n(d,p)$	α	spin
5142	2169	1	$.05 \pm .10$	3, 4 ⁺
5210	2101	1	$.22 \pm .08$	3 ⁺
5516	1795	1	$.0 \pm .10$	2 ⁺ (3),(4)
5752	1559	1	$.25 \pm .06$	4 ⁺
6465	846	1	$.11 \pm .07$	4 ⁺
6517	793	1	$.20 \pm .05$	3 ⁺
6874	437	1	$.0 \pm .07$	2 ⁺ (3)
7163	148	1	$.12 \pm .05$	4 ⁺

α is the fraction of $I+\frac{1}{2}$ capture ($0 \leq \alpha \leq 1$). Known where the 3⁺ G.S. and the 1⁺ 142 keV level. As α is almost near zero everywhere most neutrons are captured through the $I=3^-$ channel ($I_T = 7/2^-$).

A spin sequence proposed by Van Assche [2] with a 2⁺ 17 keV, 5⁺ 23 keV, 1⁺ 142 keV and a 4⁺ 148 keV is consistent with the present results.

[1] E.R. Reddingius, J.J. Bosman and H. Postma, Phys. Lett. 41B (1972) 301.

[2] P. van Assche, thesis.

1.2.5. Spin assignments to energy levels of ^{59}Fe and ^{65}Ni (R. Vennink)

Circular polarized γ -radiation, emitted by ^{65}Ni and ^{59}Fe , after capturing polarized neutrons, has been studied.

For ^{65}Ni 6 primary transitions have been investigated of which 4 spin assignments could be given (see table).

The result after measurement on 7 primary transitions of ^{59}Fe is 5 spin assignments and 1 spin prediction (see table).

^{59}Fe		^{65}Ni	
E_x (MeV)	J^π	E_x	J^π
0	$3/2^-$	0.064	$1/2^-$
0.287	$1/2^-$	0.311	$3/2^-$
0.728	$3/2^-$	0.692	$3/2^-$
1.162	$3/2^-$	1.418	$1/2^-$
1.921	$3/2^-$		
1.962	$(1/2^-)$		

1.2.6. The $^{64,66,68}\text{Zn}(n,\gamma)$ reactions measured with a pair spectrometer

(J. de Boer).

Earlier single spectrum measurements on the $^{64,66,68}\text{Zn}$ isotopes at HB4, resulted in extremely complex capture γ spectra, which were difficult to analyse.

The (n,γ) group of the KFA (Jülich) has offered us the possibility to perform these measurements with their pair spectrometer at the DIDO reactor at the KFA in Jülich.

Preliminary data from the $^{64}\text{Zn}(n,\gamma)$ reaction have shown that almost no background is disturbing.

Results for the 60 strongest transitions in ^{65}Zn are shown in the fig. In this figure transitions with intensities up to $I_\gamma \approx 0.4\%$ are drawn. At the present stage 32 primary transitions have been analysed, of which 9 were already known. Further analysis is still going on.

1.2.7. Investigation of the spin state of some energy levels in ^{45}Ca

(R. Vennink)

Primary transitions in ^{45}Ca , after capturing of polarized neutrons in ^{44}Ca , have been considered.

The circularly polarization of these transitions has been investigated. For ^{45}Ca 9 primary transitions have been seen. Till now the obtained statistics are enough to make a spin assignment to 7 levels (see table).

^{45}Ca	
E_x (MeV)	J^π
1.435	$3/2^-$
1.900	$3/2^-$
2.247	$1/2^-$
2.842	$3/2^-$
3.242	$3/2^-$
3.419	$1/2^-$
4.616	$1/2^-$

1.2.8. The study of the $^{238}\text{U}(n,\gamma)^{239}\text{U}$ reaction (J. Kopecký, R.E. Chrien* and H.I. Liou*)

Although high resolution data on the high energy gamma rays emitted after neutron capture in ^{238}U exist, little information is available on the region below 1 MeV. By using the HFBR chopper time-of-flight system, the spectra of low-energy γ -rays from resonance capture and the coincidences were measured. We distinguish prompt γ -rays from radioactivity or isomeric transitions by comparing the resonance spectra with those obtained between resonances. Approximately 60 prompt capture γ -rays have been identified from $^{238}\text{U}(n,\gamma)^{239}\text{U}$. Energies and relative intensities were established using calibrated radioactive sources. The strongest line in the low energy region, reported by Sheline et al. at 552 keV is seen to be a doublet of 551.92 ± 0.03 and 553.97 ± 0.03 keV. About 2/3 of the lines can be placed in the level scheme of Bollinger & Thomas.

Circular polarization of 18 primary transitions (with $I_\gamma \geq 0.2$) has been measured at the HFR in Petten. Unique spin assignments have been made for 8 levels. For the remaining levels spin restrictions could be made.

*) Brookhaven National Laboratory

1.2.9. Spin states in ^{43}Ca using the $^{42}\text{Ca}(n,\gamma)$ reaction (R. Vennink)

Spin assignments are made to levels in ^{43}Ca with the circular polarization set-up at the H.F.R.

After capturing polarized neutrons, circular polarized radiation is emitted. A polarization analyzer, placed in front of a detector causes an asymmetry in the intensity of the emitted radiation.

The measured asymmetry is compared with the theoretical value, the so-called R-value. On assuming pure dipole radiation the R-value can be +1, in the case of a transition between capture state $J^\pi = \frac{1}{2}^+$ and final state $J^\pi = \frac{1}{2}^-$ or can be -0.5 in the case of a transition to a final state with $J^\pi = \frac{3}{2}^-$.

In the table the results are shown. The spin-state of the p-levels 593 and 2046 were already known and spin assignments to all mentioned levels have already been suggested from the J-dependence on angular distributions from (d,p) work and are confirmed now by these measurements. This confirmation shows that the so-called Lee-Schiffer method of spin assignments by means of the (d,p) reaction is reliable for ^{43}Ca .

^{43}Ca

E_x (keV)	R	ΔR	J^π
593	-0.50	0.11	$3/2^-$
2046	-0.50	0.03	$3/2^-$
2611	0.79	0.19	$1/2^-$
2878	0.6	0.3	$1/2^-$
2944	-0.55	0.18	$3/2^-$
3286	-0.3	0.2	$3/2^-$
3573	-0.4	0.2	$3/2^-$
4207	0.98	0.15	$1/2^-$
4902	0.80	0.5	$(1/2^-)$

1.2.10. M2-strength in neutron capture (J. Kopecky)

Primary neutron capture transitions between states with opposite parity have always been assumed to have a pure E1-mode. Recent conclusions [1,2] on the existence of non-zero M2-admixtures turned our attention to this effect, since it would have a serious implication on the analysis of many (n, γ) polarization experiments.

A large wealth of data originating from the capture of polarized neutrons can be used to test the E1-assumption. If one restricts the analysis only to even targets, the uncertainty caused by the spin interference in the capturing state is eliminated, while the parity interference is negligible for thermal neutrons.

The circular polarization data (R-values) are then subject to the following errors:

1. An unknown peak (overlapping the analysed peak) influences the magnitude of the R-value. With the present knowledge of γ -ray spectra this error could be considered as negligible.
 2. A systematic error in the calibration of the circular polarization due to the non-validity of the E1-assumption for the 5.42 MeV γ -ray in $^{32}\text{S}(n,\gamma)$ reaction.
 3. A variable systematic error in the analysis of the polarization spectra, which influences the R-values and/or their errors.
- A high consistency between external and internal errors for analysed samples indicates the absence of significant systematic errors.

To test the E1-assumption for sulphur calibration $39(1/2^+ \rightarrow 1/2^-, R_{\text{theor}} = +1)$ γ -rays have been analysed and a mean value of $\bar{R} = 1.004 \pm 0.009$ establishes the limit for the M2-admixture as $\delta(M2/E1)_{5.42 \text{ MeV}} < 0.007$.

The analysis of 57 circularly polarized $(1/2^+ \rightarrow 3/2^-, R_{\text{theor}} = -0.5)$ γ -rays (in 17 doubly even targets with $40 < A < 68$) yielded the mean value of $\bar{R} = -0.495 \pm 0.007$. It can be shown, that the sample distribution around this mean value is consistent with a normal one, having a standard deviation of $\sigma = 0.05$. From this value a limit for the M2 admixture can be derived as $\delta(M2/E1) < 0.04$. The influence of such admixtures can be neglected for the circular polarization analysis for odd targets, if one considers the present experimental accuracy.

Comparing the present results with the earlier works [1,2] the following conclusions can be made:

- 1) The mean values of δ are in a reasonable agreement considering the value of $\delta \sim 0.03$ resulting from both earlier experiments.
- 2) The highly admixed ($\delta \sim 0.1 - 0.2$) transitions found with a solid significance in ref. [1] are not found in our work. This fact is rather striking, if one takes into account the 20 accurately measured transitions ($AR \leq 0.1$), which would enable one to measure the above mentioned admixtures as significant as 3-10 standard deviations. As a matter of fact, we have not found any individual transition with a significant presence ($> 99.9\%$ confidence limit) of M2-radiation. The absence of such mixed transitions in our analysis refreshes the old question [3], whether interference effects in the analysis of the angular distribution of γ -rays in ref. [2] has been fully accounted for.

-
- [1] R. Moreh et al., Physics Letters 36B (1971), 71.
 - [2] J.W. Maas, Thesis, Utrecht Uni., 1976.
 - [3] B. Arad, Phys. Rev. C7 (1973), 749.

1.2.11. Investigation of ^{137}Ba and ^{139}Ba (J.R. Balder)

Isotopically enriched targets of $^{136,138}\text{Ba}$ were measured at the HB7 circular polarization set-up. Also a single spectrum was recorded at HB4.

Both target nuclei have $J^\pi = 0^+$ (even-even nuclei) and due to the (almost) closed neutron-shell a relatively simple level scheme.

As yet, two levels in ^{138}Ba and two in ^{136}Ba could be given a definitive spin assignment.

In the ^{136}Ba spectrum two strong lines were seen. One could be identified as a primary transition to the 2179 keV level. From (d,p) work J^π was known to be $1/2^-$ or $3/2^-$, which we now could reduce to $J^\pi = 3/2^-$. The other one is, when we look at its intensity and energy, almost certainly a primary transition, in which case we can assign a $J^\pi = -1/2$ to the 2179 level.

<u>^{138}Ba</u>			<u>^{136}Ba</u>		
E_x	R	J^π	E_x	R	J^π
627.26	$-.41 \pm .04$	$3/2^-$	2179	$-.48 \pm .06$	$3/2^-$
1081.9	$.84 \pm .09$	$1/2^-$	2646	$1.29 \pm .24$	$1/2^-$

Publications

- K. Abrahams; Radiative capture of polarized thermal neutrons.
Neitrona Fizika; Proceedings conference Kiev, USSR, 9-13 June 1975.
Part 3, 254-274.
- K. Abrahams; Binding energies of valency nucleon states.
Proceedings International conference on selected topics in nuclear
structure, Dubna, USSR, 15-19 June 1976, 118.
- K. Abrahams, J.B.M. de Haas and R. Vennink; Simple p-wave neutron states.
Proceedings International conference on the interactions of neutrons
with nuclei, Lowell, Mass., 6-9 July 1976, Vol. II, 1431.
- J. Kopecky; Anomalous M1 capture in mass region $A = 20-40$.
Proceedings International conference on the interactions of neutrons
with nuclei, Lowell, Mass., 6-9 July 1976, Vol. II, 1285.
- J. Kopecky and A.M.J. Spits; Direct capture in the $^{37}\text{Cl}(n,\gamma)$ reaction.
Proceedings International conference on the interactions of neutrons
with nuclei, Lowell, Mass., 6-9 July 1976, Vol. II, 1286.
- J. Kopecky, R.E. Chrien, R.C. Greenwood and M. Stelts.
The $^{87,88}\text{Sr}(n,\gamma)$ reactions at 2- and 24 keV.
Proceedings International conference on the interactions of neutrons
with nuclei, Lowell, Mass., 6-9 July 1976, Vol. II, 1287.
- A.M.J. Spits and J. Kopecky; The reaction $^{35}\text{Cl}(n,\gamma)^{36}\text{Cl}$ studied with
non-polarized and polarized thermal neutrons.
Nucl. Phys. A264 (1976), 1, p. 63-92.

2. R.J. Van de Graaff Laboratory, State University, Utrecht, The Netherlands.

List of publications in the year 1976

M.A. van Driel, H.H. Eggenhuisen, G.A.P. Engelbertink, L.P. Ekström and J.A.J. Hermans; Model independent J^π assignments in ^{38}Ar from γ -ray experiments in heavy ion induced reactions.

Nuclear Physics A272 (1976) 466-492.

P.M. Endt; Nuclear spectroscopy in the sd shell.

Nukleonika, Vol. 21, no. 6/76.

F.E.H. van Eijkern, G. van Middelkoop, W.A. Sterrenburg and A.F.C. Buijense; Spectroscopy of ^{32}P (II).

Nuclear Physics A260 (1976) 124-140.

F.E.H. van Eijkern, G.A. Timmer, F. Meurders and P.W.M. Glaudemans; Shell-model calculations in $A = 28-32$ nuclei.

Z. Physik A278, 337-345 (1976).

R.E. Horstman, H.A. Doubt, J.L. Eberhardt and G. van Middelkoop; A magnetic moment measurement of the first-excited 2^+ state of ^{22}Ne . Hyperfine interactions 2 (1976) 383-384.

H. Lancman[†], R.J. Sparks^{††} and C. van der Leun; Nuclear resonance fluorescence in ^{54}Fe .

Nuclear Physics A257 (1976) 29-36

F. Meurders, P.W.M. Glaudemans, J.F.A. van Hienen and G.A. Timmer; Shell-model calculations with an adjusted surface-delta interaction. (I) Application to spectroscopic factors in $A=24-28$ nuclei.

Z. Physik A 276 (1976) 1113-126.

R.J. Sparks^{††}; Investigation of the reaction $^{34}\text{S}(p,\gamma)^{35}\text{Cl}$.

(I) Resonances at proton energies above 2 MeV.

Nuclear Physics A265 (1976) 416-428.

R.J. Sparks^{††}, H. Lancman[†] and C. van der Leun; Resonant gamma-ray absorption in ^{208}Pb .

Nuclear Physics A259 (1976) 13-19.

[†] On sabbatical leave from Brooklyn College of CUNY, USA.

^{††} On leave from Institute of Nuclear Sciences, DSIR, New Zealand.

P.C. Zalm, J.L. Eberhardt, R.E. Horstman, G. van Middelkoop and H. de Waard^{*}; The use of a single-crystal iron frame in transient field g-factor measurements.

Physics Letters, Volume 60B, number 3 (1976).

J.L. Eberhardt[†], R.E. Horstman^{††}, P.C. Zalm, H.A. Doubt^{†††} and G. van Middelkoop; Large transient magnetic fields at high ion velocities in polarized iron.

Hyperfine Interaction (in press).

P.M. Endt; Spectroscopic factors for single-nucleon transfer in the A = 21-44 region.

Accepted for publication in Atomic Data and Nuclear Data Tables 19.

G.A.P. Engelbertink, L.P. Ekström, D.E.C. Scherpenzeel and H.H. Eggenhuisen; Phenomenological restrictions for spin-alignment attenuation factors in heavy-ion induced fusion-evaporation reactions.

Accepted for publication in Nuclear Instruments & Methods.

R.E. Horstman^{††}, J.L. Eberhardt[†], P.C. Zalm, H.A. Doubt^{†††} and G. van Middelkoop; Recoil-distance measurements of the g-factor of $^{22}\text{Ne}(2_1^+)$. Accepted for publication in Nuclear Physics.

J.E. Koops and P.W.M. Glaudemans; Shell-model calculations on Ni and Cu isotopes.

Accepted for publication in Zeitschrift für Physik A.

W.A. Sterrenburg, G. van Middelkoop and F.E.H. van Eijkens; Spectroscopy of states in ^{33}S by means of neutron-gamma angular correlation measurements.

Accepted for publication in Nuclear Physics.

R. Brenn⁺, H. Spehl⁺, A. Weckherlin⁺, H.A. Doubt^{†††} and G. van Middelkoop; Nuclear Deorientation for heavy ions recoiling in vacuum and low pressure gas.

Submitted for publication.

* Lab. voor Algemene Natuurkunde, R.U. Groningen, The Netherlands.

† Present address: Institute of Physics, University of Aarhus, Denmark.

†† Present address: Philips' Natuurk. Laboratorium, Eindhoven, The Netherlands.

††† Present address: Nuclear Physics Laboratory, Oxford OX1-3RH, England.

+ Fakultät für Physik der Universität, D 78 Freiburg, West-Germany.

H.H. Eggenhuisen, L.P. Ekström, G.A.P. Engelbertink, H.J.M. Aarts and J.A.J. Hermans; High-spin states in ^{40}K investigated with the $^{26}\text{Mg} + ^{16}\text{O}$ reaction.

Submitted for publication.

L.P. Ekström, H.H. Eggenhuisen, G.A.P. Engelbertink, J.A.J. Hermans and H.J.M. Aarts; Spin-parity assignments to yrast states of ^{42}K .

Submitted for publication.

J.A.J. Hermans, G.A.P. Engelbertink, L.P. Ekström, H.H. Eggenhuisen and M.A. van Driel; High-velocity DSA measurements in the 1-20 ps lifetime region; Comparison between DSA and RD.

Submitted for publication.

PROGRESS REPORT FROM NORWAY

Thermal neutron activation cross-sections and resonance activation integrals of some (n,γ) reactions induced in platinum metal isotopes.

Reaction	σ_{th} barns	I_0^* barns
$^{96}\text{Ru}(n,\gamma)^{97}\text{Ru}$	0.29 ± 0.02	7.34 ± 0.08
$^{102}\text{Ru}(n,\gamma)^{103}\text{Ru}$	1.21 ± 0.07	4.2 ± 0.1
$^{104}\text{Ru}(n,\gamma)^{105}\text{Ru}$	0.32 ± 0.02	4.3 ± 0.1
$^{108}\text{Pd}(n,\gamma)^{109m+g}\text{Pd}$	8.3 ± 0.6	244 ± 4
$^{191}\text{Ir}(n,\gamma)^{192m1+g}\text{Ir}$	1350 ± 60	4460 ± 120
$^{193}\text{Ir}(n,\gamma)^{194}\text{Ir}$	270 ± 10	2900 ± 20
$^{194}\text{Pt}(n,\gamma)^{195m}\text{Pt}$	0.117 ± 0.009	3.1 ± 0.1
$^{196}\text{Pt}(n,\gamma)^{197m+g}\text{Pt}$	0.58 ± 0.03	7.1 ± 0.2
$^{198}\text{Pt}(n,\gamma)^{199m+g}\text{Pt}$	4.8 ± 0.3	84 ± 3

*Including "1/v-tail".

Epithermal activation is performed under a 0.7mm cadmium filter.

For the flux monitor, ^{198}Au , the values $\sigma_{th} = 98.8$ barns and

$I_0 = 1550$ barns were adopted.

J.P. Rambæk and E. Steinnes, Institutt for atomenergi, Kjeller, Norway, personal communication (1977)

NEANDC (OR) - 146 "L"

INDC (SWT) - 010 / L

PROGRESS REPORT TO NEANDC
FROM SWITZERLAND

June 1976

T. Hürlimann

Swiss Federal Institute for Reactor Research
Würenlingen

NOT FOR PUBLICATION

PREFACE

This document contains information of a preliminary or private nature and must be used with discretion. Its contents may not be quoted, abstracted, reproduced, transmitted to libraries or societies or formally referred to without the explicit permission of the originator.

CONTENTS

	page
I. Institut de Physique, Université de Neuchâtel	155
II. Laboratorium für Kernphysik, Eidg. Technische Hochschule, Zürich	158
III. Institut für Physik der Universität Basel	165
IV. Physik-Institut der Universität Zürich	167
V. Eidg. Institut für Reaktorforschung, Würenlingen	170

I. Institut de Physique, Université de Neuchâtel

(Dir.: Prof. Jean Rossel)

1. $D(n,n)D$; $D(\vec{n},n)D$ and $D(\vec{n},\vec{n})D$ elastic scattering at low energy

D. Bovet, P. Chatelain, Y. Onel, R. Viennet and J. Weber

The depolarization factor $D(\theta)$ for the scattering of neutrons from deuteron was measured for several angles at 2.45 MeV and the results including some ERA analyses were presented to the 4th International Symposium on Polarization Phenomena, Zürich 1975 {1,2}.

The test of the fast neutron-gamma discriminator {3} has been completed. The performance of this module was of great interest since the discrimination did work up to an average counting rate of 300 KHz, even at low energies.

This module was used in the measurement of the polarization $P(\theta)$ for $\theta_L = 100^\circ$ at 2.45 MeV which was part of the set of measurements submitted to the International Conference on the Interaction of Neutrons with Nuclei, Lowell Mass., 1976 {4}*). The previous determination of the nd differential cross sections at low energies were not adequate for fitting the data with the available models, even the simplest fit with the orthogonal polynomials was not significant.

Then it has been concluded that there was a need for more accurate differential cross section data, especially at the angles larger than 140° or 150° (CM). Therefore we have started to measure the differential cross sections by using the method of recoil energy spectrum {5}.

In this measurement, the scatterer is a NE 213 deuterated liquid scintillator of small dimensions (1 x 1 cm). An associated particle time-of-flight system for the $d(d,n)^3\text{He}$ reaction has been developed for producing neutrons of 2.45 MeV. The measurements are in progress.

The measurements of the angular variation of the depolarization factor and other Wolfenstein parameters will be resumed later on.

References

- {1} Proceedings of this Conference, contributed papers p. B3
- {2} Ibid p. B5
- {3} P. Betz et al., Nucl. Instr. & Methods 119 (1974) 199
- {4} Proceedings of this Conference, contributed papers (to be published)
- {5} D. Bovet, P. Chatelain, Y. Onel, R. Viennet and J. Weber
(to be published)

*) This paper also presents some new ERA analyses which include our P(θ) data.

2. Neutron-neutron quasifree scattering at 14.1 MeV

E. Bovet, F. Foroughi, C. Nussbaum and J. Rossel

The differential cross section for the D(n,nn)p reaction has been measured in two different kinematic configurations favouring n-n quasifree scattering where the spectator proton has nearly zero energy. These measurements are a continuation of the preliminary measurements {1} which proved the feasibility of such an experiment without detecting the spectator proton practically at rest in the C_6D_{12} target. The two symmetrical configurations, $\theta_1 = \theta_2 = 40^\circ$, $\theta_{12} = 180^\circ$ ($E_p^{\min} = 0$) and $\theta_1 = \theta_2 = 30^\circ$ ($E_p^{\min} = 180$ keV), were chosen to favour comparison with existing "exact" theoretical predictions, for which such configurations are particularly well suited {2}. The electronic signals directly related to the deuteron break-up, as well as those controlling the stability of the experiment were processed and stored by a PDP 15/20 computer. In addition, the simultaneous measurements of the yields from the D(n,n)D and $^{12}C(n,n)^{12}C$ elastic reactions which are used to monitor the break-up reaction, were also recorded by the computer.

The data analysis shows:

- a) that such an experiment can be successfully performed without detecting the spectator proton ($\sim 2 \cdot 10^3$ true events for $2,2 \cdot 10^3$ counts in 2000 hours);
- b) that the differential cross section at $\theta_1 = \theta_2 = 40^\circ$ ($E_p = 0$) is smaller than that of $\theta_1 = \theta_2 = 30^\circ$ by a factor of about 2, whereas the "exact" {3} theory (Faddeev equations with separable two-body potentials) predicts a factor of only 1.3;
- c) that the shape of the differential cross section obtained at 30° shows evidence of a pronounced relative minimum for $E_p = E_p^{\min} = 180$ keV. This structure is predicted by neither the simpler {4} nor the more sophisticated "exact" theoretical models using s-wave nucleon-nucleon interaction..

References

- {1} E. Bovet, F. Foroughi and J. Rossel, *Helv. Phys. Acta* 48 (1975) 137
- {2} M. Jain, J. G. Rogers and D. P. Saylor, *Phys. Rev. Lett.* 31 (1973) 838
- {3} W. Ebenhöh, *Nucl. Phys.* A191 (1972) 97
- {4} F. Foroughi and E. Bovet, *Helv. Phys. Acta* 48 (1975), 577

II. Laboratorium für Kernphysik, Eidg. Technische Hochschule Zürich

(Dir.: Prof. Dr. J. Lang)

1. Measurement of the analysing powers in ${}^3\text{He}(\vec{d},d){}^3\text{He}$ Scattering

B. Jenny, W. Grüebler, V. König, P. A. Schmelzbach, R. Risler,
D. O. Boerma and W. G. Weitkamp

Some time ago, a phase shift analysis based on the cross section and all analysing power components of d - ${}^3\text{He}$ elastic scattering has been tried. Measurements of iT_{11} , T_{20} , T_{21} and T_{22} exist in the energy range between 4.0 and 11.5 MeV [1]. Due to the relatively complicated spin structure of the scattering problem and the existence of open reaction channels, the scattering matrix contains a large number of independent elements. In fact, the phase shift analysis showed clearly the need for extended and more precise data in order to determine the matrix elements accurately. Measurements in smaller energy steps and at lower energies were also desirable.

New angular distributions of iT_{11} , T_{20} , T_{21} , T_{22} , and of the unpolarized differential cross section have been measured for ten deuteron bombarding energies between 2.0 and 11.5 MeV, each containing up to 50 data points with a relative error in the analysing powers of typically 0.005. It was possible to extend the measurements to c. m. angles of 12.5° and 165° using a special gas target with 0.9 mg/cm^2 mylar foil entrance and exit windows. The ${}^3\text{He}$ gas pressure was 200 Torr. The beam polarization was determined with a polarimeter mounted behind the target.

Fig. 1 shows two of the measured analysing powers. Circles indicate data points obtained by detecting the recoil ${}^3\text{He}$ particles. A comparison with measurements of ${}^3\text{H}(\vec{d},d){}^3\text{H}$ scattering [2] at the same deuteron energies is interesting. Generally they agree remarkably well with ${}^3\text{He}(\vec{d},d){}^3\text{He}$ scattering, thus confirming the similarity of ${}^5\text{He}$ and its mirror nucleus at higher excitation energies, where a series of $T = 1/2$ levels is predicted by theoretical calculations [3,4,5]. One part of the occurring significant deviations

may probably be ascribed to the 0.24 MeV higher excitation of the ^5He nucleus resulting from the different threshold energies. The discrepancies of T_{22} at 5.0 MeV between 30° and 60° and those at 8.0 MeV seem to be caused by other reasons. A phase shift analysis of the new data is now in progress at this laboratory.

References

- {1} V. König, W. Grüebler, R. E. White, P. A. Schmelzbach and P. Marmier, Nucl. Phys. A185 (1972) 263
- {2} A. A. Debenham, V. König, W. Grüebler, P. A. Schmelzbach, R. Risler and D. O. Boerma, Nucl. Phys. A216 (1973) 42
- {3} P. Heiss and H. H. Hackenbroich, Nucl. Phys. A162 (1971) 530
- {4} R. F. Wagner and C. Werntz, Phys. Rev. C4 (1971) 1
- {5} F. S. Chwieroth, R. E. Brown, Y. C. Tang and D. R. Thompson, Phys. Rev. C8 (1973) 938

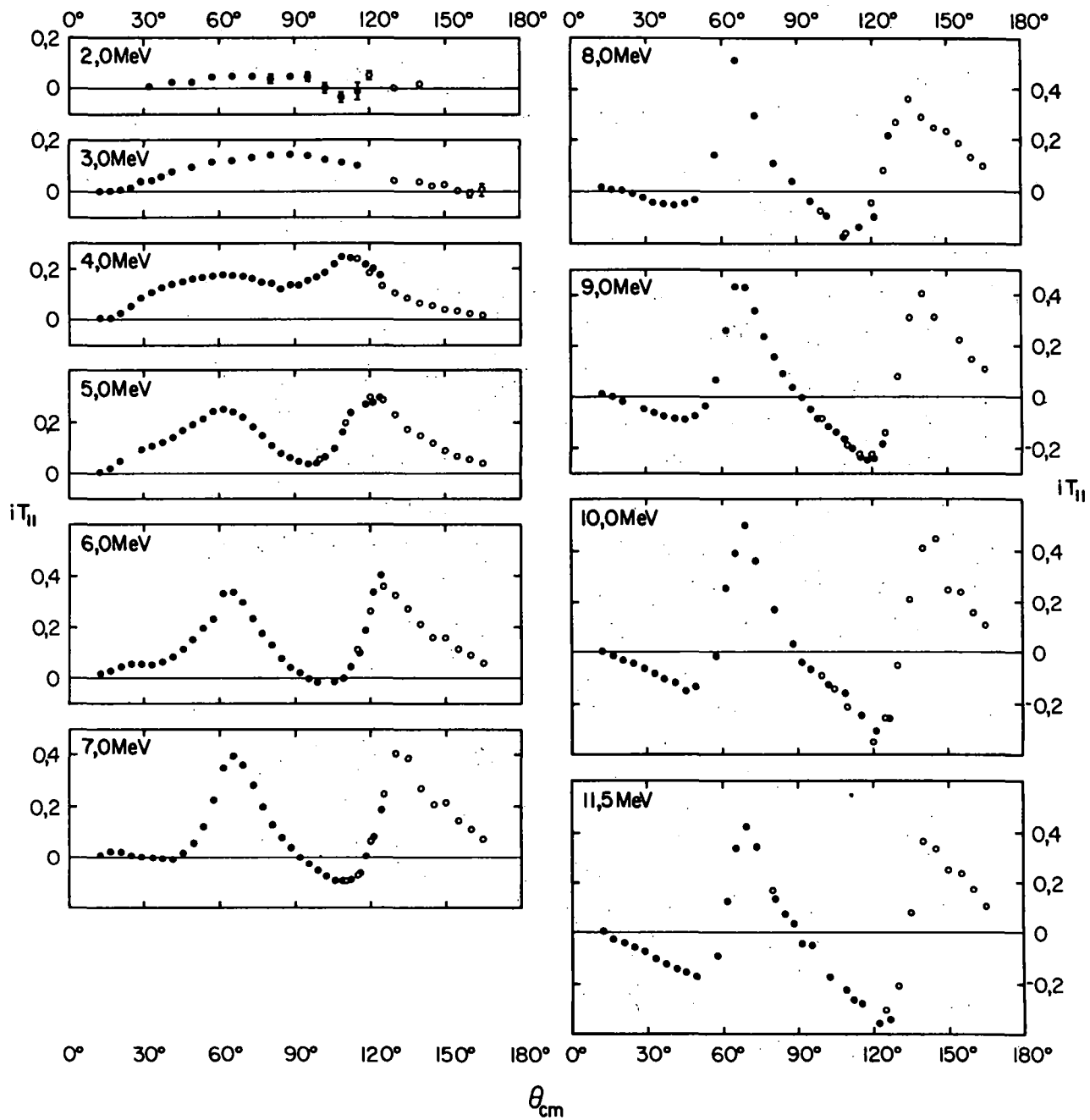


Fig. 1: Vector analysing power iT_{11} in ${}^3\text{He}(\vec{d},d){}^3\text{He}$ scattering

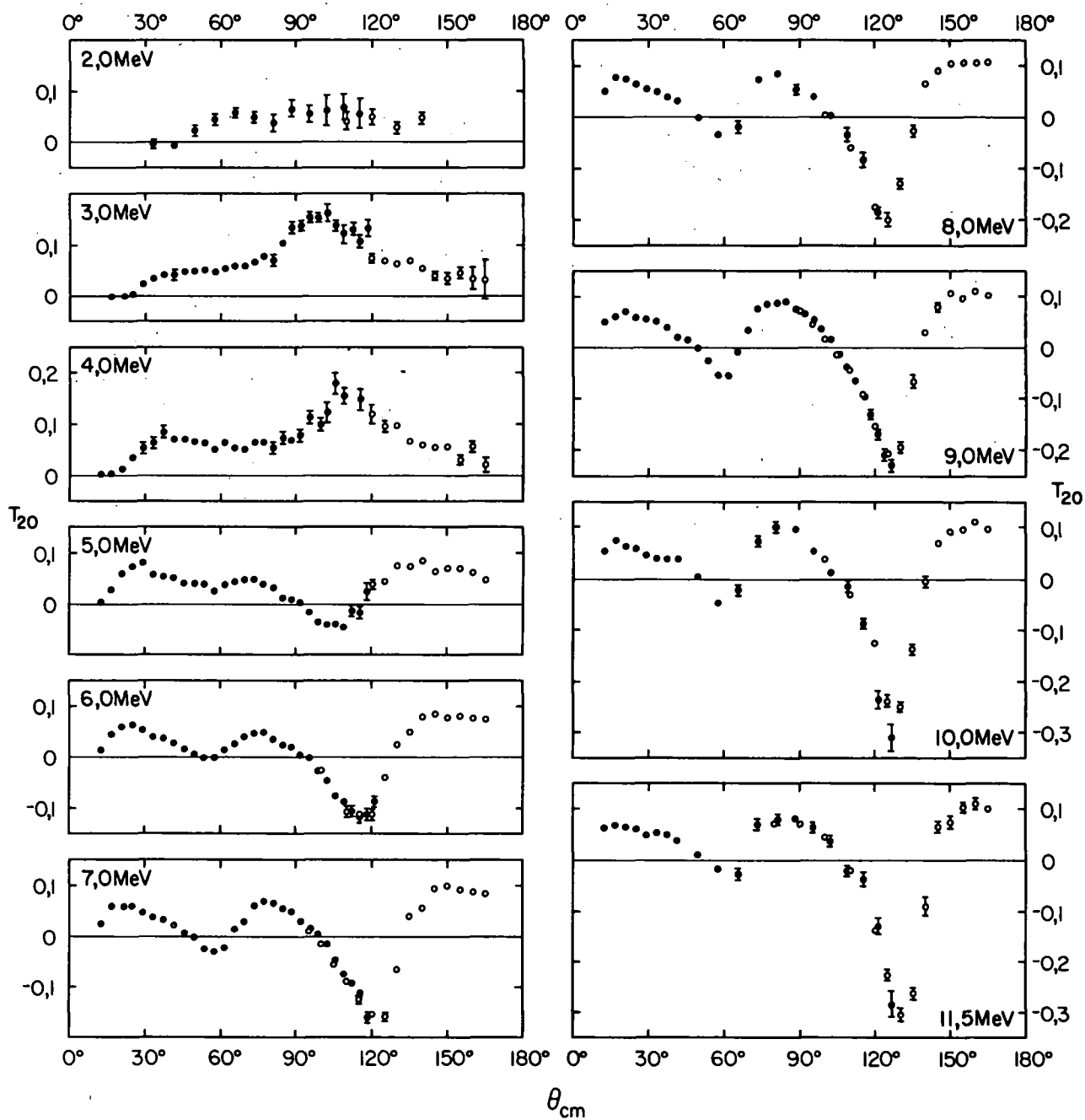


Fig. 2: Tensor analysing power T_{20} in ${}^3\text{He}(d,d){}^3\text{He}$ scattering

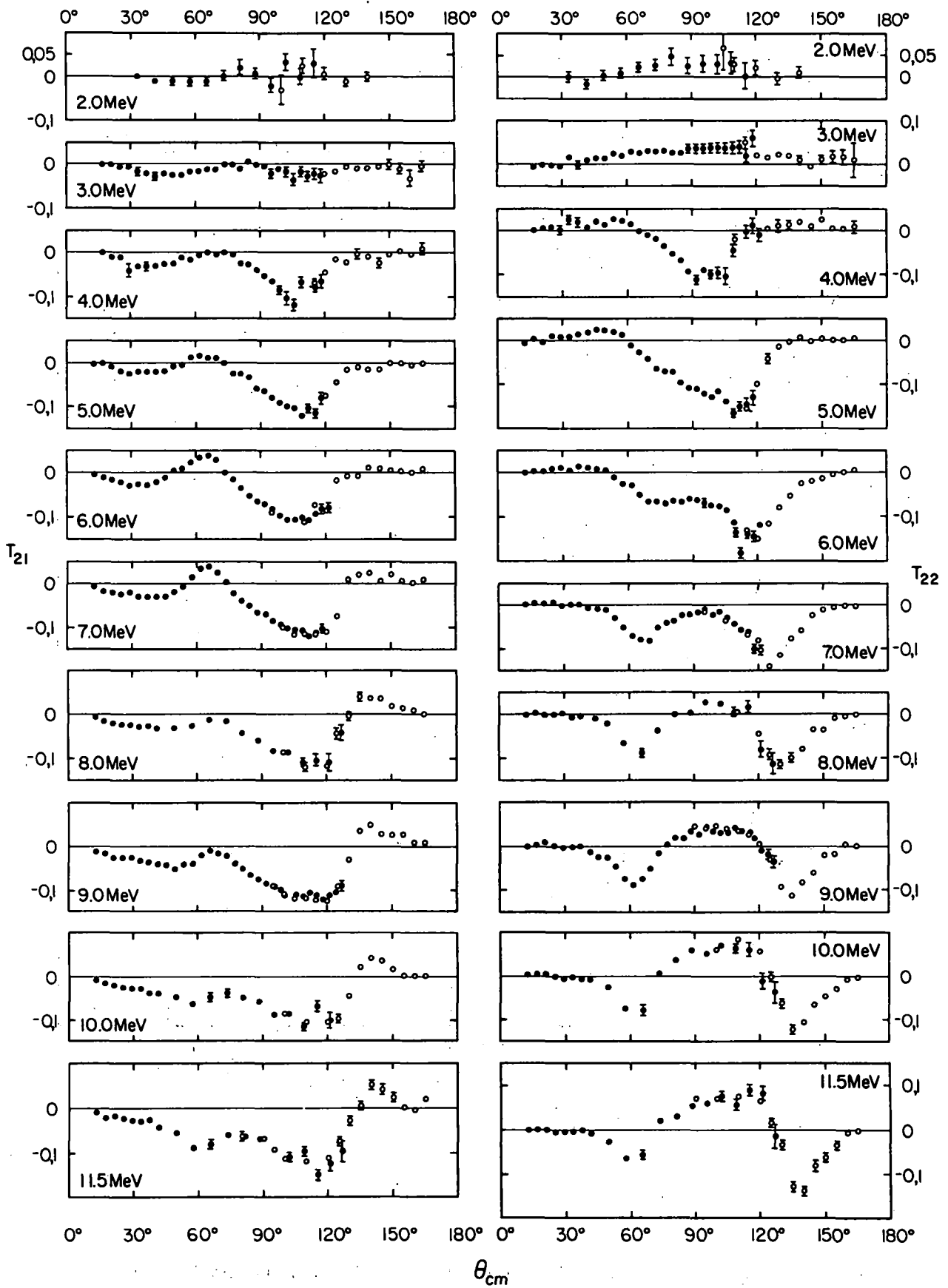


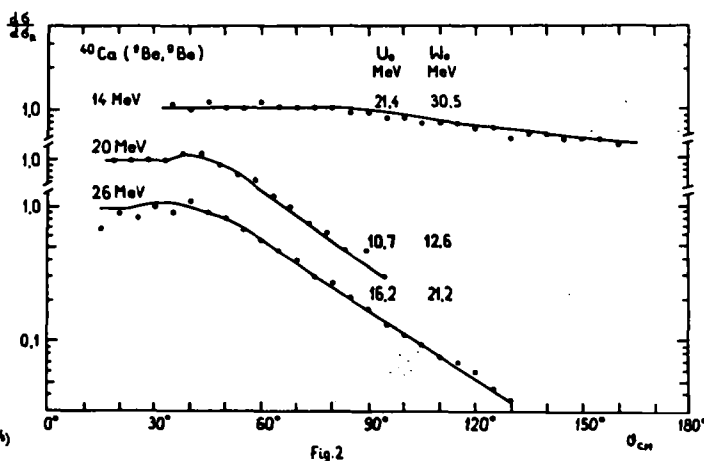
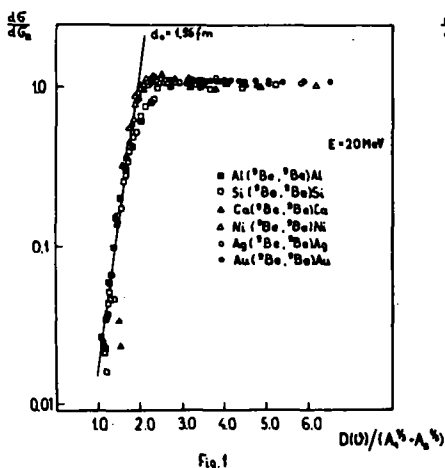
Fig. 3: Tensor analysing powers T_{21} and T_{22} in ${}^3\text{He}(d,d){}^3\text{He}$ scattering

2. Elastic Scattering of ^9Be Ions

J. Lang, R. Müller, E. Ungricht and J. Unternährer
 L. Jarczyk[†], A. Strzalkowski[†] and R. Bukowska[†]

The angular distribution for elastic scattering of ^9Be ions on different nuclei were measured using the ^9Be beam from the ETH tandem accelerator in Zürich [1]. The measurements were performed for the target nuclei ^9Be , ^{12}C , ^{24}Mg , ^{27}Al , ^{28}Si , ^{40}Ca , ^{58}Ni and ^{108}Ag at the three beam energies 14, 20 and 26 MeV. The angular region from 10° to 100° (Lab) and in some cases up to 160° was covered in 5° intervals.

Except for the lightest investigated nuclei ^9Be and ^{12}C where some structure in the angular distributions was observed, only a smooth decrease of the cross section above some angle could be noticed, characteristic for the strong absorption and domination of Coulomb interaction. Following a procedure used in [2], experimental results at 20 MeV are presented in Fig. 1 in function of $d = D(\theta) / (A_1^{1/3} + A_2^{1/3})$, where $D(\theta)$ is the distance of closest approach corresponding to the classical Coulomb orbit. This representation



shows that the distance D_0 for which nuclear effects set in varies proportional to $(A_1^{1/3} + A_2^{1/3})$ resulting in an approximately constant d_0 of 1.96 fm. This value is, however, greater than the distances found in ^{16}O or ^{12}C scattering. The optical model can, of course, be used to fit the cross sections.

It is well known that the optical model parameters cannot be determined in an unique way from such measurements. Therefore, the geometrical parameters were fixed arbitrarily to $R=1,27 (A_1^{1/3} + A_2^{1/3})$ fm and $a=0,647$ fm and only the depths of the real and imaginary potentials varied. An example is given in Fig. 2.

References

- {1} R. Balzer, contribution to Heavy Ion Conference, Caen, September 1976
- {2} G. R. Satchler, Reaction between Complex Nuclei, Tennessee 1974

† Institute of Physics, Jagellonian University, 30059 Cracow, Poland

III. Institut für Physik der Universität Basel

(Dir.: Prof. E. Baumgartner)

Spectroscopic Factors for Energy Levels of $^{41,43,45,49}\text{Ca}$

H. Schär, D. Trautmann and E. Baumgartner

In this work we briefly describe the determination of spectroscopic factors by means of (d,p) reactions on some Calcium isotopes in the vicinity of the Coulomb barrier.

Differential (d,p) cross-sections on $^{40,42,44,48}\text{Ca}$ were measured at 2.5 MeV incident deuteron energy in 5 degree intervals between 40 and 160 degrees. The excitation energies of the final nuclei range from 0 to 5.5 MeV.

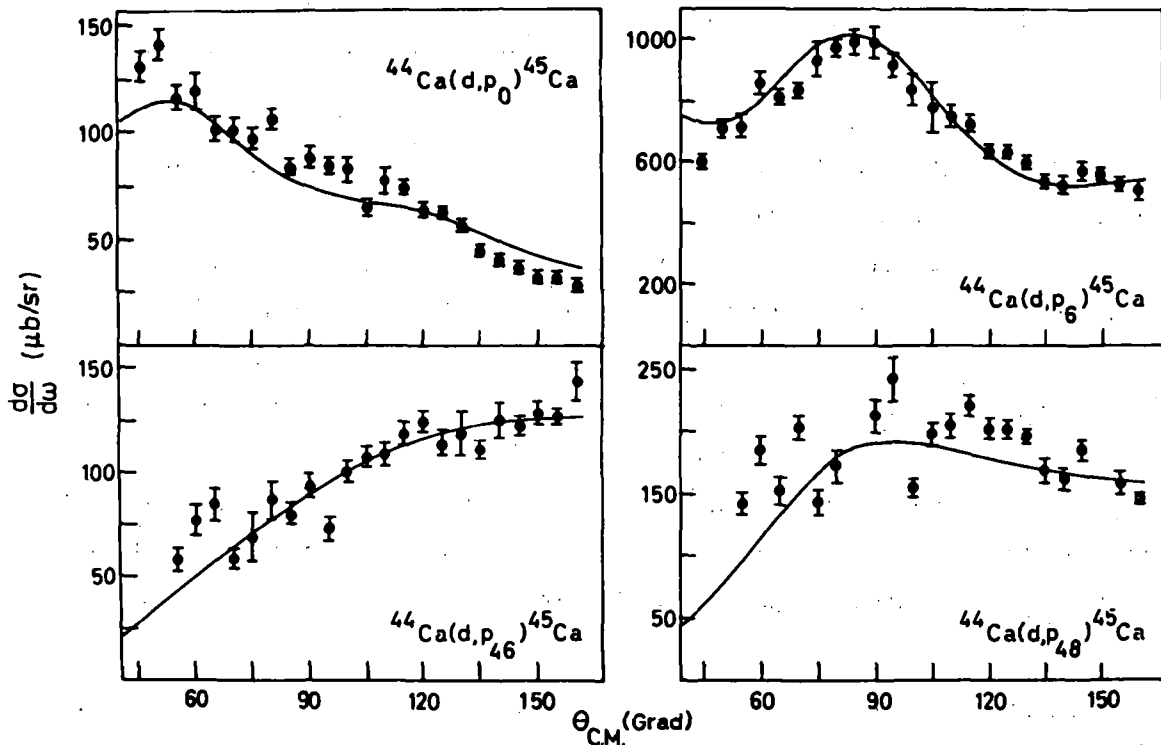


Fig. 1: Measured and calculated angular distributions of the reactions $^{44}\text{Ca}(d,p)^{45}\text{Ca}$ at 2.5 MeV deuteron energy. The corresponding level energies and spectroscopic factors are summarized in table 1. The quantity j is the total angular momentum.

Theoretical angular distributions are calculated with the Born approximation. However, as usual the plane waves are replaced by waves calculated in an optical model potential, using the computer codes DWUCK {1} and LOLA {2}. A least squares' fit of these angular distributions to the measured cross-sections gives the spectroscopic factors.

Fig. 1 shows selected angular distributions; the dots are the experimental values, the full lines represent the results obtained with the code DWUCK.

Table 1: Spectroscopic Information for ^{45}Ca

level No.	excitation energy (MeV)	l	$2j$	$(2j+1)S$
0	0.000	3	7	3.6
6	1.904	1	3	2.5
46	4.837	2	5	0.5
48	4.919	0	1	0.1

When the energies of the incoming deuteron and the outgoing proton are both well below the Coulomb barrier, the spectroscopic factor is almost independent of the optical scattering potentials; it is only influenced by the optical model parameters describing the bound neutron wave-function.

Unfortunately, pure subcoulomb conditions cannot be realized for every energy level in the final nucleus because of the high reaction Q values {3}. Possible compound nuclear contributions to the cross-section, and ambiguities in the choice of the optical model parameters render an exact determination of spectroscopic factors difficult.

References

- {1} P. D. Kunz, University of Colorado, Internal Report COO-535-613
- {2} R. M. de Vries, Phys. Rev. C8, 951 (1973)
- {3} F. K. Mc Gowan and W. T. Milner, Nucl. Data Tables 11, 1 (1972)

IV. Physik-Institut der Universität Zürich

(Dir.: Prof. E. Brun)

^3He Induced Activation Cross Sections on ^{10}B , ^{16}O and ^{19}F

J. Gass and H. H. Müller

With respect to the interpretation of activation analyses, activation cross sections for the reactions $^{10}\text{B}(^3\text{He},\text{d})^{11}\text{C}$, $^{16}\text{O}(^3\text{He},\text{p})^{18}\text{F}$ and $^{19}\text{F}(^3\text{He},\alpha)^{18}\text{F}$ have been determined in the energy range of the incident particle between 1.5 and 4.6 MeV. The production yield of activated nuclei in a thick target was measured as a function of the incident particle energy. The cross section values have been determined by differentiation of the yield curves.

In Fig. 1 are shown the activation cross sections obtained in the present measurements along with those of Hahn et al {1} for the reactions $^{16}\text{O}(^3\text{He},\text{p})^{18}\text{F}$ and $^{19}\text{F}(^3\text{He},\alpha)^{18}\text{F}$ and of Patterson et al {2} for the reaction $^{10}\text{B}(^3\text{He},\text{d})^{11}\text{C}$. A summary of the numerical data is given in Table 1.

A more detailed article to this subject will be published in Nuclear Instruments and Methods.

References

- {1} R. L. Hahn and E. Ricci
Physical Review 46 (1966) 650
- {2} J. P. Patterson, J. M. Poate, E. W. Titterton and B. A. Robson
Proc. Phys. Soc. 86 (1965) 1297

Table 1: Numerical values of the activation cross sections $\sigma(E_0)$ (in mb)

Energy interval (MeV)	$^{16}_O(^3\text{He,p})^{18}_F$	$^{19}_F(^3\text{He},\alpha)^{18}_F$	$^{10}_B(^3\text{He,d})^{11}_C$
1,2 -1,4			0,31 ± 0,02
1,4 -1,6			1,08 ± 0,07
1,5 -1,75	0,71 ± 0,01		
1,6 -1,8	0,76 ± 0,02		2,40 ± 0,20
1,75 2,0	1,93 ± 0,04		
1,8 -2,0	1,82 ± 0,09		5,17 ± 0,45
2,0 -2,125	3,85 ± 0,12		
2,0 -2,2	3,61 ± 0,21		8,7 ± 0,9
2,0 -2,5		0,33 ± 0,10	
2,125-2,25	7,05 ± 0,22		
2,2 -2,4	11,2 ± 0,6		5,7 ± 1,3
2,25 -2,375	16,9 ± 0,5		
2,25 -2,5		0,82 ± 0,03	
2,375-2,5	23,3 ± 0,7		
2,4 -2,5	21,0 ± 1,9		30,6 ± 4,1
2,5 -2,6	19,1 ± 2,7		29,0 ± 6,1
2,5 -2,625	14,4 ± 0,9	3,9 ± 0,2	
2,6 -2,8	27,3 ± 2,1		14,9 ± 3,9
2,625-2,75	21,9 ± 1,1	4,5 ± 0,3	
2,75 -2,875	31,1 ± 1,6	6,9 ± 0,5	
2,8 -3,0	43,3 ± 3,5		33,4 ± 5,5
2,875-3,0	59,3 ± 2,4	4,3 ± 0,6	
3,0 -3,125	50,7 ± 2,9	5,0 ± 0,7	
3,0 -3,2	70,7 ± 5,8		26,1 ± 7,0
3,125-3,25	62,2 ± 3,7	16,8 ± 1,0	
3,2 -3,4	95,1 ± 9,0		22,4 ± 8,5
3,25 -3,375	53,9 ± 4,4	6,9 ± 1,2	
3,375-3,5		9,0 ± 1,5	
3,4 -3,6	86 ± 12		28 ± 10
3,5 -3,625		18,4 ± 1,8	
3,6 -3,8	108 ± 16		15 ± 11
3,8 -4,0	129 ± 20		17 ± 12
4,0 -4,2	171 ± 26		63 ± 14
4,2 -4,4	205 ± 33		47 ± 17
4,4 -4,6	139 ± 39		75 ± 21

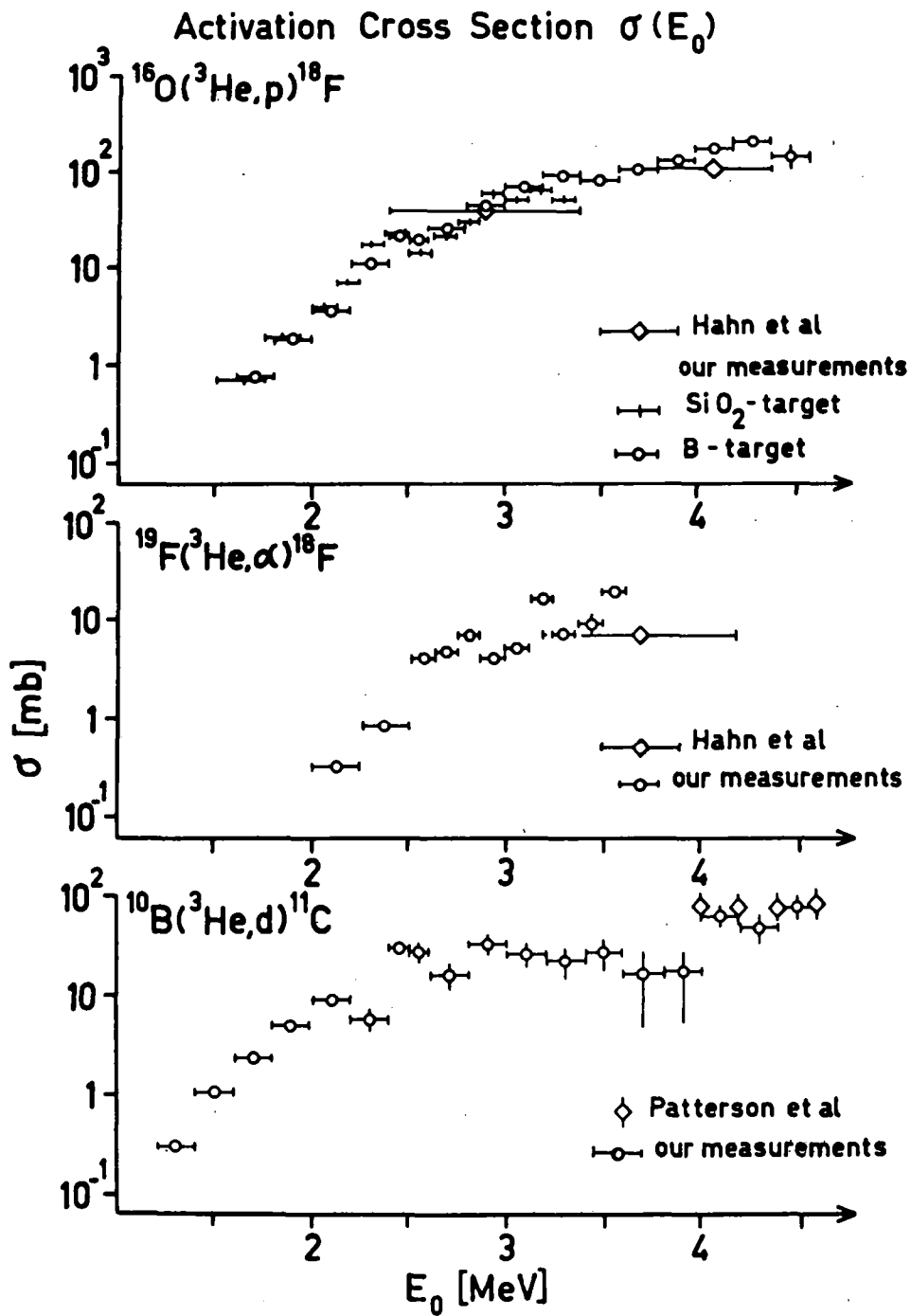


Fig. 1: Activation cross sections as functions of energy. As target material for the reaction $^{16}\text{O}(^3\text{He},p)^{18}\text{F}$ we used clean quartz glass (SiO_2), CaF_2 -powder pressed to tablets for the reaction $^{19}\text{F}(^3\text{He},\alpha)^{18}\text{F}$ and tablets of natural boron-powder for the reaction $^{10}\text{B}(^3\text{He},d)^{11}\text{C}$. Relative oxygen cross section values could also be extracted from the boron measurements, as the boron-powder was partially oxidized.

V. Eidg. Institut für Reaktorforschung, Würenlingen

(Dir.: Prof. H. Gränicher)

1. Dynamic Fission Barriers of Even-Even Actinides Nuclei

K. Junker

Based on the concept of dynamic fission paths (1) the fission barrier of about 60 nuclei in the range from Th to Ku have been calculated. Using a realistic shell model potential (deformed Woods-Saxon potential including the Coulomb potential for the protons {2,3}) to generate the single particle states, the potential energy surfaces of the actinide nuclei have been determined by applying Strutinskys' energy renormalization method {4}. The shape parametrization of H. C. Pauli {5} has been used and supplemented by a further deformation parameter describing deviations from axial symmetry. The calculation included elongation, constriction and axial asymmetry at the inner barrier and elongation, constriction and mass asymmetry at the outer barrier. Fig. 1 shows the calculated barriers as a function of Z^2/A of the fissioning nuclei. The values are given with respect to the groundstate and include 0,5 MeV zero point energy. In Fig. 2 the expected mass asymmetry χ (ratio of the volume of the heavy fragment to that of the light fragment) determined at the outer dynamic barrier is shown as a function of the mass number A. Preliminary investigations for the Pu isotopes showed a remarkable instability of the outer, mass symmetric barrier against axially asymmetric distortions. As much as 2 MeV barrier reduction is obtained by including axial asymmetry in the calculations. As a consequence the difference ΔE_B between mass symmetric and mass asymmetric outer barriers was calculated to be approximately 1,5 MeV independent of the neutron number N. This fits nicely to the experimental results {6} which never showed the pronounced maximum of about 4 MeV at a neutron number $N \approx 146$ predicted by all previous calculations.

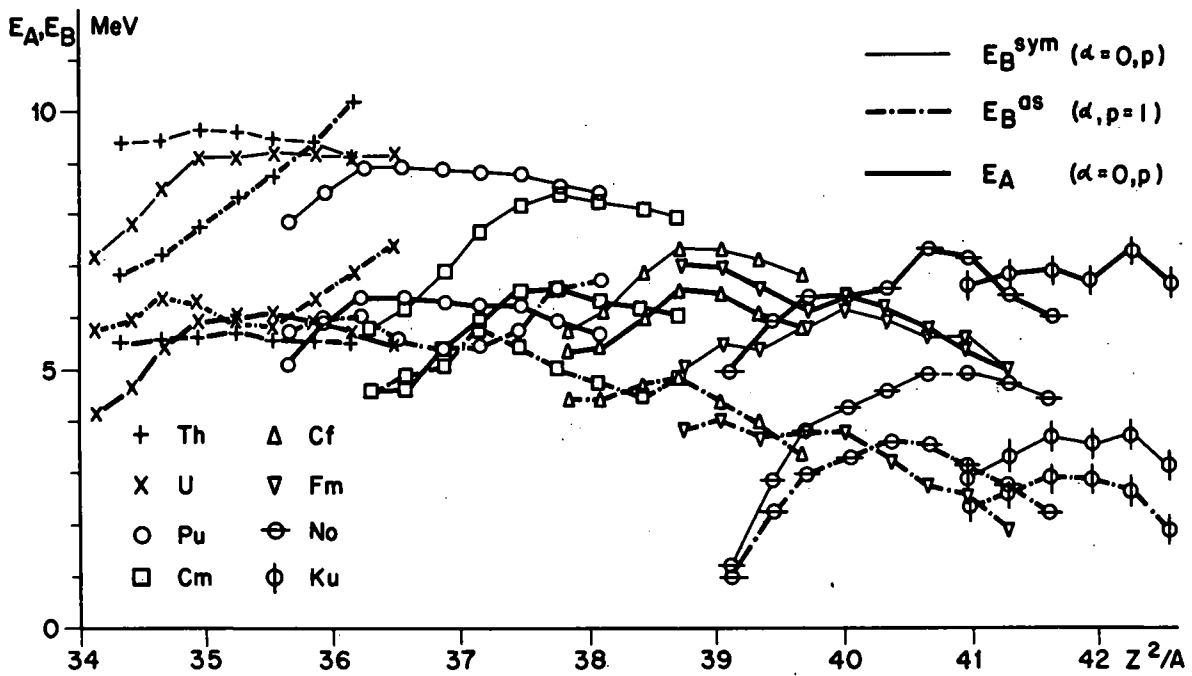


Fig. 1: Fission barriers as a function of Z^2/A (E_A : inner barrier, E_B : outer barrier). Values are given with respect to the groundstate energy, including 0.5 MeV zero point energy.

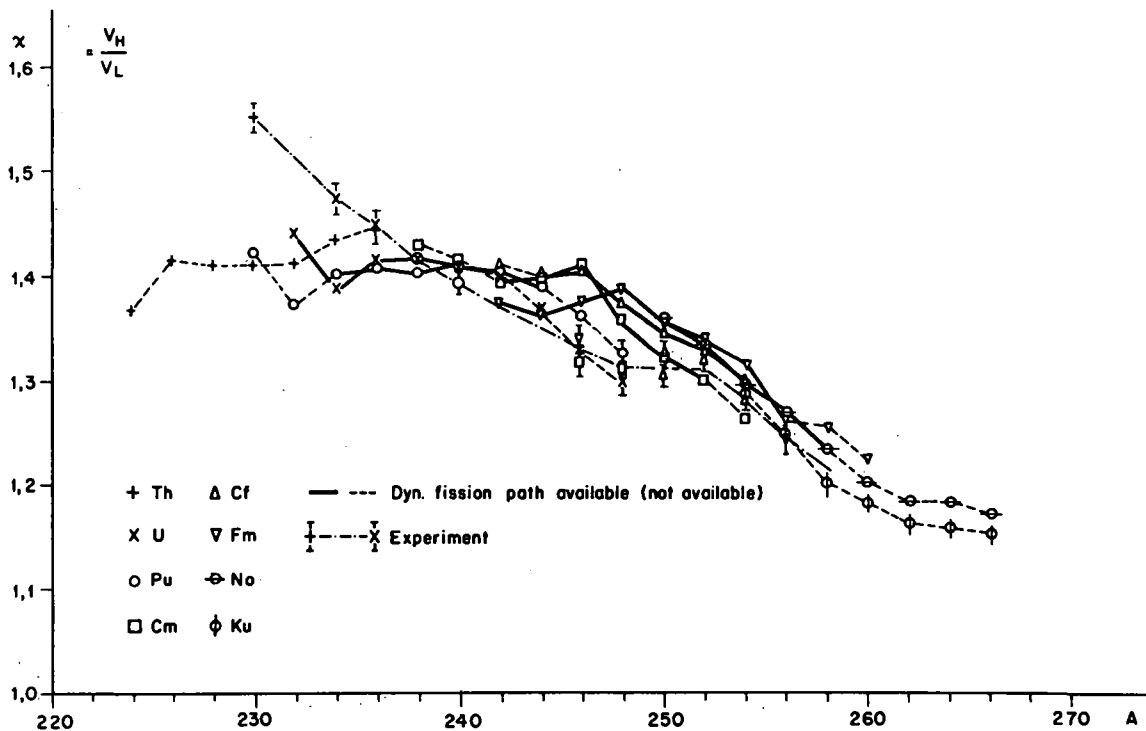


Fig. 2: Mass asymmetry determined at the outer dynamic fission barrier

References

- {1} T. Ledergerber and H. C. Pauli, Nucl. Phys. A207 (1973), 1
- {2} K. Junker, Acta Phys. Austr. 40 (1974), 335
- {3} K. Junker, Acta Phys. Austr. 43 (1975), 221
- {4} V. M. Strutinsky, Nucl. Phys. A122 (1968), 1
- {5} H. C. Pauli, Phys. Rep. 7C (1972)
- {6} H. J. Specht, Proc. Seventh Masurian School in Nucl. Phys.,
Part3, Nukleonika 20 (1975), 717

2. Production of Radioisotopes with 500 MeV Protons

J. Hadermann

The feasibility of ^{123}I production by 500 MeV protons from different target nuclei is investigated. Cross sections for spallation and peripheral reactions are calculated in the framework of a parametric representation [1]. Table 1 gives a comparison of available experimental and calculated cross sections in the mass and energy region of interest. Cumulative cross sections are indicated by curly brackets. Generally calculated and experimental values agree reasonably well. It would, however, be useful to fill some of the experimental gaps and to check some of the larger discrepancies.

In table 2 cumulative activities for different Xenon isotopes* were calculated taking into account the radioactive decay chains of the isotopes produced. For the beam and target specifications shown in the table caption activities between 650 mCi and 2Ci were obtained. The ratio $R = \frac{^{123}\text{Xe activity}}{^{121}\text{Xe activity}}$ is important in minimizing the most unwanted ^{121}I contamination. The isotopes ^{134}Ba and ^{135}Ba would be the most suitable targets for ^{123}I production. However, as a readily available target material ^{133}Cs is competing favorably.

* For the production of ^{123}I Xenon is blown out from the irradiated target enhancing the purity of the desired iodine isotope.

Table 1a

Product	^{139}La - Target			^{123}Cs - Target		
	Calc.	Exp.	Ref	Calc.	Exp.	Ref
^{118}I	1.3	6	a)			
^{119}I	4.2	13	a)			
^{120}Xe	1.8	8.5	a)			
^{120}I	6.6	15	a)			
^{121}Cs	1.9	} 21	a)			
^{121}Xe	3.6		a)			
^{121}I	14.8		18	a)		
^{122}Cs	4.6	} 42	a)			
^{122}Xe	12.3		a)			
^{123}Ba	0.2	} 36 ± 5 45 ± 6 57 ± 9 12	b)	49.4	} 4.21 ± 0.94	e)
^{123}Cs	12.6		c)			
^{123}Xe	17.5		b)			
^{123}I	11.7		a)			
^{124}I	5.8	9.3	a)			
^{125}Ba	2.7	} 57 ± 9 43 6.7	b)	53.5	} 95.8 ± 13.5	e)
^{125}Cs	27.5		a)			
^{125}Xe	16.3		a)			
^{125}I	3.4		a)			
^{126}I	1.3	5.1	a)			
^{127}La	2.4	} 45 ± 7 29 ± 8 59 53 ± 11	b)	14.1	} 24.4 ± 0.5	e)
^{127}Ba	18.7		c)			
^{127}Cs	11.9		d)			
^{127}Xe	5.1		b)			
^{128}I	0.2	1.3	a)			
^{129}La	21.2	} 68 ± 14 51 ± 8 35	b)	24.8	14.0 ± 0.15	e)
^{129}Ba	22.3		c)			
^{129}Cs	3.0		d)			
^{130}Cs				34.3	55.3 ± 6.4	e)
^{130}I	0.12	0.33	a)			
^{131}Cs				49.5	47.2 ± 2.6	e)
^{131}I	0.05	0.15	a)			
^{132}Cs	11.7	6.1 ± 1.8	c)	61.2	63.6 ± 1.7	e)
^{136}Cs	0.32	0.86 ± 0.03	c)			

Table 1b

Product	^{nat}Ba - Target			^{nat}Ce - Target			^{141}Pr - Target		
	Calc.	Exp.	Ref.	Calc.	Exp.	Ref.	Calc.	Exp.	Ref.
^{127}La	-			2.7	} 54 ± 8		3.4	} 49 ± 8	
^{127}Ba	20.1	} 21 ± 5	c)	18.6		c)	20.3		c)
^{127}Cs	21.0			7.8			4.9		
^{129}La	-			20.0	} 66 ± 9		22.9	} 58 ± 8	
^{129}Ba	50.0	} 27 ± 5	c)	39.2		c)	29.6		c)
^{129}Cs	23.4			1.7			0.96		
^{132}Cs	25.9	12 ± 3	c)	1.0	2.8 ± 0.6	c)	0.11	0.23 ± 0.06	c)
^{136}Cs	21.8	7.7 ± 2	c)	0.06	0.12 ± 0.05	c)	0.005	0.011 ± 0.008	c)

a) Ref. 2

b) ref. 3

c) Ref. 4

d) Ref. 5

e) Ref. 6

Tables 1a and 1b: Comparison between experimental and calculated cross sections. Units are mb. Calculations are done for 590 MeV proton energy and do not vary appreciably in an energy range of 40 MeV. Proton energies were 600 MeV for references b), 550 MeV for reference e) and 590 MeV otherwise

Table 2

Product	T a r g e t - n u c l e u s													
	^{133}Cs	nat Ba	^{139}La	nat Ce	^{141}Pr	^{130}Ba	^{132}Ba	^{134}Ba	^{135}Ba	^{136}Ba	^{137}Ba	^{138}Ba	^{140}Ce	^{142}Ce
^{120}Xe	1.25	0.31	0.27	0.29	0.36	7.32	2.96	1.26	0.81	0.51	0.31	0.19	0.31	0.12
^{121}Xe	2.83	0.75	0.66	0.69	0.82	9.33	5.63	2.79	1.86	1.22	0.79	0.50	0.74	0.31
^{122}Xe	1.01	0.30	0.27	0.26	0.29	1.77	1.49	0.96	0.69	0.48	0.33	0.22	0.28	0.13
^{123}Xe	6.09	3.10	2.71	2.53	2.53	4.12	6.44	7.70	6.24	4.70	3.43	2.43	2.68	1.44
^{125}Xe	1.21	1.01	0.73	0.54	0.41	0.58	0.73	0.88	0.83	1.08	1.06	1.01	0.55	0.51
^{127}Xe	0.012	0.007	0.004	0.003	0.003	0.004	0.004	0.008	0.007	0.007	0.006	0.006	0.003	0.003
R	2.15	4.55	4.11	3.70	3.10	0.44	1.14	2.76	3.35	3.85	4.35	4.84	3.61	4.57

Table 2: Xenon activities produced by 4 hours of irradiation of different targets. Units are 10^{10} decays/sec. A proton flux of $2.4 \cdot 10^{13}$ / cm^2 sec of 500 MeV energy is taken. The targets consist of $5 \cdot 10^{22}$ atoms. Also shown is the ratio $R = ^{123}\text{Xe}$ activity / ^{121}Xe activity.

References

- {1} R. Silberberg and C. H. Tsao, *Astrophys. J. Suppl.* 25 (1973) 315,
ibid. 25 (1973) 335
- {2} R. Silberberg and C. H. Tsao, *Cross Sections of Proton-Nucleus Interactions at High Energies*, Naval Research Laboratory Report 7593, Washington 1973
- {3} A. E. Ogard et al. in *Accelerator-Produced Radioisotope Program*, La-5249 PR, Los Alamos 1973
- {4} K. L. Scholz et al., *Int. J. Appl. Rad. and Isotopes* 25 (1974) 302
- {5} K. L. Scholz et al., *Am. Assoc. Phys. in Medicine, Quarterly Bull.*, June 1972, p. 80
- {6} M. A. Molecke in *Nuclear Chemistry Research of High Energy Nuclear Reactions at Carnegie-Mellon University Annual Progress Report 1971-1972*, Pittsburgh 1972

3. Yields of (μ^-, pxn) reactions

A. Wyttenbach, P. Baertschi, H. S. Pruys[†], E. A. Hermes[†]

When a nucleus (with charge Z) captures a negative muon, the resulting compound nucleus deexcites almost exclusively by emission of neutrons and γ -rays, giving products with charge $Z-1$. Emission of a proton, leading to products with charge $Z-2$, has a very low probability. Up to now this process was only known to occur in light nuclei ($Z < 20$) with a few percent probability {1}; for medium nuclei an upper experimental limit of 1 to 3 percent was observed {2}.

The usual experimental technique of measuring de-excitation γ -rays in time-relation to the μ -stop is not useful to detect rare events such as (μ^-, pxn) , because these are drowned by the signals from the much more abundant (μ^-, xn) reactions. We therefore had to resort to activation experiments. In these experiments it is possible to choose targets in such a way that the (μ^-, xn) reactions lead almost entirely to stable and/or to very short or very long-lived activities; it is thus possible to measure instable products of (μ^-, pxn) reactions practically free from interferences, what in turn gives the activation method the necessary sensitivity for these rare events.

The activities were performed at the SIN superconducting μ -channel. The number of muons stopped in the target were recorded by a conventional counter telescope. Targets with a thickness of 2 to 3 g/cm^2 were used. After activation, they were removed from the μ^- -beam and measured on a Ge(Li) detector. γ -ray spectra were evaluated by an appropriate computer program {3}, and γ -ray intensities are used to calculate activities.

The results of these measurements, some of which still have a provisional character, are given in Table 1 and Figure 1. The errors given are standard deviations as obtained from one to four experiments for each target; they do not take into account systematic errors associated with the μ^- -beam-monitoring or with the decay schemes used. (μ^-, pn) and $(\mu^-, p2n)$ reactions on a given nucleus have roughly the same probability. The probability of a (μ^-, p)

reaction is lower by a factor of 5. It can further be seen that the yields of all three reactions decrease approximately exponentially with the Coulomb barrier of the target nucleus. It is thought that these results can be explained by a neutron evaporation mechanism. Indeed for a given target there is roughly a constant ratio between the yields for (μ, xn) reactions (as calculated for an evaporation mechanism and barring direct neutron emission {4}) and the experimentally determined yields of the (μ, pxn) reactions.

Future work will supplement the experimental data, and the theoretical considerations will be refined.

References

- {1} P. Singer, Springer Tracts in Modern Physics, 71, 39 (1974);
S. Charalamabus, Nucl. Phys. A166, 145 (1971)
- {2} C. Petitjean et al., Nucl. Phys. A178, 193 (1971)
- {3} P. A. Schubiger, J. Radioanal. Chem. 25, 141 (1975)
- {4} J. Hadermann, private communication

† Physics Institute, University Zürich

Table 1

Yields of (μ^-, pxn) reactions (in units of 10^{-3} /stopped μ^-)

Target	(μ^-, p)	(μ^-, pn)	$(\mu^-, p2n)$
⁵⁵ Mn	2.0 ± 0.2	10.8 ± 0.7	8.7 ± 0.1
⁵⁹ Co	1.8 ± 0.1	22.7 ± 0.6	9.8 ± 0.2
⁷⁵ As	1.3 ± 0.1	6.9 ± 0.2	4.8 ± 0.2
⁹⁴ Zr		4.3 ± 0.8	
¹³³ Cs	0.46 ± 0.02	2.4 ± 0.3	1.8 ± 0.1
²⁰⁹ Bi	0.07 ± 0.03		

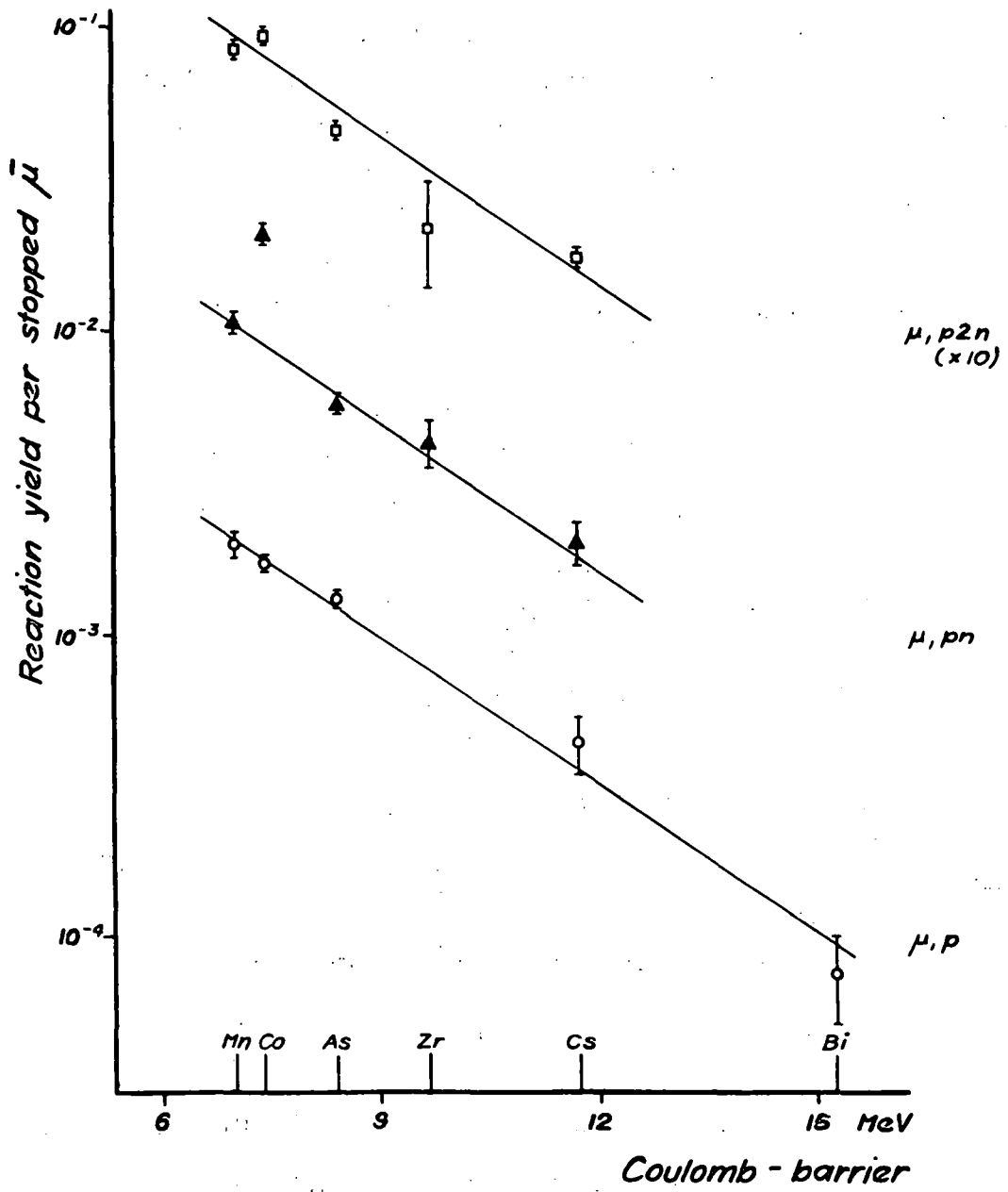


Fig. 1: Experimentally determined yields of (μ^-, pxn) reactions

PROGRESS REPORT TO NEANDC AND INDC

SOME RECENT REACTOR PHYSICS ACTIVITIES AT
THE ÇEKMECE NUCLEAR RESEARCH AND TRAINING
CENTER (ÇNAEM), İSTANBUL, TURKEY

BY

ÇETİN ERTEK

1977

ÇEKMECE NUCLEAR RESEARCH AND TRAINING CENTER
(ÇNAEM), POST BOX 1, HAVA ALANI, İSTANBUL
TURKEY

On the Negative Slowing-down Densities in the Multi-group Transport Theory Calculations of the Fast Neutron Energy Spectrum

(by Ç. Ertek and N. Çakmak)

The reason of appearance of the negative slowing-down densities in the multi-group calculations of the fast neutron density energy spectrum is discussed. When and why these negative values decrease in number is investigated using 25 and 54 group calculations. These multi-group formulations have been established using the Fourier transform of Boltzmann transport equation by P-approximation for slab geometry and homogeneous medium. The appearance of the negative slowing-down densities is discussed for a 1.143% enriched uranium water-moderated sub-critical reactor lattice for three different volume ratios using both 25 and 54 group calculations.

The following conclusions and discussions can be derived from this study:

-The calculation of fast and epithermal neutron energy spectrum in nuclear reactors by Greuling-Goertzel approximation provides the risk of producing negative slowing-down densities under some conditions.

-It is found absolutely necessary to print out the slowing-down density values together with their signs for each energy in the calculations. If the computer program internally calculates the slowing-down densities and prints out only the energy-dependent flux for each energy group one can encounter misleading results.

-If one finds some negative values for slowing-down densities it is not correct to proceed further. Because, the negative slowing-down densities do not

correspond to any physical meaning, such as up-scattering. We suggest that the only thing to be done in this case is to increase the number of energy groups if another cross-section library is available.

-As far as we know, a systematical investigation of the occurrence of these negative slowing-down densities has not been done up to now by taking into account leakage, number of energy groups, fuel and moderator interfaces and absorption effects. It is absolutely needed.

-As supported by R.Ehrlich's conclusions, we have also found that if the number of energy groups increases the appearance of oscillations and negative slowing-down densities decreases.

-This study does not completely yield parallel results with R.Ehrlich's conclusions as far as the negativities and the absorption of the medium are concerned as is discussed in detail in Section 2 in the following reference;

" On the negative slowing-down densities in the multi-group calculations of the fast neutron energy spectrum " by Ç.Ertek and N.Çakmak, Atomkernenergie Bd.27(1976) Lfg.4,S. 250-252.

On the numerical difference between homogeneous and heterogeneous calculations of uranium 238 capture rate ratios in light water reactors

(by Ç. Ertek and Y. Özbir)

In this work, we briefly try to illustrate the effect of the space-dependent heterogeneous treatment on the uranium 238 reaction rate calculations and these results are compared with homogeneous calculations.

In this short search we concentrated on 0.600 inch diameter, 1.0 % enriched uranium metal rod lattice with volume ratio (water to uranium) W/U:4.0. Brookhaven National Laboratory, USA, calculations and measurements have been made of β^{28} the ratio of episcadmium-to-subcadmium captures in U-238 foils placed in a typical cross-section of the lattice fuel rod. In table 1 of reference (1) the theoretical and experimental values of β^{28} are tabulated. For the 0.600 inch diameter, 1.0 % enriched uranium metal rod lattice with volume ratio W/U:4.0 the β^{28} value theoretically found by heterogeneous treatment is $\beta^{28} = 0.624$. BNL experimental value is 0.60 ± 0.05 .

Taking the neutron energy spectrum from Fig. 1 of Ref. 1 for the lattice in question and taking the cross section values for neutrons below 0.625 eV energy from TEMPEST library and for neutrons above 0.625 eV energy from MUFT library, we have calculated the β^{28} value and found it to be $\beta^{28} = 0.755$. In this calculation the resonance integral of U 238 is taken into account and spectrum is taken as 1/E for resonance region in question.

In short, we have illustrated the large difference between the two different calculations if one treats the reaction rate calculation as a straightforward numerical integration knowing the energy spectrum of neutrons properly.

In reactor design, if a theory predicts well the

material buckling of the system, it does not necessarily mean that the energy spectrum of the neutrons inside the reactor can be predicted correctly(2).

As it is stated by Strawbridge(3) "in addition to buckling uncertainties other effects that increase the standard deviation of the calculated results include impurities in the fuel, clad and moderator(impurities were neglected in the calculations), and uncertainties in physical parameters such as dimensions, densities and enrichments".(3).

In order to check the energy spectrum of the reactor, one has to make reaction rate ratio measurements and spectrum indices measurements, and these results must be compared with sophisticated reaction rate calculations including perturbations and heterogeneities of the system. A proper recipe for β^8 calculation of this kind is given by D.R.Oden Jr(4).

1. On the numerical difference between homogeneous and heterogeneous calculations of uranium 238 capture rate ratios in light water reactors by C.Ertek and Y.Ozbir Atomkernenergie, Bd.26(1975) Lfg.1, S 68-69.

2. Ertek, Ç, Yalçın A., İnel Y., An accurate determination of the cadmium ratio of neutron capture rates in U238 in slightly enriched uranium. NSE 36(1969) 209-219.

3. Strawbridge, L.E., Barry Criticality calculations for uranium water moderated lattices NSE 23(1965) 58-73.

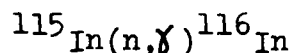
4. Oden, Jr., D.R. BNWL-1637 Special Distribution Jan 1972.

5. Stehn, J.R. MUFT code KAPL-M-JRS-13, General Electric Co. W-31-109 Eng.52

6. Stehn, J.R., M.D. Goldberg, B.A. Magurno, R.W. Chasman BNL 325 (2nd ed.) Suppl. No. 2 (physics-TID-4500, 32nd ed.) Sigma Center, Brookhaven National Lab.

7. Honeck, H.C. The calculation of the thermal utilization and disadvantage factor in uranium/water lattices. NSE 18(1964) 49-68.

An investigation on the thickness dependence of the total and capture cross-section determination of



(by Ç. Ertek)

In this work(1), a detailed investigation of the capture and total cross-section measurements for the $^{115}\text{In}(n,\gamma)^{116}\text{In}$ capture reaction around the 1.456 eV first resonance has been discussed. Sample thickness determination criteria are reviewed from the statistical and systematic point of view. It has been established(2) that most of the results from old activation measurements on radiative-capture cross-sections of 14-15 MeV neutrons are in error due to the fact that corrections for secondary neutron capture in the sample have been ignored. Present work shows clearly the amount of systematic error involved in the radiative-capture cross section and possibly total cross section determination in the electron volt range for the above capture reaction.

The work investigates in detail the specific activation rates (activity per nucleus per second) for a variety of target foil thicknesses ranging from 1.10^{-4} cm to 23.10^{-4} cm around the 1.456 eV resonance energy.

Special attention is paid to the energy distribution of neutrons after going into the thin targets. The thickness dependence of the competition between absorption and scattering events are investigated in detail.

It is concluded that the $N\sigma t \ll 1$ criteria is not satisfied in most of the early transmission measurements because of the trend to make the statistical error minimum in a short counting time. For example in the resonance parameters measurements of Cd-113 which was a joint effort between Brookhaven National Laboratory and Cekmece Nuclear

Research Center, the thinnest sample used had a 0.002809cm thickness and it gives $N\sigma_d$ value to be 1.0004 which is not very much smaller than 1 rather higher(3).

The experimental results show clearly the deep penetration of neutrons toward the sample is more than is foreseen due to the fact that pointed out in this work.

Almost all total cross-section measuring centers have or have had the effective cross-section value at that particular energy for a particular thickness of that sample but this information is not considered separately during the final evaluation of resonance parameters (such as σ_0) and it is finally lost. It is actually that value we need for the activation detector used in the neutron spectrum measurements by taking into account the appropriate resolution and Doppler broadening corrections. What is usually done is to chose a set of samples and try to find E_r (resonance energy), σ_0 and total width (Γ) by least squares analysis for that particular resonance energy. For activation detector which is irradiated in reactor or elsewhere to find the neutron spectrum in the vicinity we again try to find a correction factor for selfshielding for its thickness. The resonance peak values are usually measured in mono-energetic beam geometry and it is questionable to use self shielding factors from that cross-section for the detector foil which is irradiated in the isotropic neutron flux. The development has been restricted, in the isotropic case, to foils irradiated in a void or in water whereas often the foil or its cadmium cover is embedded in a scattering and absorbing medium. In the latter case, the impinging flux may no longer be isotropic, thereby violating one of the basic assumptions of calculations.

1. An investigation on the thickness dependence of the total and capture cross-section determination (PHI/I 13) by C. Ertek, 1976 International Conf. on the Interactions of Neutrons with Nuclei, Lowell, Massachusetts, USA.

2. NEANDC Topical Conference on Capture Cross-section Measurements Harwell, 9th April, 1975. Report AERE-R 8082 p. 19 (unpublished).

3. Akyüz R.O., Cansoy C., Domaniç F., Parameters for the first neutron resonance of Cd-113 ÇNAEM Report No. 36, 1967.

Digital Determination of TR-I Control Rod Worths
and Time Behaviour of Neutron Flux

(by Ç. Ertek)

15

In this work, the control rod reactivity worth of the swimming-pool type reactor (TR-I) in ÇNAEM, Çekmece Nuclear Research and Training Center has been measured digitally and the mean neutron lifetime of neutrons has been estimated by a special miniature fission chamber with 60 nanosecond resolving time. The time behaviour of thermal neutrons is also compared with reactor control console results. The following conclusions could be derived from this study;

-The control rod reactivity worths are usually calibrated at low power levels (1 to 10 W) and the calibration values should not depend on the reactor power levels. But if we try to measure the reactivity value of some change from the reactor console at high-power level e.g. at 1 kW or 10 kW levels, it is found that this change is underestimated.

-Neutron measuring devices are highly sensitive to gamma rays and gamma-ray build-up effects and attention must be paid to the instant and unknown reactivity effects seen by the control console at especially high-power levels.

-Miniature fission chambers are found to be also sensitive to gamma rays and gamma-ray build-up effects for the reactor power levels of more than 10 kW. In this work it is also found that if we try to measure the reactivity value of a control rod at 1 kW power level and if we apply

this power by lowering the reactor power from 1 MW to 1 KW, even the miniature fission chamber gives misleading results due to the high gamma radiation field and gamma build-up.

-The digital method gave very good agreement with differential doubling-time measurements which were performed only at 10 W low-power level and the former method was giving reliable results even up to 1kW power level.

-Large contribution from gamma rays are experimentally verified even for the so-called "compensated" ionization chambers.(1).

1. Digital determination of TR-I control rod worths and time behaviour of neutron flux, by Ç. Ertek, Atomkernenergie(ATKE) Bd.27(1976) Lfg.2.

Fast neutron spectrum and absolute fast flux measurements
in TR-I Reactor core and its reflector

(by Ç. Ertek and A. İsyar)

(IAEA Project No. TUR/1/10)

In this work, the energy spectrum and amplitude of fast neutrons have been measured in 4 different positions inside the TR-I core and the reflector with the aid of analytical formulation proposed by J.P. Genthon(1).

If one compares the results obtained by P. Mas et. al.(2) in MELUSINE and TRITON Reactors and the results obtained in this work, one can indicate some interesting factors that affect the fast neutron spectrum.

Measurements have been performed in TR-I swimming-pool type reactor's D-34, D-47, D-48 and D-49 positions. The reason of direct comparison of these 3 reactors was mainly to understand the effect of 2 lines graphite

reflectors in TR-I reactor core . The situation is more similar for Melusine reactor case but Melusine has no graphite reflector instead it has only light water as a reflector. Fuel element types are identical for all these three reactors.

As a result analytical formulation of fast neutron spectrum has been investigated. The strong assumption in this formulation is that the energy dependence of fast neutrons in the reactor core (having the energy greater than 1 MeV) has the $E^{-0.775}$ analytical shape.

The existence of two rows of graphite reflector in the water reflector of TR-I Reactor increases the β value from 1 to 1.28 for D-47 position and 1.4 for D-49 position. The energy spectrum for fast neutrons are found for these four different positions.

The fast neutron energy spectrum of TR-I Reactor has also been calculated using MUFT Code by our calculational group for the actual fuel composition and volume fractions. 25 and 54 energy group calculations have both shown that the fast neutron flux for 2.7 MeV energy gives a maximum in the energy distribution. In our experiment by detector foils we have also found this result. The experimental result found here, agree very well with the Herdade's (3) results. In that case the fast neutron spectrum was measured by a proton-recoil telescope. The contribution of gamma-ray pulses to the background is important for proton energies below 2.5 MeV for a 0.45mm thick crystal and below 6 MeV for a 0.93mm thick crystal.

Foil activation and proton-recoil telescope techniques can also be compared with shielded-diode data which show a higher intensity of fast neutrons (4).

1. Genthon J.P. 1964, Rapport CEA-R 2403.
2. Mas P., Lloret, R., Comera J., Rapport CEA-R 3180, 1967.
3. Neutron dosimetry, Proceedings of Symposium Harwell, 10-14 Dec. 1962 p.409.
4. Neutron Physics Div., Annual Progress Report, Aug. 1963 by E.P. Blizard p.101 ORNL-3499.Voll.

The mean neutron life-time determination by
reactor noise measurement

(by Ç. Ertek)

(Submitted to ATOMKERNENERGIE for publication)

In the previous work(1), the control rod reactivity worth of the swimming-pool type reactor (TR-I) in ÇNAEM, Çekmece Nuclear Research and Training Center was measured digitally and the mean neutron life-time was estimated by a special miniature fission chamber.

In the present work, an entirely different method (the noise analysis) is applied in order to determine the same quantity "the mean neutron life-time" and the results are compared.

The mean neutron life-time value is found to be $\bar{\ell} = 3.92\text{ms}$. This value differs from our previous result only by 20.9 %. This agreement can be considered very satisfactory if one considers the various noise sources generated in a reactor and the factors involved in these two completely different techniques.

-As discussed in detail in the previous(1) work gamma ray compensation effects must be considered very seriously in the mean neutron life-time measurement.

-The noise measurements have serious signal-to-noise problems due to background noise sources for the two signals are physically different in most cases a strong correlation between them should not exist(2).

-Luckily, the two entirely different techniques are applied to the same source, mainly, the same core as shown in Fig.I, p.99 of reference(1).

-The reactor power in the previous work(1) was 1KW and in the present work was 50KW. From the noise analysis point of view if we increase the reactor power more than that new sources of noise may be exited. On the other hand at low power statistics may suffer.

-In zero power reactors the primary source of the observed fluctuations, namely the random nature of the neutron production, scattering and absorption processes, follows probability laws which are incorporated into theoretical models. Such models considered simple homogeneous reactor neutronics, but recently detailed theories have been developed to take into account(3) spatial and energy dependence, neutron transport effects, neutron detectors, lattice heterogeneity etc.

1. Ertek, Ç., Digital determination of TR-I control rod worths and time behaviour of neutron flux. Atomkernenergie (ATKE)27,1976, No.2, p.99.

2. Wright S.A., Albrecht R.W., and Edelman M.F., Cross correlation of neutronic and acoustic noise signals from local boiling, KFK 2069, p.8, Oct.1974.

3. Greef C.P., Measurements of temperature fluctuations in a gas-cooled power reactor, research dept., Berkeley Nuclear Lab. RD/B/N 2942, p.14, Feb.1974.

The analysis of a fictitious accident due to loss
of control on the shim rods in MITR-II

(by T. Yarman)

The analysis of an accident concerning the withdrawal of the shim rods in MITR-II is considered. Thus the two-dimensional, time dependent, three group diffusion equations for the proposed designed core of the MIT Reactor are written with an extra source term accounting for the photoneutrons generated in the D_2O reflector. An analytical expression is developed for this term. Then an approximate flux composed of two spatial shapes chosen beforehand, each having an unknown time coefficient is inserted into the time dependent multigroup equations and the weighted residual criteria is applied. The results obtained through OZAN, the code written to perform computations required by the present work, has suggested that a space dependent analysis is required to analyze the accident postulated.

(ÇNAEM Report No. R-152, by T. Yarman, 1975.

A method for calculating plutonium source
LMFBR accidents

(by M.Kirbiyik)

The objective of this work was to estimate upper limits for the generation of vaporized plutonium during disassembly and during subsequent expansion of the fuel in a large core-disruptive accident. Fuel-vapor generation during disassembly was calculated using the VENUS-II code(2). The expansion after disassembly was assumed to be isentropic. The fuel was allowed to expand to low pressure; and in this process further fuel vapor was formed. Heat transfer and mixing prior to expansion might reduce fuel-vapor source while at the same time generating sodium vapor.

1. A method for calculating plutonium source LMFBR accidents by M.Kirbiyik, CNAEM Report No.151.
2. J.F.Jackson and R.B.Nicholson, VENUS-II, An LMFBR Disassembly Program, Argonne National Lab., ANL-7951, 1972.

Etude thermique du coeur TR-I constitué par des
éléments combustibles A 23 plaques

(par Ş. Erk)

Le but de cette étude est de comparer les conditions de refroidissement du coeur de TR-I fonctionnant à 1 MW, et utilisant respectivement les éléments combustibles de types S-10 et SI-23 et d'étudier des extensions futures et, si besoin, des augmentations de puissance.

1. Etude thermique du coeur TR-I constitué par des éléments combustibles a 23 plaques, par Ş Erk CNAEM Report No.150, 1975.

Dosage radiometrique du thorium dans les
minerais de Turquie

(par R.Uzmen et B.İpekoğlu)

There is a great need for rapid and continuous analysis of thorium during the physical enrichment processes of the turkish thorium minerals; consequently a quantitative determination curve of Pb^{212} which is in isotropic equilibrium with Th^{232} . The use of standard thorium component was useless, since quantitative determination of thorium in the mineral was carried out beforehand by chemical methods.

1. Dosage radiometrique du thorium dans les minerais de Turquie, par R.Uzmen et B. İpekoğlu ÇNAEM Report No.147, 1975.

SOME NUCLEAR DATA ACTIVITIES AT
MIDDLE EAST TECHNICAL UNIVERSITY, ANKARA, TURKEY
AND
HACETTEPE UNIVERSITY, ANKARA, TURKEY

1977

Ranges in Al of Fragments From Spontaneous
Fission of ^{252}Cf by Using a Ge(Li) detector*

Isotope	Avarage R ($\frac{\text{mgAl}}{\text{cm}^2}$)
^{95}Zr (64d)	4.14 ± 0.08
^{95}Nb (35d)	4.00 ± 0.04
^{97}Zr (16h)	3.87 ± 0.05
^{99}Mo (66h)	3.84 ± 0.02
^{103}Ru (39d)	3.82 ± 0.02
^{105}Ru (4.5h)	3.73 ± 0.03
^{105}Rh (36h)	3.69 ± 0.07
^{115}Cd (53h)	3.64 ± 0.03
^{131}I (8d)	3.44 ± 0.03
^{132}Te (78h)	3.40 ± 0.02
^{132}I (2.5h)	3.42 ± 0.03
^{133}I (21h)	3.43 ± 0.06
^{133}Xe (5d)	3.39 ± 0.04
^{135}I (7h)	3.31 ± 0.04
^{135}Xe (9h)	3.28 ± 0.03
^{140}Ba (13d)	3.05 ± 0.03
^{140}La (40h)	3.14 ± 0.03
^{141}Ce (33d)	3.08 ± 0.02
^{142}La (1.5h)	3.02 ± 0.06
^{143}Ce (34h)	2.96 ± 0.04
^{147}Nd (11d)	2.90 ± 0.04
^{149}Nd (1.7h)	2.81 ± 0.07
^{153}Sm (47h)	2.56 ± 0.03

*G.Yener and O.Birgöl, Department of Physics, Hacettepe
University, Ankara, Turkey

N.K.Aras, Department of Chemistry, Middle East Technical
University, Ankara, Turkey.

^{252}Cf (s.f.)

Table of Calculated Fractional Independent Yields (FIY)
versus $Z-Z_p$ with $\sigma=0.58$ †

$Z-Z_p$	FIY	$Z-Z_p$	FIY	$Z-Z_p$	FIY
0.00	0.6158	0.48	0.4680	0.96	0.2060
0.02	0.6155	0.50	0.4571	0.98	0.1967
0.04	0.6146	0.52	0.4461	1.00	0.1875
0.06	0.6131	0.54	0.4349	1.02	0.1790
0.08	0.6112	0.56	0.4240	1.04	0.1704
0.10	0.6086	0.58	0.4126	1.06	0.1621
0.12	0.6054	0.60	0.4011	1.08	0.1540
0.14	0.6035	0.62	0.3896	1.10	0.1462
0.16	0.5973	0.64	0.3780	1.12	0.1386
0.18	0.5924	0.66	0.3655	1.14	0.1316
0.20	0.5870	0.68	0.3544	1.16	0.1245
0.22	0.5813	0.70	0.3432	1.18	0.1178
0.24	0.5749	0.72	0.3321	1.20	0.1112
0.26	0.5683	0.74	0.3204	1.22	0.1050
0.28	0.5610	0.76	0.3091	1.24	0.09920
0.30	0.5532	0.78	0.2922	1.26	0.09344
0.32	0.5451	0.80	0.2868	1.28	0.08794
0.34	0.5365	0.82	0.2759	1.30	0.08270
0.36	0.5278	0.84	0.2652	1.32	0.07766
0.38	0.5184	0.86	0.2546	1.34	0.07319
0.40	0.5091	0.88	0.2446	1.36	0.06859
0.42	0.4992	0.90	0.2344	1.38	0.06412
0.44	0.4890	0.92	0.2244	1.40	0.06000
0.46	0.4786	0.94	0.2146	1.42	0.05574

$Z-Z_p$	FIY	$Z-Z_p$	FIY	$Z-Z_p$	FIY
1.44	0.05205	1.80	0.01219	2.16	0.002382
1.46	0.04856	1.82	0.01187	2.18	0.002147
1.48	0.04523	1.84	0.01091	2.20	0.001930
1.50	0.04214	1.86	0.009988	2.22	0.001713
1.52	0.03927	1.88	0.009123	2.24	0.001555
1.54	0.03652	1.90	0.008336	2.26	0.001369
1.56	0.03391	1.92	0.007610	2.28	0.001260
1.58	0.03144	1.94	0.006947	2.30	0.001129
1.60	0.02914	1.96	0.006362	2.32	0.001015
1.62	0.02698	1.98	0.005762	2.34	0.0009070
1.64	0.02496	2.00	0.005147	2.36	0.0007856
1.66	0.02306	2.02	0.004780	2.38	0.0007097
1.68	0.02135	2.04	0.004313	2.40	0.0006425
1.70	0.01970	2.06	0.003876	2.42	0.0005605
1.72	0.01815	2.08	0.003270	2.44	0.0005064
1.74	0.01670	2.10	0.003148	2.46	0.0004440
1.76	0.01536	2.12	0.002880	2.48	0.0004067
1.78	0.01409	2.14	0.002631	2.50	0.0003604

† H.N.Erten and N.K.Aras, submitted to the Physical Review (1977).

Empirical Z_p Values, Average Neutron Numbers and
Chain Yields in the Spontaneous Fission of $^{252}\text{Cf}^\dagger$

A	ν	Z_p	Chain Yield	A	ν	Z_p	Chain Yield
85	0.53	33.63	0.05	105	1.77	41.89	6.78
86	0.59	34.04	0.10	106	1.83	42.31	6.15
87	0.65	34.46	0.14	107	1.89	42.72	6.68
88	0.72	34.87	0.20	108	1.96	43.13	6.36
89	0.78	35.29	0.34	109	2.02	43.55	6.61
90	0.84	35.70	0.40	110	2.08	43.96	5.90
91	0.90	36.11	0.63	111	2.14	44.37	5.13
92	0.96	36.52	0.74	112	2.20	44.78	4.31
93	1.02	36.93	0.88	113	2.27	45.17	4.46
94	1.09	37.35	1.10	114	2.33	45.55	3.20
95	1.15	37.76	1.37	115	2.39	45.92	2.69
96	1.21	38.18	1.59	116	2.45	46.30	2.10
97	1.27	38.59	1.92	117	2.51	46.67	1.06
98	1.33	39.00	2.40	118	2.58	47.05	0.90
99	1.40	39.42	2.92	119	2.64	47.43	0.50
100	1.46	39.83	3.40	120	2.70	47.80	0.30
101	1.52	40.24	4.35	121	2.76	48.18	0.15
102	1.58	40.65	3.92	122	2.82	48.57	0.020
103	1.65	41.07	5.09	123	2.89	48.96	0.015
104	1.71	41.48	5.70	124	2.95	49.34	0.010

A	ν	Z_p	Chain Yield	A	ν	Z_p	Chain Yield
125	0.90	48.91	0.010	146	2.20	57.26	4.80
126	0.96	49.29	0.030	147	2.27	57.68	4.29
127	1.03	49.69	0.13	148	2.33	58.09	3.60
128	1.09	50.08	0.40	149	2.39	58.51	2.57
129	1.15	50.48	0.60	150	2.45	58.92	2.50
130	1.21	50.88	1.0	151	2.51	59.33	2.11
131	1.27	51.25	1.49	152	2.58	59.75	1.50
132	1.34	51.64	2.32	153	2.64	60.16	1.31
133	1.40	52.01	3.72	154	2.70	60.57	1.0
134	1.46	52.38	4.22	155	2.76	60.98	0.80
135	1.52	52.76	4.39	156	2.82	61.40	0.68
136	1.58	53.13	4.85	157	2.89	61.81	0.50
137	1.65	53.55	4.66	158	2.95	62.22	0.40
138	1.71	53.96	5.45	159	3.01	62.63	0.30
139	1.77	54.38	5.66	160	3.07	63.05	0.20
140	1.83	54.79	5.88	161	3.13	63.46	0.14
141	1.89	55.20	5.67	162	3.20	63.88	0.10
142	1.96	55.72	6.0	163	3.26	64.29	0.080
143	2.02	56.03	6.52	164	3.32	64.70	0.050
144	2.08	56.44	5.53	165	3.38	65.11	0.030
145	2.14	56.85	5.30				

† H.N.Erten and N.K.Aras, Submitted to the Physical Review (1977).

Laboratory: Department of Chemistry
Middle East Technical University
Ankara-Turkey

Names : H.N.Erten, O.Birgül and N.K.Aras

Facility : Cf-252 source

Experiment: Measurement of yields and isomer ratio
in A=134 chain for the spontaneous
fission of Cf-252.

Method : Measurements were made/^{by}radiochemical
separations and using γ -ray spectrometry
with Ge(Li) and NaI(Tl) detectors. The
accuracy of the measurements is about ± 5 %.

Completion
Date : The experimental measurements have been
completed. Results submitted to J.Inorg.
Nucl.Chem.

Laboratory: Department of Chemistry
Middle East Technical University
Ankara-Turkey

Names : L.Toppare, H.N.Erten and N.K.Aras

Facility : Cf-252 source

Experiment: Measurement of cumulative and independent yields of products with half-lives less than one hour by direct γ -ray counting using Ge(Li) detectors. The accuracy of the measurements is between 5-15 %.

Completion

Date : The experimental measurements have been completed.

Laboratory: Department of Chemistry
Middle East Technical University

Names : H.N.Erten and N.K.Aras

Purpose : Examine charge distribution in the
spontaneous fission of Cf-252

Method : Treatment of experimental fractional
cumulative yields and comparing with
U-235(n_{th}, f)

Completion
Date : Has been completed. Empirical charge
distribution parameters Z_p and σ are
obtained. Results submitted as an
article to the Physical Review.

YIELDS OF PRODUCTS FROM SPONTANEOUS FISSION OF $^{252}\text{Cf}^\dagger$

Isotope	Reference Nuclide	Cumulative Yields
^{101}Mo	^{108}Ru	3.23 ± 0.4
^{104}Tc	^{141}Ba	5.5 ± 0.4
^{106}Tc	^{139}Xe	4.68 ± 0.2
^{109}Ru	^{139}Xe	5.18 ± 0.2
^{116}Ag	^{139}Xe	1.6 ± 0.2
^{131}Sb	^{134}Te	1.2 ± 0.2
^{133}mTe	^{141}Ba	3.14 ± 0.2
^{135}I	^{134}Te	4.0 ± 0.1
^{136}mI	^{139}Xe	$0.6 \pm 0.1^*$
^{137}Xe	^{139}Xe	4.6 ± 0.2
^{138}Cs	^{141}Ba	5.61 ± 0.1
^{141}Ba	^{108}Ru	6.0 ± 0.2
^{144}La	^{139}Xe	5.4 ± 0.2
^{146}Ce	^{141}Ba	3.82 ± 0.1
^{149}Nd	^{134}Te	2.42 ± 0.1
^{151}Nd	^{134}Te	1.72 ± 0.1

* = Independent Yields

† = L.Toppare, H.N.Erten and N.K.Aras (Unpublished) 1977